Host response to tissue derived decellularised crosslinked biomaterials

Thesis submitted in accordance with the requirements of the University of Liverpool for the degree of Doctor in Philosophy

By

Helen Ashwin

June 2016

Abstract

Tissue derived implants are used in a wide range of tissue repair applications. They can be sourced either from human donors (allograft) or from animals (xenograft), with harvest locations including dermis, small intestine submucosa and pericardium. To help reduce antigenicity and provide the desired characteristics of the implant, all these materials are processed. These manufacturing processes can include delipidation, decellularisation, crosslinking and sterilisation. Balancing host immune response to tissue derived implants is a critical component of wound healing, with excessive and inadequate interactions being detrimental to patient recovery and implant functionality.

In these studies the effect of using 1,6 hexamethylene diisocyanate (HMDI) to impart varying levels of crosslinking to acellular porcine dermal collagen decellularised using the propriety Permacol™ process was assessed. HMDI is incorporated into the amino acid structure of collagen by reacting with the amine groups found on lysine and hydroxylysine side chains.

Biophysical characterisation established the direct effect varying crosslinking levels present in the implants had on resistance to enzyme degradation, thermal stability and mechanical properties. Potential leukocyte activation was measured *in vitro* via reactive oxygen species (ROS) generation. Leukocytes are one of the first immune cell populations recruited to implantation sites, possessing formidable secretomes capable of significantly accelerating material degradation, particularly through extracellular release of ROS.

In addition, subsets of the implants produced were implanted subcutaneously in a rat model to evaluate the host immune response in relation to the crosslinking level.

The addition of HMDI crosslinks into acellular porcine dermal collagen decellularised using the propriety Permacol™ process was shown to increase resistance to enzyme degradation and thermal stability but had minimal effect *in vitro* on mechanical properties and ROS production. Low levels of HMDI crosslinking were required to impart resistance to enzyme degradation. *In vivo* low levels of HMDI crosslinks, such as those present in Permacol™ surgical implant, did not affect the host immune response. Higher levels of HMDI crosslinking *in vivo* was shown to delay the resolution of the host's immune response.

Acknowledgments

I would firstly like to thank my supervisors Prof. John Hunt and Dr Judith Curran for giving me the opportunity to do a PhD at the University of Liverpool. I am very grateful to John for his patience, support, encouragement and expertise throughout my research.

I would like to thank my managers Steve Bloor and Stephen Wholert at Covidien along with colleagues at Swillington, Trevoux and North Haven sites. Steve Bloor for his belief in me when we first spoke about my studies and his wealth of knowledge regarding biologics and processing techniques. Stephen Wholert for making me part of his team in Trevoux and continued support through to the end of my research.

During my time at Liverpool I worked with great colleagues at the Department of Clinical Engineering. I would like to extend my gratitude to everyone for their friendship, encouragement, support and feel privileged to know you all. There is a special mention for Dr Nick Bryan, for his expertise and invaluable advice in histology and immunology.

I am most grateful to my family and friends for all the support and patience, especially through the write up. Maintaining my sanity at work through coffee and cake and tromping through the hills and dales.

Lastly, Richard for his support, patience, belief, encouragement and love throughout.

Contents

Abstract ..... **i**

Acknowledgments ..... **ii**

Abbreviations ..... **vi**

List of figures ..... **vii**

List of tables ..... **xvi**

List of equations ..... **xviii**

1 Introduction **1**

1.1 Collagen 1

1.2 Collagen biomaterials 8

1.2.1 Chemical crosslinking collagen biomaterials 9

1.2.2 Soft tissue repair 13

1.3 Immune response 15

1.3.1 Cells of the immune response 16

1.3.2 Wound healing 21

1.3.3 Biomaterials and wound healing 21

1.4 Thesis Aims and Objectives 23

2 Materials and Methods **24**

2.1 Acellular porcine collagen scaffold preparation 24

2.2 Biophysical characterisation techniques 25

2.2.1 Amino acid analysis 25

2.2.2 Thermal stability of crosslinked material 27

2.2.3 Collagenase assay 28

2.2.4 Uniaxial tensile testing 30

2.2.5 Ball burst tensile testing 30

2.3 *In vitro* reactive oxygen species testing 31

2.4 *In vivo* immune response testing 34
2.4.1 Animal model..... 34
2.5 Histological analysis.....38
2.5.1 Embedding 38
2.5.2 Tinctoral staining 40
2.5.3 Immunohistochemistry..... 43
2.6 Image analysis 46
2.7 Statistical analysis 47
2.7.1 ANOVA 47
3 Biomaterial Characterisation.....48
3.1 Introduction 48
3.2 Aim.....49
3.3 Results 49
3.3.1 Comparison of amino acid composition of crosslinked collagen matrix 49
3.3.2 Evaluation of the effect of crosslinking on resistance to enzyme degradation..... 70
3.3.3 Evaluation of the effect of crosslinking on denaturation temperature. 73
3.3.4 Tensile Testing..... 80
3.4 Discussion 85
4 Effect of crosslinking on leukocyte activation 91
4.1 Introduction 91
4.2 Aim.....92
4.3 Results 93
4.3.1 Material stimulated Leukocyte activation..... 93
4.4 Discussion 105

5 Effect of Crosslinking on Immune Response 110

5.1 Introduction 110

5.2 Aim 111

5.3 Results 111

5.3.1 Day 2 implant observations 117

5.3.2 Day 7 implant observations 130

5.3.3 Day 14 implant observations 143

5.3.4 Day 28 implant observations 151

5.3.5 Overall implant observations 159

5.4 Discussion 170

6 General Discussion and Conclusions 175

6.1 General Discussion 175

6.2 Conclusions 181

6.3 Suggestions for future work 182

7 References 184

Abbreviations

AA	Amino acid
ANOVA	Analysis of Variance
APTES	3-aminopropyl triethoxysilane
BSA	Bovine serum albumin
DSC	Differential scanning calorimetry
ECM	extra cellular matrix
EDC	1-ethyl-3-(3-dimethyl aminopropyl)carbodiimide
EDTA	Ethylenediamine tera-acetic acid
ETOH	Ethanol
HCl	Hydrochloric acid
HDMI	Hexamethylene diisocyanate
HPLC	High performance liquid chromatogrphy
IL	Interlukins
IFN	Interferon
MHC	Major Histocompatability Complex
N	Newton
NADPH	Nicotinamide adenine dinucleotide phosphate
NK	Natural killer
PBS	Phosphate buffer saline
ROS	Reactive oxygen species
SD	Standard deviation
TCP	Tissue culture plastic
Td	Denaturation temperature
TGF	Transforming Growth Factor
Th	T helper
TNF	Tumour necrosis factor

List of figures

Figure 1.1 Hierarchical structure of collagen from single α chain to collagen fibre 2

Figure 1.2 Collagen molecule triple helix space fill model after the propeptide ends have been cleaved [12]..... 3

Figure 1.3 Type I procollagen being cleaved by ADAMTS-2 and BMP-1 [10]. ... 4

Figure 1.4 Collagen microfibril space fill model (helical portion of 5 collagen molecules) [12]..... 5

Figure 1.5 Hydrogen bonds between collagen triple helices to help stabilise microfibril and fibril formation. 5

Figure 1.6 Aldimine (immature) crosslink between C-telopeptide and triple helix portions of collagen molecules..... 6

Figure 1.7 Illustration of collagen D-period. 6

Figure 1.8 SEM photograph of Permacol™ showing collagen fibres with banding from D-period, red highlights in top left corner indicate dark bands caused by gap in D-period. 7

Figure 1.9 HHL (mature) crosslink between C-telopeptide and triple helices of collagen molecules. 8

Figure 1.10 Schematic of EDC, NHS crosslinking reaction with collagen molecules. 10

Figure 1.11 Glutaraldehyde crosslinking pathways with collagen [32]..... 11

Figure 1.12 Schematic of HMDI crosslinking reaction with collagen..... 12

Figure 1.13 Genipin crosslinking reaction with collagen. 13

Figure 1.14 *Cells and proteins of the innate and adaptive immune systems (based on Dranoff 2010* [36]*).* 16

Figure 1.15 T cell activation and differentiation into cytotoxic T cells (CD8+) and T helper (Th) cells (CD4+). Cytokines produced by Th cells and there role in immune cell activation. 20

Figure 2.1 DSC profile, temperature (°C) vs heat flow, of indium from Mettler-Toledo DSC 821e processed using STARe System software. 28

Figure 2.2 Dog bone dimensions used in uniaxial tensile test. 30

Figure 2.3 Ball burst test set up, picture a sand paper placed over fixture, picture b specimen placed on top of fixture and picture c specimen secured by circular plate, spherical probe in position. 31

Figure 2.4 Reagents used in leukocyte activation test[59]. 32

Figure 2.5 Randomised Delivery Schematic for Subcutaneous Implantation of Non crosslinked collagen and Permacol™. Red, pink and blue circles represent other biological materials that were implanted at the same time, data not included. 35

Figure 2.6 Randomised Delivery Schematic for Subcutaneous Implantation of collagen crosslinked with 200ml HMDI/kg collagen for 50 hours. Red circles represent other biological materials that were implanted at the same time, data not included. 36

Figure 2.7 Immunohistochemistry schematic 45

Figure 2.8 Example of where fields of view may be counted for an implant 46

Figure 3.1 Schematic of HMDI reaction with amine groups in collagen molecule. 49

Figure 3.2 Example HPLC chromatogram for AA analysis, glutamic acid, proline, glycine and alanine are all off scale. 51

Figure 3.3 Average normalised concentrations for arginine, aspartic acid, histadine and isoleucine across all materials. 52

Figure 3.4 Average normalised concentrations for leucine, methioine, phenylalanine and serine detected across all materials. 53

Figure 3.5 Average normalised concentrations for threonine, tyrosine and valine detected across all materials. 54

Figure 3.6 Average normalised concentrations for lysine detected in all materials. 55

Figure 3.7 Average normalised concentrations for lysine detected in all materials. 55

Figure 3.8 Normalised hydroxylysine concentration varying the amount of HMDI added to the reaction, squares 20 hour exposure, circles 0.5 hour exposure, triangle 50 hour exposure, error bars ± standard deviation. 57

Figure 3.9 Normalised lysine concentration varying the amount of HMDI added to the reaction squares 20 hour exposure, circles 0.5 hour exposure, triangle 50 hour exposure, error bars ± standard deviation. 58

Figure 3.10 Normalised hydroxylysine concentration varying the duration of exposure to HMDI, square 2ml HMDI/kg collagen, diamond no HMDI, cross 200ml HMDI/kg collagen, error bars ±standard deviation. 58

Figure 3.11 Normalised lysine concentration varying the duration of exposure to HMDI: square 2ml HMDI/kg collagen, diamond no HMDI, cross 200ml HMDI/kg collagen, error bars ±standard deviation. 59

Figure 3.12 Collagenase resistance assay, collagen remaining after enzyme digestion, varying the quantity of HMDI, duration of the crosslinking reaction 20 hours, error bars ± standard deviation. 71

Figure 3.13 Collagenase resistance assay, collagen remaining after enzyme digestion, using 2 ml of HMDI per kg of collagen, varying the duration of the crosslinking reaction error bars ± standard deviation. 71

Figure 3.14 Collagenase resistance assay, collagen remaining after enzyme digestion, number of crosslinks present in the material per 1000 AA, error bars ± standard deviation. 72

Figure 3.15 Collagen denaturation temperature, varying the quantity of HMDI, duration of the crosslinking reaction; diamonds 20 hour exposure, squares 0.5 hour exposure, triangle 50 hour exposure, green line unprocessed collagen, error bars ± standard deviation 74

Figure 3.16 Collagen denaturation temperature, using 2 ml of HMDI per kg of collagen, varying the duration of the crosslinking reaction; diamonds 2ml HMDI/kg collagen, squares no HMDI, triangle 200ml HMDI/kg collagen, error bars ± standard deviation. 74

Figure 3.17 Collagen denaturation temperature v's number of crosslinks present in material per 1000 AA, error bars ± standard deviation. 76

Figure 3.18 Graphical representation of stress strain curve. Line A represents ultimate tensile strength, the slope between points B is Young's modulus and C represents extension at maximum load. 80

Figure 3.19 Ultimate tensile strength varying the number of crosslinks present in the material per 1000 AA. Error bars ± standard deviation. 83

Figure 3.20 Young's modulus varying the number of crosslinks present in the material per 1000 AA. Error bars ± standard deviation. 83

Figure 3.21 Extension at maximum load varying the number of crosslinks present in the material per 1000 AA. Error bars ± standard deviation. 84

Figure 4.1 The role of NADPH oxidase in ROS production[89]..... 92

Figure 4.2 Leukocyte ROS production in response to acellular porcine dermal matrix with a crosslinking level of 1.7 crosslinks per 1000 AA. Each line represent mean RLU production n=3, for donors 1-3 (D1, D2 and D3) response to different sheets (red, white, orange, blue and green)..... 94

Figure 4.3 Mean total RLU, 3 donors, varying levels of crosslinked material and the average total RLU production for all 3 donors. Each point (except the average, purple diamonds) represent mean RLU production n=3, for donors 1-3 (D1, D2 and D3) response to different sheets (red, white, orange, blue and green)..... 96

Figure 4.4 Mean total RLU production for donor 3, green blue and white sheets with varying crosslinking levels (n=3), red line represents average RLU across all materials, error bars +standard deviation. 97

Figure 4.5 Mean total RLU production for 4 different donor's whole blood to material with -0.2, 0, 1.7, 2.6 and 11.4 crosslinks per 1000 AA (n=3), error bars + 1 standard deviation from the mean. 99

Figure 4.6 Mean ROS production from 10 donor's whole blood to materials with 0.0, 1.7 and 11.4 crosslinks per 1000 AA (n=3) and the combined mean of all 10 donors (n=30). * P<0.05 ** p<0.01, error bars + standard deviation. 100

Figure 4.7 Mean ROS production from 10 donor's whole blood to commercialy available materials, Permacol™, AlloDerm, Strattice and Surgisis® (n=3) and the combined mean of all 10 donors (n=30). * P<0.05, error bars + standard deviation. 102

Figure 4.8 Box and whisker plot of total RLU for 10 donors blood(n=30) to material with 0.0, 1.7 and 11.4 crosslinks per 1000 AA, Alloderm, Strattice, Surgisis® and tissue culture plastic. * indicates outlier greater than ± 2 residual value away from the median value. 103

Figure 4.9 Average total RLU for the crosslinking variants (excluding donor 2 day 2), error bars ± 1 standard deviation from the mean, dashed line represents control cells exposed to TCP. 104

Figure 5.1 Pico sirus red stain of Permacol™ 14 days post implantation, a) with polarising filter b) without polarising filter (20X magnification). Host / implant interface highlighted by white line in image a and black line in image b..... 116

Figure 5.2 Implant images, Permacol™ 2 days post implantation, with a hematoma. 117

Figure 5.3 Macroscopic implant observations for day 2 implants. 118

Figure 5.4 Day 2 implants, a) non-crosslinked b)Permacol™ c) highly-crosslinked H&E 40X magnification 119

Figure 5.5 Day 2 implants, a) non-crosslinked b)Permacol™ c) highly-crosslinked H&E 20X magnification 120

Figure 5.6 Semi-quantitative histological scores for day 2 non-crosslinked, Permacol™ and highly-crosslinked implants, error bars + 1 SD from the mean, n= 6 for non-crosslinked and Permacol™ and n=4 for highly-crosslinked. 122

Figure 5.7 Quantitative cell count for day 2 non-crosslinked, Permacol™ and highly-crosslinked implants, error bars + 1 standard deviation from the mean, n= 6 for non-crosslinked and Permacol™ and n=4 for highly-crosslinked. 123

Figure 5.8 Quantitative cell percentages for day 2 non-crosslinked, Permacol™ and highly-crosslinked implants, error bars + 1 standard deviation from the mean, n= 6 for non-crosslinked and Permacol™ and n=4 for highly-crosslinked. 124

Figure 5.9 ASD staining of granulocytes, day 2 implants 20X magnification ... 125

Figure 5.10 αASD staining of monocytes, macrophages and histiocytes (20x magnification) 126

Figure 5.11 Collagen I staining of Permacol™ implant / host interface (dashed line) after 2 days implantation, 20x H&E. 127

Figure 5.12 Collagen III staining of Permacol™ implant / host interface (dashed line) after 2 days implantation, 20x H&E. 128

Figure 5.13 Quantitative collagen ratio for day 2 non-crosslinked, Permacol™ and highly-crosslinked implants, error bars + 1 standard deviation from the mean, n= 6 for non-crosslinked and Permacol™ and n=4 for highly-crosslinked. 129

Figure 5.14 Implant image, highly-crosslinked implant 7 days post implantation, with vessel visible over implant. 130

Figure 5.15 Macroscopic observations for day 7 implants 130

Figure 5.16 Day 7 implants, a) non-crosslinked b)Permacol™ c) highly-crosslinked H&E 40X magnification 132

Figure 5.17 Day 7 implants, a) non-crosslinked b)Permacol™ c) highly-crosslinked H&E 20X magnification 133

Figure 5.18 Permacol™ implant 7 days after implantation, integration of the implant with the host tissue with vessels (green arrows) along the interface (dashed line), H & E 40X magnification. 135

Figure 5.19 Semi-quantitative histological scores for day 7 implants with 0.0, 1.7 and highly-crosslinked, error bars + 1 standard deviation from the mean, n= 6 for non-crosslinked and Permacol™ and n=4 for highly-crosslinked. 136

Figure 5.20 Non-crosslinked implant, 7 days after implantation showing host implant interface, Picro sirius red (polarised light) 20X magnification..... 137

Figure 5.21 Quantitative cell count for day 7 non-crosslinked, Permacol™ and highly-crosslinked implants, error bars + 1 standard deviation from the mean, n= 6 for non-crosslinked and Permacol™ and n=4 for highly-crosslinked. 138

Figure 5.22 ASD stating of granulocytes, day 7 implant, 20x magnification..... 139

Figure 5.23 Quantitative cell percentages for day 7 non-crosslinked, Permacol™ and highly-crosslinked implants, error bars + 1 standard deviation from the mean, n= 6 for non-crosslinked and Permacol™ and n=4 for highly-crosslinked. 140

Figure 5.24 Immunohistochemistry stain CD68 for activated macrophages, host tissue right and implant left (20X magnification). 141

Figure 5.25 Quantitative collagen ratio for day 7 implants with 0.0, 1.7 and highly-crosslinked, error bars + 1 standard deviation from the mean, n= 6 for non-crosslinked and Permacol™ and n=4 for highly-crosslinked. 142

Figure 5.26 Macroscopic observations for day 14 implants 143

Figure 5.27 Day 14 implants, a) non-crosslinked b)Permacol™ c) highly-crosslinked H&E 40X magnification 144

Figure 5.28 Day 14 implants, a) non-crosslinked b)Permacol™ c) highly-crosslinked H&E 20X magnification 145

Figure 5.30 Semi-quantitative histological scores for day 14 implants with 0.0, 1.7 and highly-crosslinked, error bars + 1 standard deviation from the mean, n= 6 for non-crosslinked and Permacol™ and n=4 for highly-crosslinked. 147

Figure 5.31 Quantitative cell count for day 14 non-crosslinked, Permacol™ and highly-crosslinked implants, error bars + 1 standard deviation from the mean, n= 6 for non-crosslinked and Permacol™ and n=4 for highly-crosslinked. 148

Figure 5.32 Quantitative cell percentages for day 14 non-crosslinked, Permacol™ and highly-crosslinked implants, error bars + 1 standard deviation from the mean, n= 6 for non-crosslinked and Permacol™ and n=4 for highly-crosslinked. 149

Figure 5.33 Quantitative collagen ratio for day 14 non-crosslinked, Permacol™ and highly-crosslinked implants, error bars + 1 standard deviation from the mean, n= 6 for non-crosslinked and Permacol™ and n=4 for highly-crosslinked. 150

Figure 5.34 Macroscopic observations for day 28 implants. 151

Figure 5.35 Day 28 implants, a a) non-crosslinked b)Permacol™ c) highly-crosslinked H&E 20X (a, b) 40X (c) magnification 152

Figure 5.36 Semi-quantitative histological scores for day 28 implants with 0.0, 1.7 and highly-crosslinked, error bars + 1 standard deviation from the mean, n= 6 for non-crosslinked and Permacol™ and n=4 for highly-crosslinked. 154

Figure 5.37 Permacol™ implant after 28 day implantation, implant showing basket weave pattern, Picro siris red (polarised light) 20X magnification. 155

Figure 5.38 Quantitative cell count for day 28 non-crosslinked, Permacol™ and highly-crosslinked implants, error bars + 1 standard deviation from the mean, n= 6 for non-crosslinked and Permacol™ and n=4 for highly-crosslinked. 156

Figure 5.39 Quantitative cell percentages for day 28 non-crosslinked, Permacol™ and highly-crosslinked implants, error bars + 1 standard deviation from the mean, n= 6 for non-crosslinked and Permacol™ and n=4 for highly-crosslinked. 157

Figure 5.40 Non-crosslinked ASD staining of granulocytes, day 28 implant 20X magnification..... 158

Figure 5.41 Semi-quantitative histological scores for all implant timepoints for non-crosslinked, Permacol™ and highly-crosslinked implants, error bars + 1 standard deviation from the mean, n= 24 for non-crosslinked and Permacol™ and n=16 for highly-crosslinked. 162

Figure 5.42 Semi-quantitative histological scores for all implants from days 2, 7, 14 and 28, error bars + 1 standard deviation from the mean, n= 21. 164

Figure 5.43 Quantitative histological analysis for non-crosslinked, Permacol™ and highly-crosslinked implants, error bars + 1 standard deviation from the mean, n= 24 for non-crosslinked and Permacol™ and n=16 for highly-crosslinked. 167

Figure 5.44 Quantitative histological score for 2, 7, 14 and 28 day implants, error bars + 1 standard deviation from the mean, n= 15. 169

List of tables

Table 1.1 Commercially available biomaterials for soft tissue repair. 14

Table 2.1 Crosslinking parameters HMDI concentration read vertically and duration read horizontally. Green ticks indicate variants manufactured, red crosses indicate parameters not manufactured. 25

Table 2.2 Delivery profiles used for each time point and material. 37

Table 2.3 Primary antibodies used for immunohistological staining..... 44

Table 3.1 Relationship of change in lysine / hydroxylysine concentration to HMDI concentration or duration of exposure to HMDI..... 60

Table 3.2 Tukey's post hoc test at 95% level for statistical significance between lysine concentration data sets. Boxes highlighted in red are statistically different means, boxes highlighted in green are statistically similar means..... 61

Table 3.2 (continued) Tukey's post hoc test at 95% level for statistical significance between lysine concentration data sets. Boxes highlighted in red are statistically different means, boxes highlighted in green are statistically similar means..... 62

Table 3.3 Tukey's post hoc test at 95% level for statistical significance between hydroxylysine concentration data set. Boxes highlighted in red are statistically different means, boxes highlighted in green are statistically similar means..... 63

Table 3.3 (continued) Tukey's post hoc test at 95% level for statistical significance between hydroxylysine concentration data set. Boxes highlighted in red are statistically different means, boxes highlighted in green are statistically similar means. 64

Table 3.4 Non-crosslinked collagen matrix AA break down..... 66

Table 3.5 Determination of molecules used in crosslinking reaction. 68

Table 3.6 Collagen denaturation temperature for varying crosslinking levels. 75

Table 3.7 Tukey's post hoc test at 95% level for statistical significance between the denaturation temperature by the number of crosslinks per collagen molecule. Boxes

highlighted in red are statistically different means, boxes highlighted in green are statistically similar means. 78

Table 3.8 Crosslinking variants tensiometry results 81

Table 5.1 Statistical results for semi-quantitative histological scoring, P values determined by general linear model. 160

List of equations

Equation 2.1 equation used for normalising the AA concentrations. 26

Equation 2.2 equation for calculating mean percentage weight of collagen remaining after incubation. 29

Equation 2.3 equation for correcting percentage of collagen remaining allowing for absorption of buffer during incubation. 29

Equation 3.1 Percentage of available lysine and hydroxylysine molecules available for crosslinking. 66

Equation 3.2 Determination of molecules used in crosslinking reaction. 67

Equation 3.3 Linear regression equation for collagen denaturation temperature v's number of crosslinks in material per 1000 AA. 76

1 Introduction

1.1 Collagen

Over 45 types of collagens and collagen like proteins are included in the vertebrate collagen superfamily, 28 which are present in humans [1]–[3]. They can be grouped into 3 main subfamilies; fibrillar, nonfibrillar and novel collagens. The fibrillar collagens (types I, II, III, V, XI, XXIV and XXVII) are of most interest for biomaterials [1], [4]–[6]. Type I is most abundant accounting for up to 90 % of collagen in the body and can be found in many tissues includingskin, tendons, bone, ligaments, vasculature and corneas [7], [8].

Dermal collagen is made up of approximately 97% type I and III collagens and 3% elastin [9]. The natural structure of collagen is maintained by a series of crosslinks. These vary depending on collagen type, this introduction will concentrate on type I collagen.

Collagen is a highly structured material made up of polypeptide (amino acid) chains (figure 1.1). Three AA chains interact with each other to form a collagen molecule. Five of the collagen molecules are organised to form microfibrils. These microfibrils then join together into fibrils, which in turn combine to form collagen fibres.

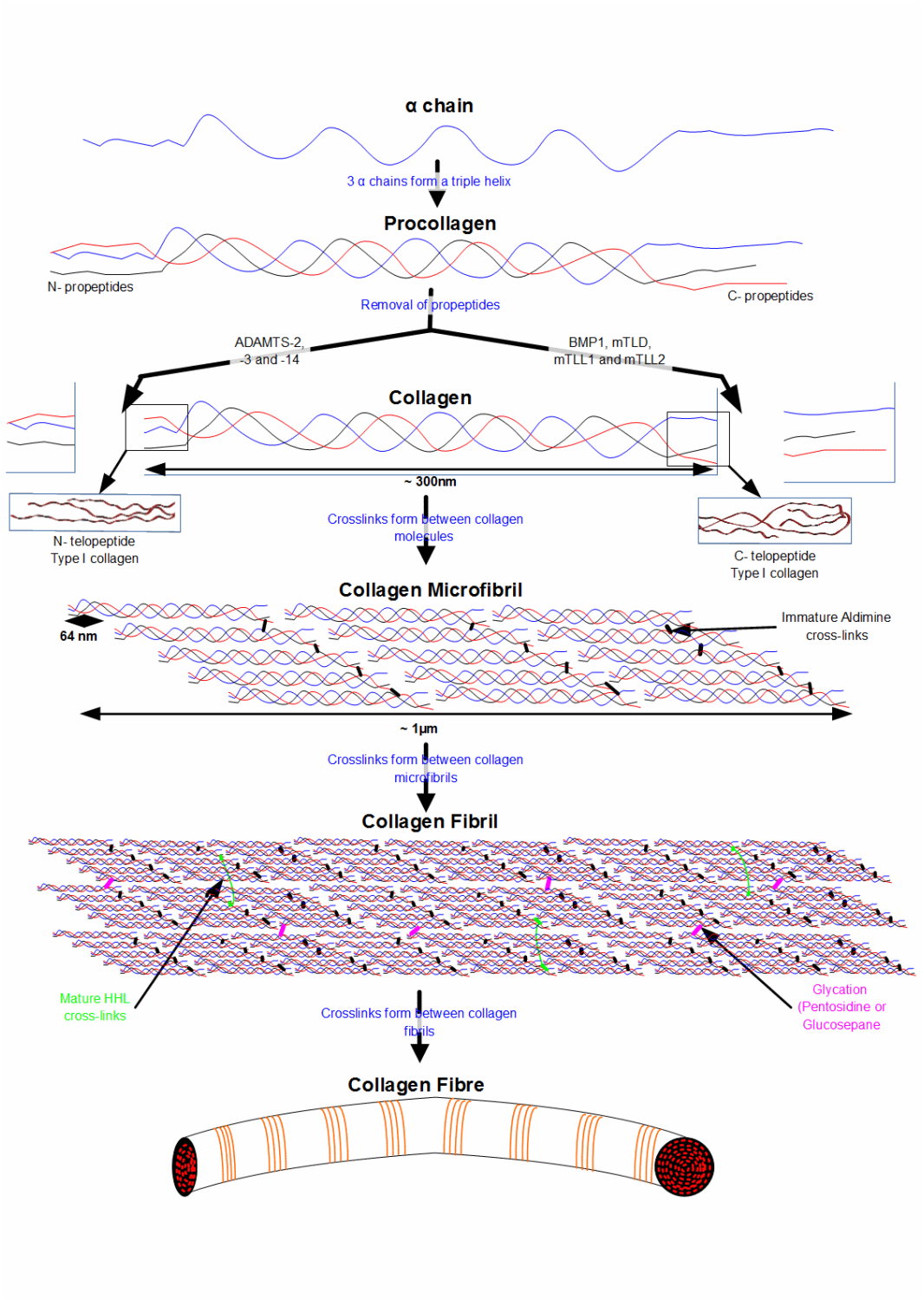

Figure 1.1 Hierarchical structure of collagen from single α chain to collagen fibre

The polypeptide (AA) chains have a central portion that is made up of a repeating sequence, glycine-x-y, where x is normally proline and y is normally hydroxyproline. These chains can either be homotrimeric (3 identical chains) or heterotrimeric (up to 3 different chains) [1], [10], [11]. Porcine dermal collagen is made up of 97% type I (heterotrimer with 2 identical α1 chains and 1 α2 chain) and type III (homotrimeric) [1]. Each procollagen molecule has a triple helix mid-section (figure 1.2) and a propeptide at each end (N-propetide the NH_2 polypeptide chain end and a C-propeptide on the COOH polypeptide chain end). The triple helical mid-section has a right turn with 3.6 residues per turn. In this section the glycine side chain (hydrogen atom) is positioned in the centre of the triple helix, this is the only AA side chain that is small enough to fit in the available space.

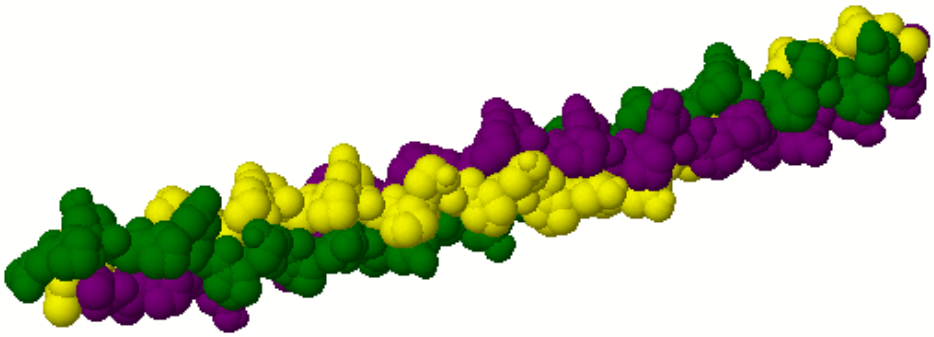

Figure 1.2 Collagen molecule triple helix space fill model after the propeptide ends have been cleaved [12]

Propeptides are naturally enzymatically removed from procollagen molecules (figure 1.3). The N-propetides are removed by multi domain proteins ADAMTS (a disintegrin and a metalloproteinase with thrombospondin motifs), ADAMTS-2, -3 and 14 cleave the N-propetides from type I with ADAMTS-2 cleaving the N-propetides on type III [13]. The C-propeptides of type I and III are removed by

BMP-1 (bone morphagenic protein-1), mTLD (mammalian Tolloid), mTLD-like1 and mTLD-like2, with BMP-1 being the most active [1]. Once the propeptides have been cleaved from the procollagen the collagen molecule (approximately 300nm or 1000 residues long) is left. Each collagen molecule consists of three regions, N-telopeptide, triple helix and C- telopeptide. The telopeptides do not follow the triplet of glycin-x-y as the helical region [14].

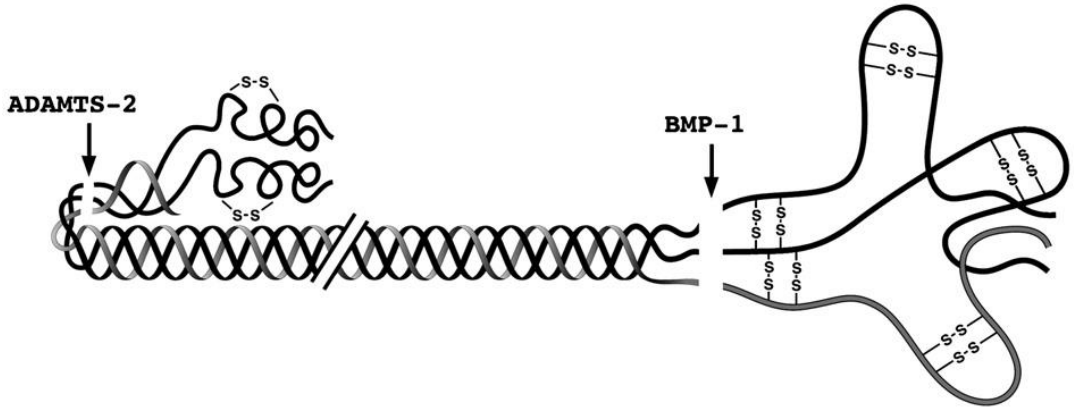

Figure 1.3 Type I procollagen being cleaved by ADAMTS-2 and BMP-1 [10].

Five collagen molecules are joined together by hydrogen bonds and immature crosslinks into microfibrils (figure 1.4). Hydrogen bonds form between the hydroxyl group of hydroxyproline and the carbonyl group of a glycine or between the hydroxyl group and carbonyl group of two hydroxyprolines (figure 1.5).

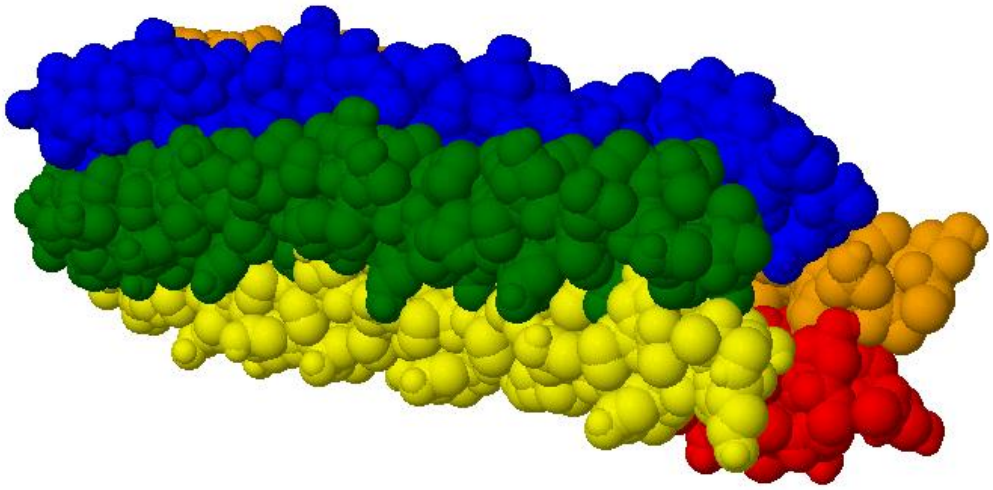

Figure 1.4 Collagen microfibril space fill model (helical portion of 5 collagen molecules) [12].

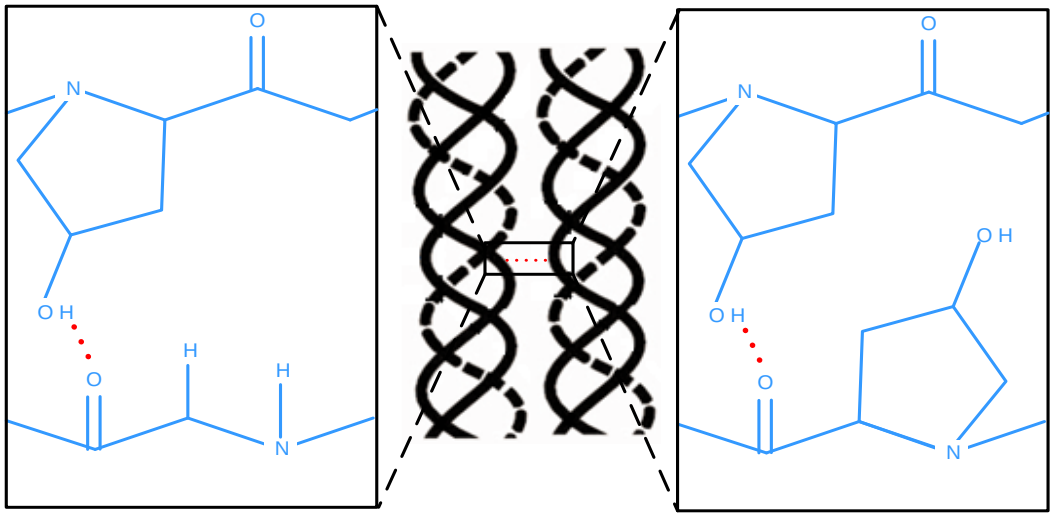

Figure 1.5 Hydrogen bonds between collagen triple helices to help stabilise microfibril and fibril formation.

Immature, reducible crosslinks are initially formed between a lysine side chain on an α1 chain C-telopeptide and a hydroxylysine side chain in the triple helix (on an α1 chain) [15], forming aldimine deH-HLNL (dehydro-hydroxylysinonorleucine), see figure 1.6 [16]. These immature crosslinks are the result of an enzymatic reaction initiated by lysyl-oxidase [17]. These immature crosslinks ensure

molecules are held together in a structured manner with all molecules in a microfibril orientated in the same direction. These immature crosslinks are easily broken by heat and enzyme digestion.

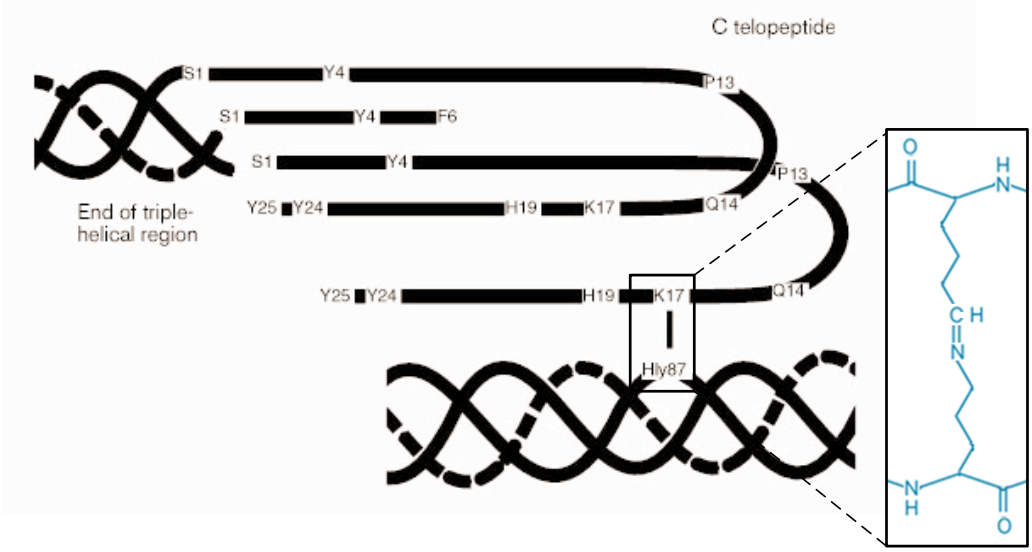

Figure 1.6 Aldimine (immature) crosslink between C-telopeptide and triple helix portions of collagen molecules.

Each collagen molecule is staggered by 67nm[18] (234 residues), the D-period (figure 1.7). The distance between the C terminal of one molecule and the N terminal of the next molecule is 0.54D and the overlap is 0.46D [19]. D-periods can be visualised by SEM photograph, figure 1.8, gaps show up as darker bands and the overlaps showing up as lighter bands.

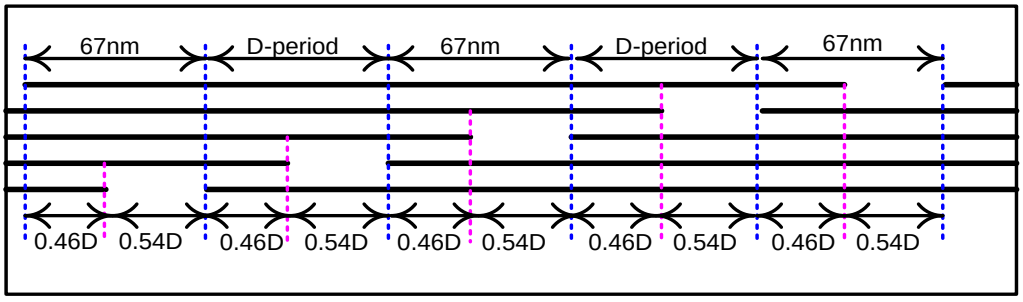

Figure 1.7 Illustration of collagen D-period.

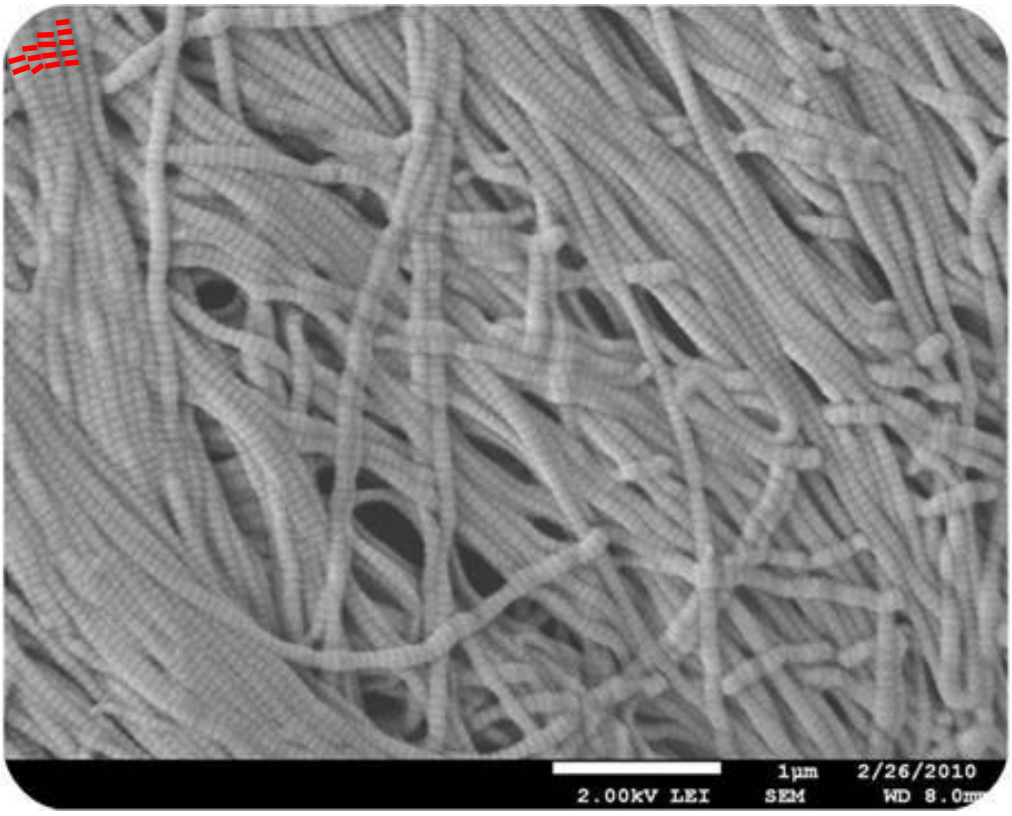

Figure 1.8 SEM photograph of Permacol™ showing collagen fibres with banding from D-period, red highlights in top left corner indicate dark bands caused by gap in D-period.

The aldimine crosslinks can react with a histadine side chain on another triple helix to form the mature trivalent crosslink histidinohydroxylysinonorleucin (HHL) (figure 1.9) [16]. The histadine side group incorporated in the HHL crosslink can form an inter or intra microfibril crosslink. These are non-reducible crosslinks that impart stability to heat and some enzyme degradation to collagenous tissues [20].

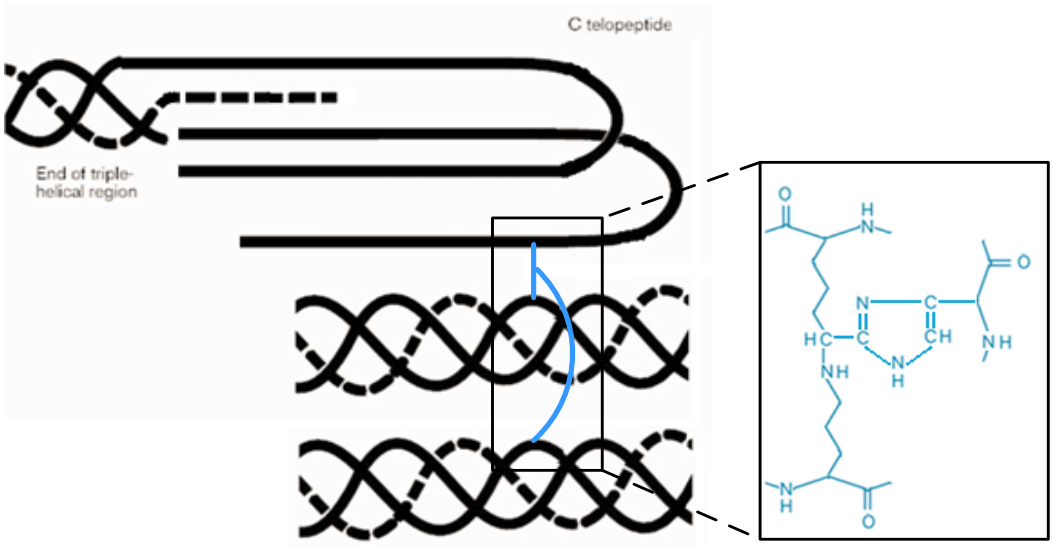

Figure 1.9 HHL (mature) crosslink between C-telopeptide and triple helices of collagen molecules.

1.2 Collagen biomaterials

Biomaterials encompasses a wide range of substrates. In 2009 Williams defined "A biomaterial is a substance that has been engineered to take a form which, alone or as part of a complex system, is used to direct, by control of interactions with components of living systems, the course of any therapeutic or diagnostic procedure, in human or veterinary medicine" [21]. To achieve this goal biomaterials are designed with properties similar to surrounding tissues and the tissue being substituted. For a health care professional to consider using a biomaterial they need to know about biocompatibility, sterility, ease of use, host integration, ease of removal if required, longevity, resulting aesthetic appearance, size or bulk, availability, storage and cost. Collagen based biomaterials have been used for centuries, catgut has been used as a suture since the middle ages [22].

As understanding of biocompatibility and sterilisation increases, the probability of a successful outcome using a biomaterial has increased [22]. Collagen was

considered to be largely nonimmunogenic until 1954 [23]. It is still considered to have low overall immunogenicity, with minimal xenogenicproduction of antibodies against collagen, possibly due to high sequence conservation between species [24]. Telopeptide regions of collagen molecules have the most variability between species, some biomaterials are treated to remove the telopeptide regions with the aim to reduce immunogenicity [25].

1.2.1 **Chemical crosslinking collagen biomaterials**

Collagen can be processed with agents that can form bridges or crosslinks between collagen molecules. These crosslinks can alter the physical properties and immune response to biomaterials produced [26].

1-ethyl-3-(3-dimethyl aminopropyl)carbodiimide (EDC) and *N*-hydroxysuccinimide (NHS) can be used to form a link between carboxylic acid (-COOH) and amine ($-NH_2$) groups (figure 1.10) [27]. Aspartic acid and glutamic acid in collagen molecules terminate in carboxylic acid groups and lysine and hydroxylysine terminate in amine groups. During the reaction EDC reacts with a free carboxylic acid, NHS then reacts with this complex. The 'activated' carboxylic acid molecule reacts with a free amine group to form a crosslink between 2 collagen molecules. Once the reaction is complete a water molecule has been removed from between the carboxylic acid and amine groups of the AA side chains forming a covalent bond [28]. No additional elements are bonded to the collagen matrix. The maximum number of crosslinking sites available in sheep dermal collagen is 20 per 1000 AA [29].

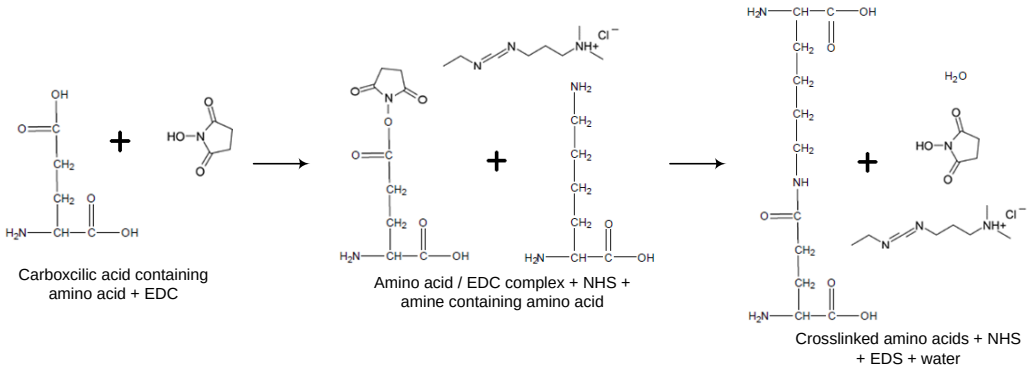

Figure 1.10 Schematic of EDC, NHS crosslinking reaction with collagen molecules.

Gluteraldehyde can be used to form covalent bonds between AA side chains containing amine groups [30]. Figure 1.11 shows the possible reaction pathways the glutaraldehyde can follow. Glutaraldehyde can react with itself as well as collagen therefore a large range of crosslinking reactions are possible. The first step in any of the pathways illustrated is the formation of the Schiff base, which is an unstable compound [31].

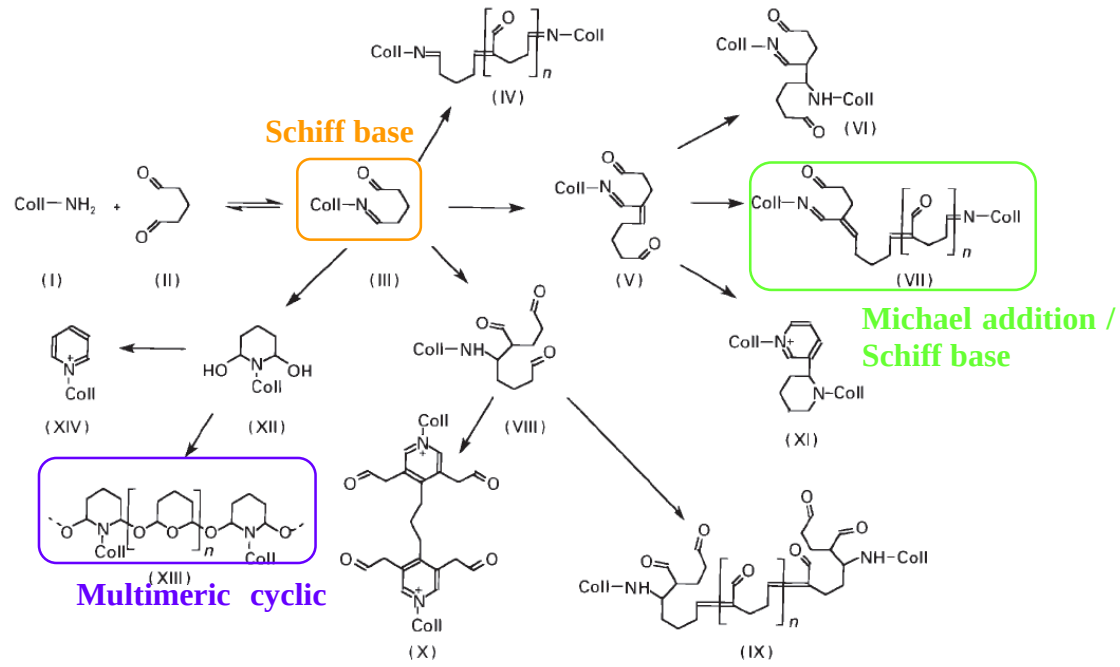

Figure 1.11 Glutaraldehyde crosslinking pathways with collagen [32].

The pH at which the reaction takes place influences the types of crosslinks that are formed. Under acidic or neutral conditions the formation of mono / multimeric cyclic hemiacetal will be formed. Under basic conditions a Michael addition / Schiff base product is most likely to form [31].

4,4'-Methylenebis(cyclohexyl isocyanate) (HMDI) is from the group of compounds that includes superglue, called isocyanates. HMDI has two isocyanate functional groups (R-N=C=O), which react with the amine groups available on the lysine and hydroxylysine AA side chains. The isocyanate functional groups are also highly reactive with water molecules therefore the reaction must take place in the absence of moisture. Figure 1.12 is a schematic of a possible crosslinking reaction with collagen.

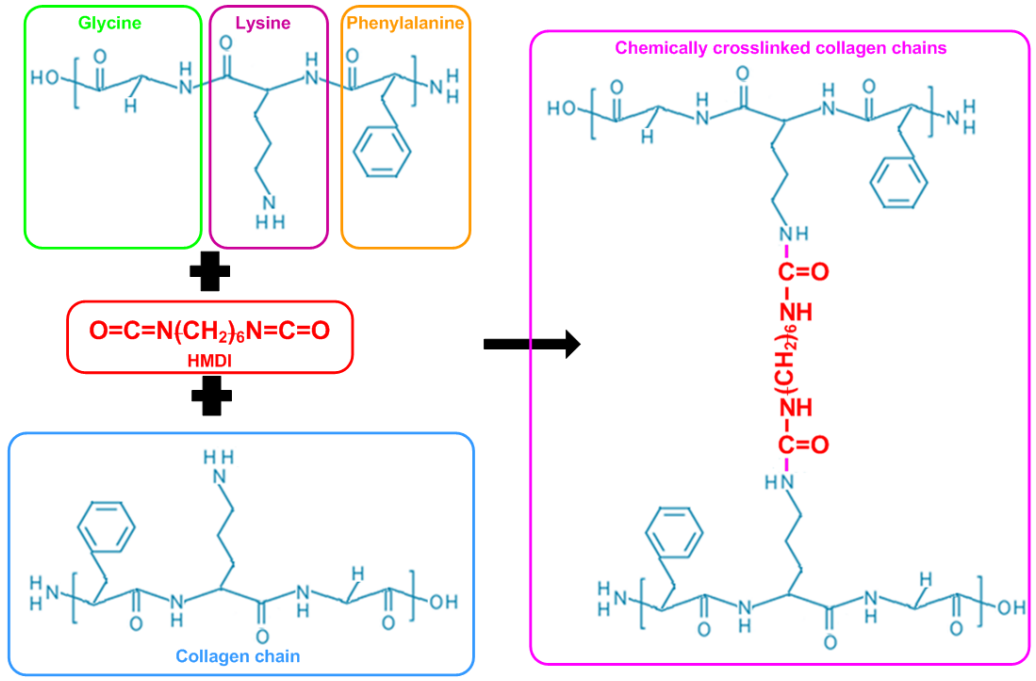

Figure 1.12 Schematic of HMDI crosslinking reaction with collagen.

Genipin is a naturally occurring aglycone derived from geniposide which is a compound present in gardenia fruit [33]. Genipin molecules will react with an amine group on the end of an AA side chain. Two of these genipin / AA complexes will react to form a crosslink between the two collagen chains (figure 1.13). Genipin has a similar crosslinking reaction to gluteraldehyde but is less immunogenic [34].

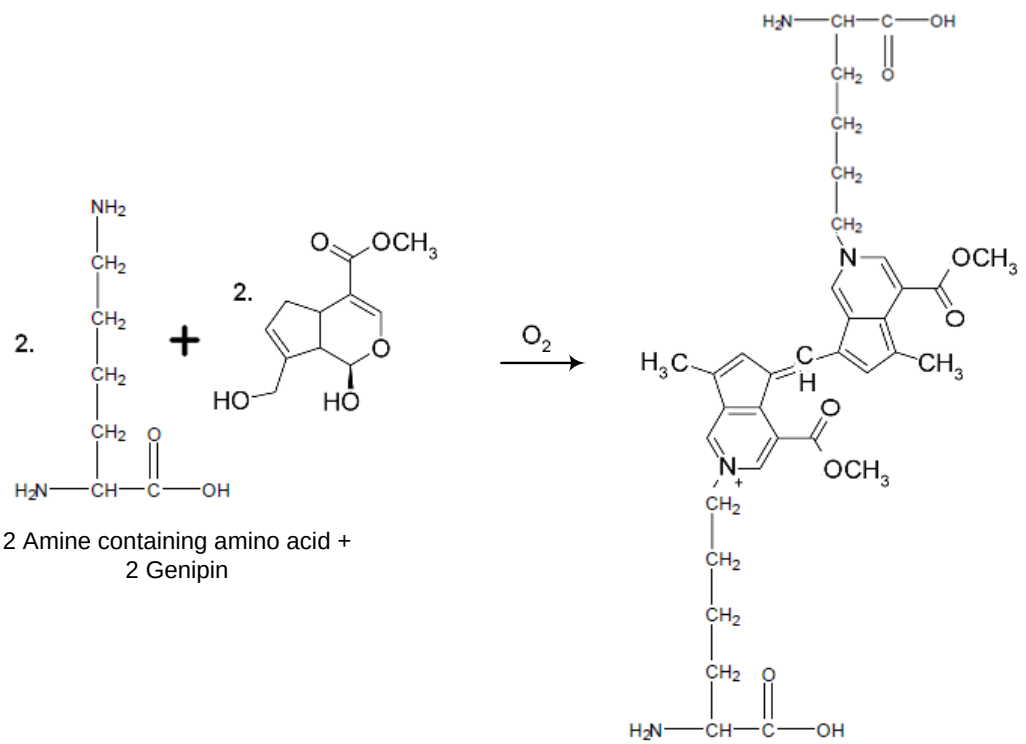

Figure 1.13 Genipin crosslinking reaction with collagen.

1.2.2 **Soft tissue repair**

Surgeons would ideally repair or replace damaged tissue with an identical tissue completely restoring its structure and function. However, due to a lack of available transplant materials many surgeons use prosthetic scaffolds. A wide range of scaffolds are available being made from synthetic fibres, allogenic tissue, xenogenic tissue or a combination of materials. Table 1.1 lists some of the currently commercially available biomaterials indicated for soft tissue repair.

Table 1.1 Commercially available biomaterials for soft tissue repair.

Product	**Manufacturer**	**Source Material**	**Crosslinked**	**Regulatory Approval**
Peri-Guard	Synovis	Bovine Pericardium	Yes (Gluteraldehyde)	510(k) & CE
ProPatch	Cryolife		No	510(k)
Veritas	Synovis		No	510(k) & CE
SurgiMend / Xenform	TEI Biosciences	Fetal Bovine Dermal Collagen	No	510(k)
Alloderm	LifeCell	Human Dermis	No	AATB
DermMatrix	Kensey Nash		No	AATB
FlexHD	MTF (Ethicon)		No	AATB
NeoForm	Tutogen (Mentor-breast)		No	AATB
MatriStem	ACell	Porcine bladder tissue	No	510(k)
Inforce	Integra	Porcine Derived Tissue	Yes (Carbodiiamide)	510(k)
CollaMend	Davol / Bard	Porcine Dermis	Yes (EDC)	510(k) & CE
Permacol™	Covidien		Yes	510(k) & CE
Strattice	LifeCell		Yes (HMDI)	510(k) & CE
XCM	Kensey Nash		No	510(k)
Meso Biomatrix	Kensey Nash	Porcine Mesothelium ECM	No	510(k)
Surgisis® / Biodesign	Cook	Porcine SIS	No	510(k) & CE

1.3 Immune response

The immune response is a biochemical cascade involving a significant number of different cell types and molecules providing protection against foreign bodies and infection. The immune response has two pathways, innate and adaptive systems.

The innate immune system is always present within the body and the body's first line of defence against pathogens and foreign bodies. Phagocytes, natural killer cells and the complement system offer a non-specific response to invasion. If the innate response is unable to eliminate the threat it may form a stimulus for the adaptive immune system [35]. The adaptive immune system is a specific response triggered by exposure to foreign antigens. Cell mediated immunity activates T lymphocytes and cytokine release. B lymphocytes are involved in humoral immunity producing antibodies to the antigens presented. Some cells presenting the antibodies remain in the body providing an immunological memory helping safeguard against future attacks. Cells of the immune system originate from bone marrow, stem cells commit to either myeloid or lymphoid lineage. Figure 1.14 shows the cells and proteins involved in adaptive and innate immune systems.

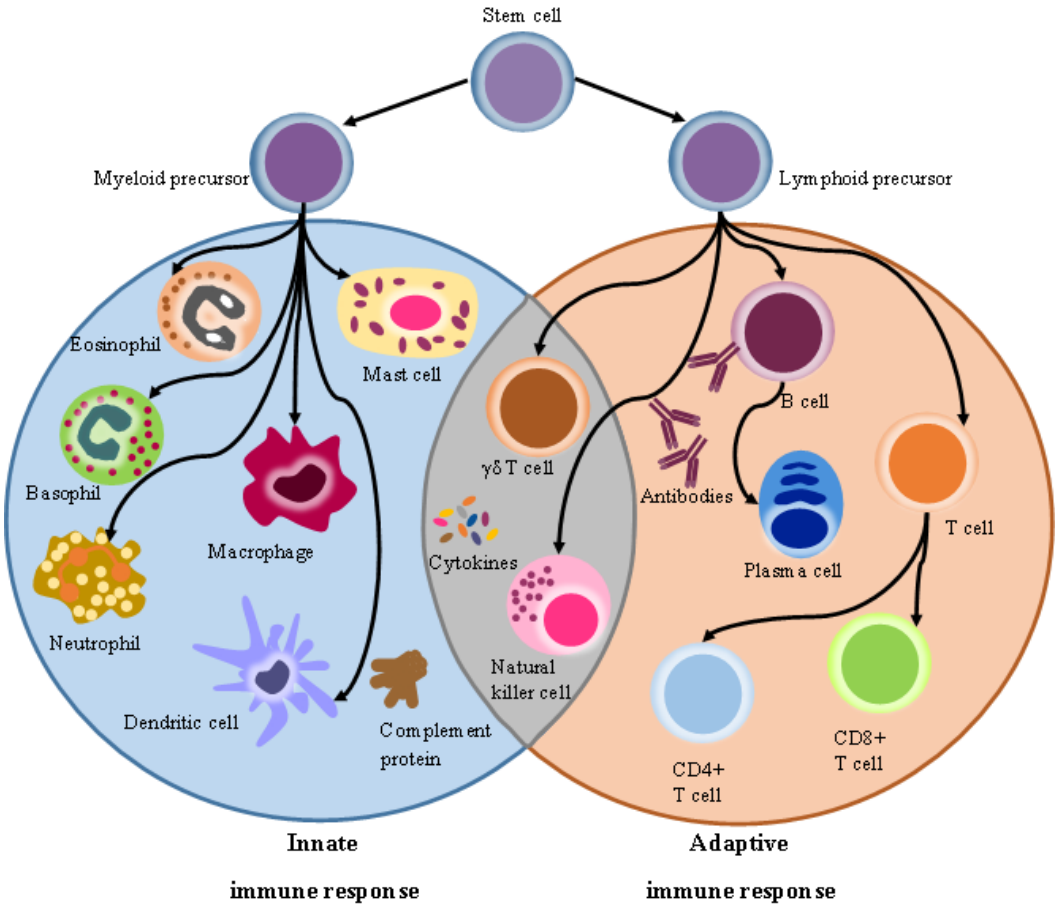

Figure 1.14 *Cells and proteins of the innate and adaptive immune systems (based on Dranoff 2010* [36]*).*

All procedures where biomaterials are implanted initiate an immune response from the initial trauma of surgery and the implantation of a material [37]. Rather than aiming to implant a completely inert material, the immune response can be used to advantage improving integration thus increasing the strength of the repair [38].

1.3.1 **Cells of the immune response**

Neutrophils, basophils, eosinophils and mast cells belong to the granulocyte class of leucocytes. These cells have intracellular granules containing, enzymes, cytokines, cytotoxic proteins and unstable chemical intermediate molecules [39], [40]. Granulocytes can release the contents of their granules to assist in the

elimination of microbes. Granulocytes perform an intrinsic role in the innate immune response.

Neutrophils are present in relatively large numbers making up 40-75% of circulating white cells [41]. Neutrophils are the first cells to migrate from the blood to sites of injury and infection, moving faster than other leucocytes. They originate from precursors in bone marrow and can be reproduced rapidly and are relatively short lived cells. Neutrophils contain two types of granules, the first type are slightly larger and contain lysozyme, lysosomal enzymes, peroxidase and cationic proteins, the second slightly smaller granules contain lysozyme, alkaline phosphatase and lactoferrin [42]. Along with degranulation neutrophils can phagocytose microbes.

Basophils are rare, generally less than 1% of circulating white cells and are mainly concerned with acute allergic reactions. Their mode of action is via degranulation, releasing histamine and cytokines [41].

Eosinophils are present in low numbers 1-6% of circulating white cells. Upon degranulation they release histamine, enzymes, growth factors and cytokines. They are involved in the destruction of parasites which are too large for phagocytosis.

Mast cells are rare in circulation normally they are found in the connective tissue surrounding small blood vessels. Their granules contain histamine, enzymes and heparin. They play an important role in early acute inflammation. Chemicals (including trypsin, venoms and immunoglobulins) and physical injury can cause degranulation.

Macrophages and dendritic cells develop from monocytes and are present in all tissue in the body. Macrophages focus on tissue integrity, dendritic cells on initiating tissue immune responses[43]. To achieve this they share much of the same functionality including T-cell activation, antigen presentation, cytokine release, phagocytosis and cytotoxicity [44]. In addition macrophages are involved in fibrosis and tumor infiltration, whereas dendritic cells are involved in tolerogenesis.

Tissue macrophages are involved in the remodelling and repair of tissues after inflammation, clearing foreign and damaged cells by their phagocytic function [43], [45]. When macrophages detect invading molecules they release proteins and reactive oxygen species recruiting a lymphocyte response where required.

Natural killer (NK) cells are found in the circulatory system and tissues. They target and kill certain virally infected cells and tumour target cells [46]. Upon contact with targeted cells, granules secreting lysozymes containing perforin are released causing target cell apoptosis. NK cells also secrete certain cytokines that help in the regulation of cell populations during inflammation [47].

Unlike many other inflammatory response cells NK cells do not require sensitisation for activity. However dendritic cells can stimulate them and signal T or B cells [48].

Cytokines play a role in the adaptive and innate immune responses. Cytokines are small proteins that are either secreted, expressed on cell membranes or contained within extracellular matrix [49]. These cytokines interact with receptors on cells coordinating the host's immune response. Cytokines are communicators between cells of the immune system, having many complex actions and interactions, these interactions can be antagonistic, additive or synergistic [50]. Cytokines can be split

into 4 main groups, interlukins (IL), interferons (IFN), tumour necrosis factor (TNF) and transforming growth factor (TGF).

Cells of the adaptive immune response, immature T cells differentiate into either T-helper (Th1 / Th2) cells (CD4+) or cytotoxic T cells (CD8+). This differentiation is triggered when T-cell receptor (TCR) interacts with major histocompatibility complex (MHC) displaying an antigen fragment. Class I MHC molecules, found on all nucleated cells, display intracellular peptides causing differentiation into CD8+ cells. CD8+ cells release perforin and granzyme causing target cell apoptosis. Class II MHC molecules, found on dendritic cells, B cells and macrophages, display extracellular peptides causing differentiation into CD4+ cells [41]. CD4+ cells can be split further into Th1 and Th2, Th1 cells secrete cytokines responsible for macrophage activation and delayed type hypersensitivity. Th2 cells secrete cytokines influencing the production and maturation of B cells into plasma cells [51], see figure 1-15.

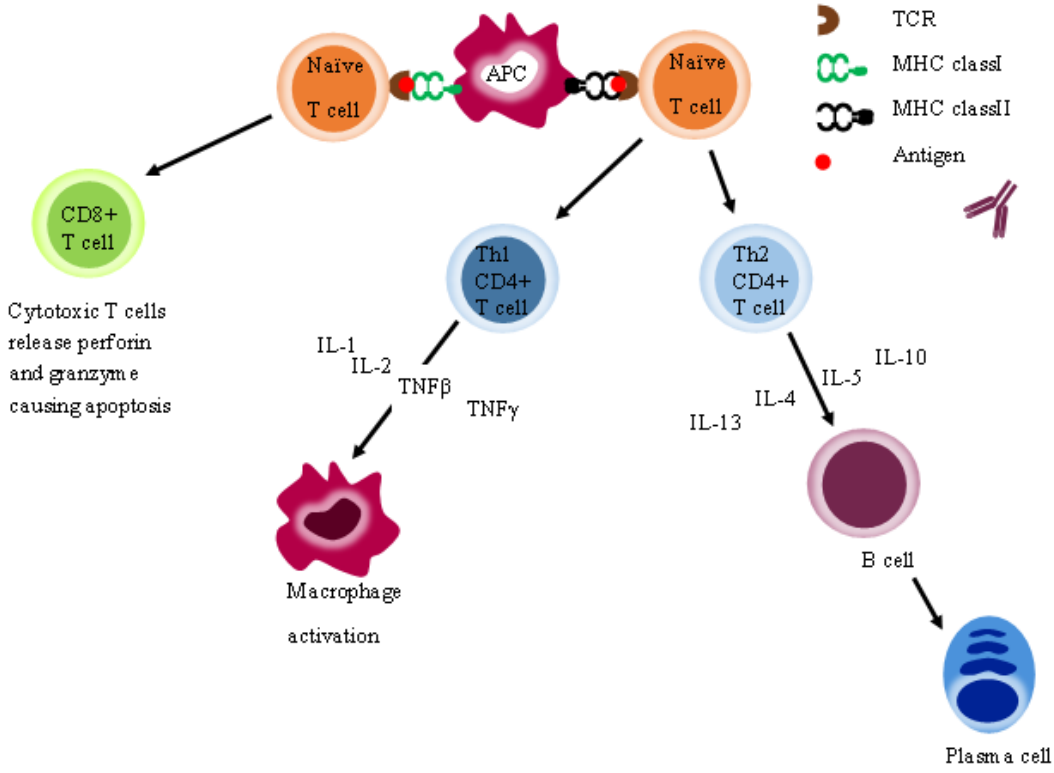

Figure 1.15 *T cell activation and differentiation into cytotoxic T cells (CD8+) and T helper (Th) cells (CD4+). Cytokines produced by Th cells and there role in immune cell activation.*

The complement system consists of a group of more than 30 membrane associated or soluble proteins. These proteins can be activated by 3 different pathways, alternative-triggered by pathogen surfaces, classical-triggered by antigen antibody complexes or lectin-triggered by bacterial surfaces. Upon activation an enzyme cascade is initiated resulting in anaphylatoxins. Anaphylatoxins are responsible for a range of responses including host cell recruitment, especially neutrophils, lysis of bacterial cell membranes by membrane attack complex and release of histamine from mast cells [52].

1.3.2 **Wound healing**

Wound healing is the process by which hosts repair injured tissue, with the objective to restore tissue surface integrity and tensile strength of tissues. Two degrees of wound healing exist, primary intention where the wound edges can be brought together and secondary intention where significant tissue loss has occurred and the wound edges cannot be brought together, instead the defect is bridged over time by wound contraction and scar tissue [42]. Wound healing process is independent of wound size, starting with the coagulation cascade forming a platelet clot with fibrin. Next is the inflammation phase with cytokines and growth factors being released causing cell proliferation and recruitment to the wound site. Neutrophils and macrophages clean the site of debris, bacteria and damaged tissue. Fibroblasts and epithelial cells are recruited to the wound site converting the clot into vascularised granulation tissue. During maturation wound tensile strength increases as type III collagen is converted into type I collagen [53], [54].

1.3.3 **Biomaterials and wound healing**

Biomaterials are used for the replacement and repair of tissue, implantation of these materials inevitably results in host tissue injury. When biomaterials are used, normal wound healing is affected provoking a prolonged inflammatory response known as foreign body reaction [55], consisting of acute and chronic inflammatory phases resulting in remodelling and tissue healing [56].

Initially plasma proteins are absorbed onto the biomaterials surface, these include fibronectin, complement, vitronectin and albumin. These proteins modulate the interaction and adhesion of cells from the innate and adaptive immune response. As with normal wound healing neutrophils are initially recruited to the wound site

and attempt to phagocytose the biomaterial resulting in “frustrated” phagocytosis [57]. Monocytes migrate to the wound site and differentiate into macrophages and adhere to the biomaterials surface, causing degradation of the biomaterial. When multiple macrophages come into contact they have the ability to fuse forming foreign body giant cells [56]. The foreign body reaction results in either the formation of a dense fibrotic tissue surrounding the biomaterial or degradation of the biomaterial [58].

Implantation of biomaterials will elicit a host response and normal wound healing from disruption of surrounding tissue and a foreign body reaction induced by the biomaterial itself. An adequate inflammatory response is essential to enable normal wound healing resulting in renewed tissue integrity and tensile strength. However, a prolonged inflammatory response, foreign body reaction or encapsulation of biomaterials is undesirable, as this could ultimately result in failure to regain tissue integrity and tensile strength. Understanding the host immune response in relation to the addition of chemical crosslinks to biomaterials will allow developments in biomaterial design.

1.4 Thesis Aims and Objectives

The overall aim of this research was to investigate the addition of chemical crosslinks into a tissue derived decellularised collagen biomaterial. Specifically, how the crosslinks affect the biomaterial's biophysical properties and immune response.

The aims of this research were achieved by the following investigations:

i. Characterisation of the biophysical properties of biomaterials prepared using various crosslinking reactions with HMDI (Chapter 3).

ii. Assessment of how biomaterial crosslinking affects leukocyte activation, using an *in vitro* reactive oxygen species assay (Chapter 4).

iii. Examine how biomaterial crosslinking affects the immune response, using an *in vivo* rat model (Chapter 5).

2 Materials and Methods

2.1 Acellular porcine collagen scaffold preparation

Porcine skin (Cheale meats Ltd, UK) was harvested and a layer of dermis approximately 1.5 mm thick was sliced out of the hides. Dermal sheets were stored at -20°C in saline until required. Sheets were defrosted, decellularised and defatted using the proprietary Permacol™ process with the exception of the hexamethylene diisocyanate (HMDI) (Sigma-Aldrich, UK) crosslinking step.

The quantity of HMDI added to acetone varied from 0 ml/kg of collagen to 200 ml/kg of collagen for the crosslinking reaction. Duration of exposure to HMDI varied from 30 minutes to 50 hours. Table 2.1 lists the 25 crosslinking variants produced, indicated by the green ticks.

Following crosslinking, sheets were packaged in foil pouches and sterilised using gamma irradiation doses between40-41 kGy (Instron, UK). Once sterilised, sheets were stored at room temperature until required.

Table 2.1 Crosslinking parameters HMDI concentration read vertically and duration read horizontally. Green ticks indicate variants manufactured, red crosses indicate parameters not manufactured.

		HMDI concentration (ml/kg collagen)									
		0	0.2	1	2	4	10	20	50	100	200
Crosslinking duration (Hours)	0.5	✓	✗	✗	✓	✗	✗	✗	✗	✗	✓
	1	✗	✗	✗	✓	✗	✗	✗	✗	✗	✗
	2	✗	✗	✗	✓	✗	✗	✗	✗	✗	✗
	3	✗	✗	✗	✓	✗	✗	✗	✗	✗	✗
	19	✗	✗	✗	✓	✗	✗	✗	✗	✗	✗
	20	✓	✓	✓	✓	✓	✓	✓	✓	✓	✓
	21	✗	✗	✗	✓	✗	✗	✗	✗	✗	✗
	45	✗	✗	✗	✓	✗	✗	✗	✗	✗	✗
	48	✗	✗	✗	✓	✗	✗	✗	✗	✗	✗
	50	✓	✗	✗	✓	✗	✗	✗	✗	✗	✓

2.2 Biophysical characterisation techniques

2.2.1 Amino acid analysis

3 mg of all materials were weighed into Pyrex™ 16x150mm heavy wall glass tubes. To each sample 2ml 5.8M constant boiling HCl (equal amounts of concentrated HCl (Sigma-Aldrich, UK) and dd H_2O) was added. A restricted neck was manufactured at the top of the tubes, each tube was connected to a vacuum line and the contents frozen by immersing the base of the tubes in liquid nitrogen (BOC Industrial gasses, UK). Vacuum was applied and samples were subjected to

(nominally) three freeze / thaw cycles to remove as much dissolved gas as possible. Following the final thaw cycle, tubes were placed in an ultrasonic water bath (VWR International, UK) until no more gas release was observed. The tubes were sealed by closing the restricted neck, whilst maintaining the vacuum. Hydrolysis was performed by placing the tubes in a heating block (Varian Inc, UK) at 110°C for 24 hours. Following hydrolysis, the top of the tube was sheared and the acid removed in a heated centrifugal evaporator. The samples were resuspended in 0.1M HCl, for analysis.

AA were separated using high performance liquid chromatography (HPLC) using a sodium buffer. Detection of the AA compounds was performed by UV/Vis detector following derivatsation with ninhydrin.

AA analysis of the samples was performed at Alta Bioscience (University of Birmingham).

In order to perform direct comparisons between samples the g/100g results are 'normalised' by Equation 2.1.

Equation 2.1 equation used for normalising the AA concentrations.

$$\frac{Individual\ amino\ acid\ result\ (g/100g)}{Total\ amino\ acids\ result\ (g/100g)} = Normalised\ amino\ acid$$

2.2.2 **Thermal stability of crosslinked material**

Into a 40µl aluminium crucible with lid (Mettler-Toledo, Switzerland) 9 – 11 mg of sample was weighed. Crucible and lid were placed into a crucible sealing press and plunger depressed; this cold welded the lid to the pan forming a hermetic seal.

The Mettler-Toledo DSC 821e (Mettler-Toledo, Switzerland) with liquid nitrogen cooling was used to analyse the samples. The DSC furnace takes two crucibles, sample pan and an empty hermetically sealed pan as a reference. All samples were run with nitrogen as a purging gas. The DSC was calibrated during each run using indium (Sigma-Aldrich, UK), using dynamic conditions starting at 145°C rising to 165°C at 3°C a minute, the peak was expected at 156°C. Figure 2.1 is an example indium calibration profile.

The calorimetric measurements for the samples were obtained under dynamic conditions starting at 30°C rising to 80°C at 3°C a minute. Denaturation temperature (Td) of the samples was calculated by Mettler Toledo STAR^e System software (Mettler-Toledo, Switzerland).

Material containing more natural or artificial crosslinks will have a higher denaturation temperature than a material with fewer natural or artificial crosslinks.

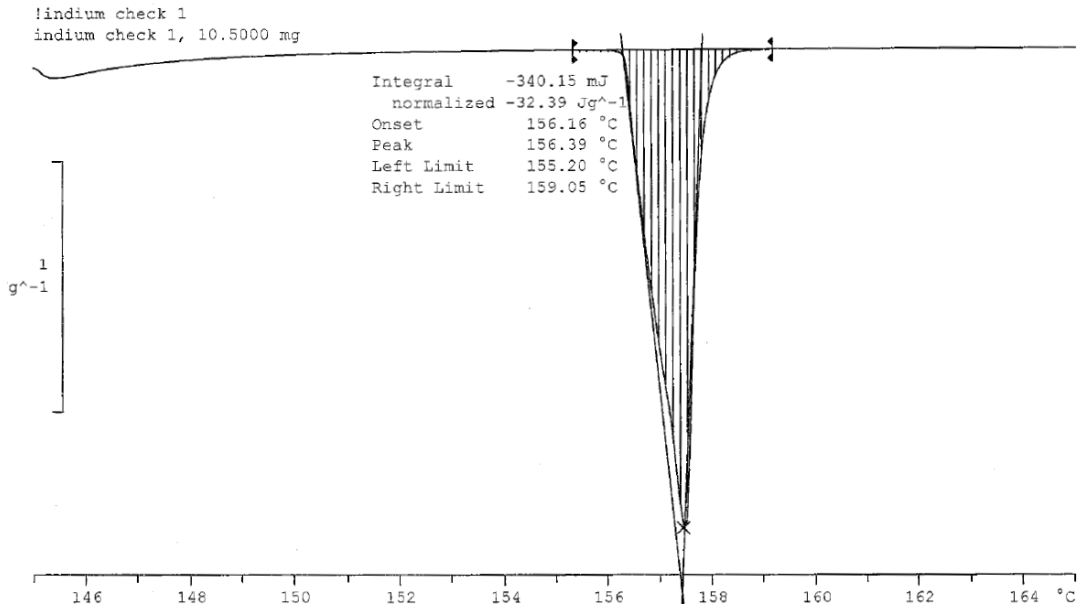

Figure 2.1 DSC profile, temperature (°C) vs heat flow, of indium from Mettler-Toledo DSC 821e processed using STARe System software.

2.2.3 **Collagenase assay**

Six samples weighing approximately 1g of each crosslinking variant were placed in an appropriately labeled falcon tube and covered with sterile saline. A positive control was prepared; the control consisted of a sheet of Permacol™ that had been placed in a beaker of boiling water for 20 minutes to denature the collagen molecules. A 0.05% w/v ovalbumin in 0.1M phosphate buffer was prepared by dissolving 25 0.1M phosphate buffer saline (PBS) tablets (Sigma-Aldrich, UK) in 500ml of ddH_2O. Once dissolved, 250mg ovalbumin (Sigma-Aldrich, UK) was added and the pH adjusted to 7.4 using 2M sodium hydroxide (Sigma-Aldrich, UK). This buffer was then used to prepare the collagenase solution at 165U/ml, collagenase was isolated from Clostridium histolyticum (Sigma-Aldrich, UK).

All samples and control pieces were blotted dry, weight recorded and transferred to individual tubes. To 5 pieces of each sample / control tubes 10ml of collagenase

buffer was added, to the remaining tube 10ml of 0.05% w/v ovalbumin in 0.1M phosphate buffer was added, acting as a negative control. All samples were incubated at 37°C ± 3°C for 22 hours ± 5 minutes.

Upon completion of the incubation the excess moisture was removed from each piece and its weight recorded.

The mean percentage weight of collagen remaining in each tube after incubation was calculated by Equation 2.2.

Equation 2.2 equation for calculating mean percentage weight of collagen remaining after incubation.

$$\frac{Final\ collagen\ weight\ (g)}{Intital\ collagen\ weight\ (g)}\ X\ 100 = \%\ Weight\ remaining$$

To take into account absorption of the buffer during incubation, % weight remaining for each sample that was incubated with collagenase buffer was corrected using equation 2.33.

Equation 2.3 equation for correcting percentage of collagen remaining allowing for absorption of buffer during incubation.

$$\frac{\%\ weight\ remaining\ (incubated\ with\ collagenase\ buffer)}{\%\ weight\ remaining\ (incubated\ with\ blank\ buffer)}\ X\ 100$$

$$= Corrected\ \%\ Weight\ remaining$$

The average corrected percentage weight remaining of each set of replicates was calculated by adding the corrected % weight remaining for each replicate together (excluding the blank) and dividing by the number of replicates (5).

2.2.4 **Uniaxial tensile testing**

Uniaxial tensile testing was carried out on an Instron 5965 (Instron, UK) tensiometer with pneumatic grips attached to a 1kN load cell. Dog bone shaped samples as illustrated in figure 2.2 were used. The sample dog bone was clamped vertically in the pneumatic grips of the tensiometer. A pre load of 0.001N was applied to the sample; the grips were then separated at a rate of 10mm/min until sample failure. The stress strain curve was recorded and the ultimate tensile strength (UTS) and modulus were recorded, Bluehill version 2.0 software (Instron, UK) was used to acquire and analyse the data. If the sample slipped from the grips the results were not used.

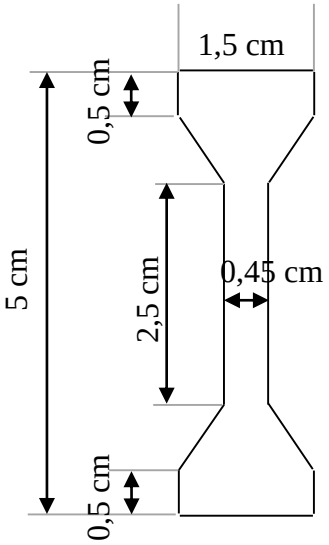

Figure 2.2 Dog bone dimensions used in uniaxial tensile test.

2.2.5 **Ball burst tensile testing**

Ball burst testing was performed based on ASTM standard D3787: Burst strength of textiles. Due to the amount of material available the test apparatus and sample size were scaled down.

Analyses were performed on a Nene M2 tensile tester (Nene Instruments Ltd., UK) in compression mode. A probe with a spherical tip ¼″ diameter was attached to either a 500N or 5KN load cell. A sample holder with a 1.3cm diameter hole in the middle was attached to the base plate. The samples were secured between 2 pieces of 80 grit sand paper with ID 1.3cm and OD 3.5cm (Figure 2.3).

A 2.5 x 2.5 cm sample was cut from a sheet, the thickness of sample was measured using callipers in 3 places across the sample. The square of material was then secured in the sample holder. The probe travelled towards the sample at 10mm/min until a 0.1N load was reached triggering data acquisition. Once triggered, the height was set to zero and the probe continued to travel at a rate of 10mm/min until the sample failed. The load and displacement at peak and yield were recorded, along with Youngs modulus, calculated by Nene software (Nene Instruments Ltd., UK).

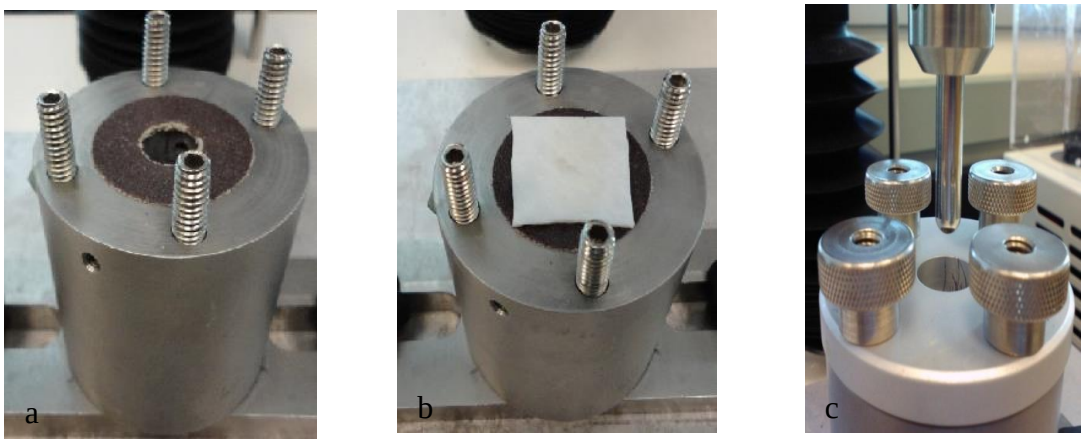

Figure 2.3 Ball burst test set up, picture a sand paper placed over fixture, picture b specimen placed on top of fixture and picture c specimen secured by circular plate, spherical probe in position.

2.3 *In vitro* reactive oxygen species testing

The Able® cell activation test kit (Knight scientific, UK) for whole blood or isolated cells with Pholasin® and Adjuvant-K™ was used to assess leukocyte activation. All reagents and substrates were reconstituted using the instructions supplied by the manufacturer.

Material was cut into 6.5mm discs which were added to the bottom of each well of a white 96 well microtiter plate. Then 90µl reconstitution and assay buffer, 20µl adjuvant-K and 50µl pholasin were added to each well [59]. Immediately after collection via finger prick, whole blood was diluted 100 fold with blood dilution buffer and 20µl was added to the appropriate wells. The 96 well plate was transferred to a FLUOstar OPTIMA plate reader (BMG LABTECH, Germany) and fluorescence was continuously measured for 150 cycles (approximately 194 minutes).

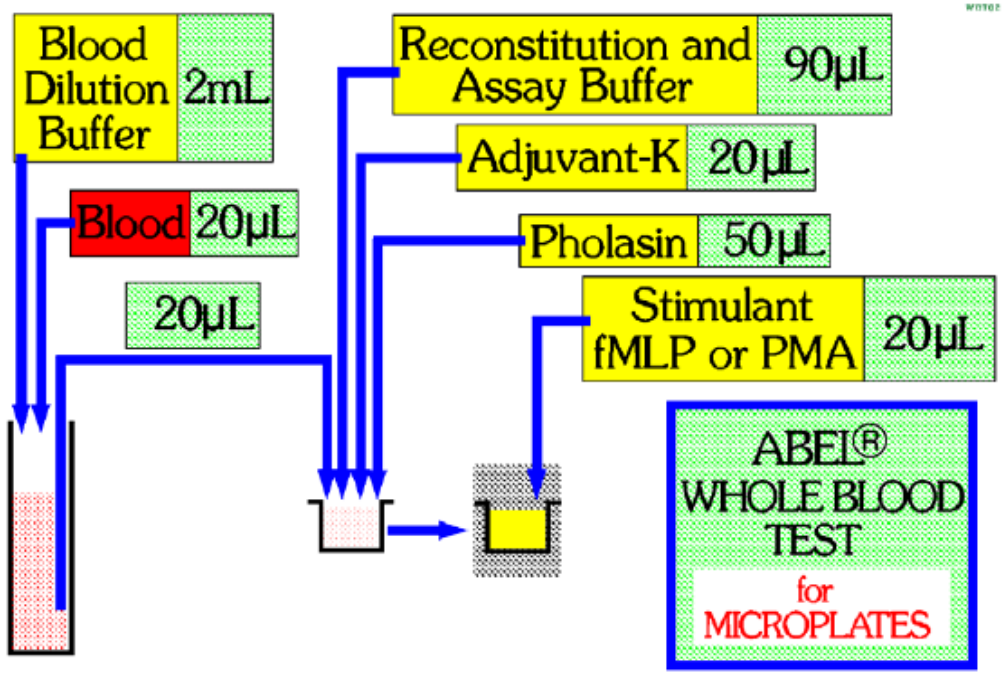

Figure 2.4 Reagents used in leukocyte activation test[59].

After 100 cycles (approximately 129 minutes) 20µl of fMLP (formyl-methionyl-leucyl-phenylalanine) was injected into each well, this solution was added as a positive control to prove any leucocytes present could be activated. After 125 cycles (approximately 161 minutes) 20µl of PMA (phorbol-myristate-acetate) was injected as a second positive control to allow degranulation and deduce the maximum extent of remaining ROS within each well.

2.4 *In vivo* immune response testing

2.4.1 Animal model

Collagen sheets were cut into 1cm squares in a class II cabinet and stored in sterile phosphate buffer saline until implantation. Only non crosslinked collagen (0 ml HMDI/kg collagen for 0.5 hours), Permacol™ (2 ml HMDI/kg collagen crosslinked for 20 hours) and 200 ml HMDI/kg collagen crosslinked for 50 hours were implanted.

Six week old male Wister rats weighing 250-270g were administered an equal ratio of O_2/N_2O supplemented with isoflurane (2-chloro-2-(difluoromethoxy-1,1,1-trifluoro-ethane) at 2% (v/v) as an inhalation anaesthetic. Once subjects were sedated (confirmed by absence of a pedal withdraw reflex) the incisional area was shaved and sterilised by swabbing using standard surgical iodine and pain relief (buprenorphine) was administered. A prophylactic antibiotic (baytril) was administered by subcutaneous injection. A 1.5cm long cutaneous incision was made in the centre of the subjects' dorsal side. Using the single incision 4 subcutaneous channels were created by blunt dissection, such that channels terminated approximately above each shoulder and hip. The materials were inserted into these channels one per channel following the randomised delivery schematic (Figure 2.5and Figure 2.6). Profiles used for each material and time point are listed in table 2.2. The wound was closed using 3 interrupted sutures (Polysorb 5-0, Tyco, USA).

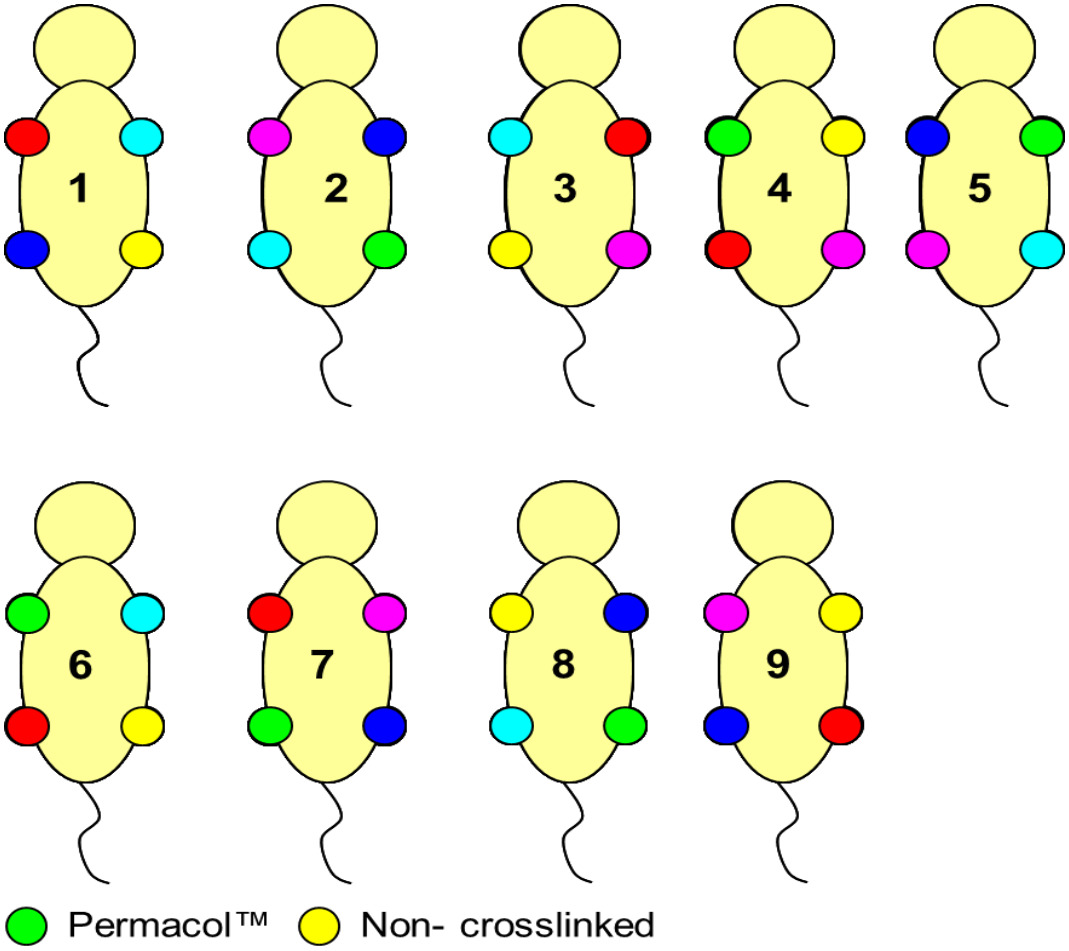

Figure 2.5 Randomised Delivery Schematic for Subcutaneous Implantation of Non crosslinked collagen and Permacol™. Red, pink and blue circles represent other biological materials that were implanted at the same time, data not included.

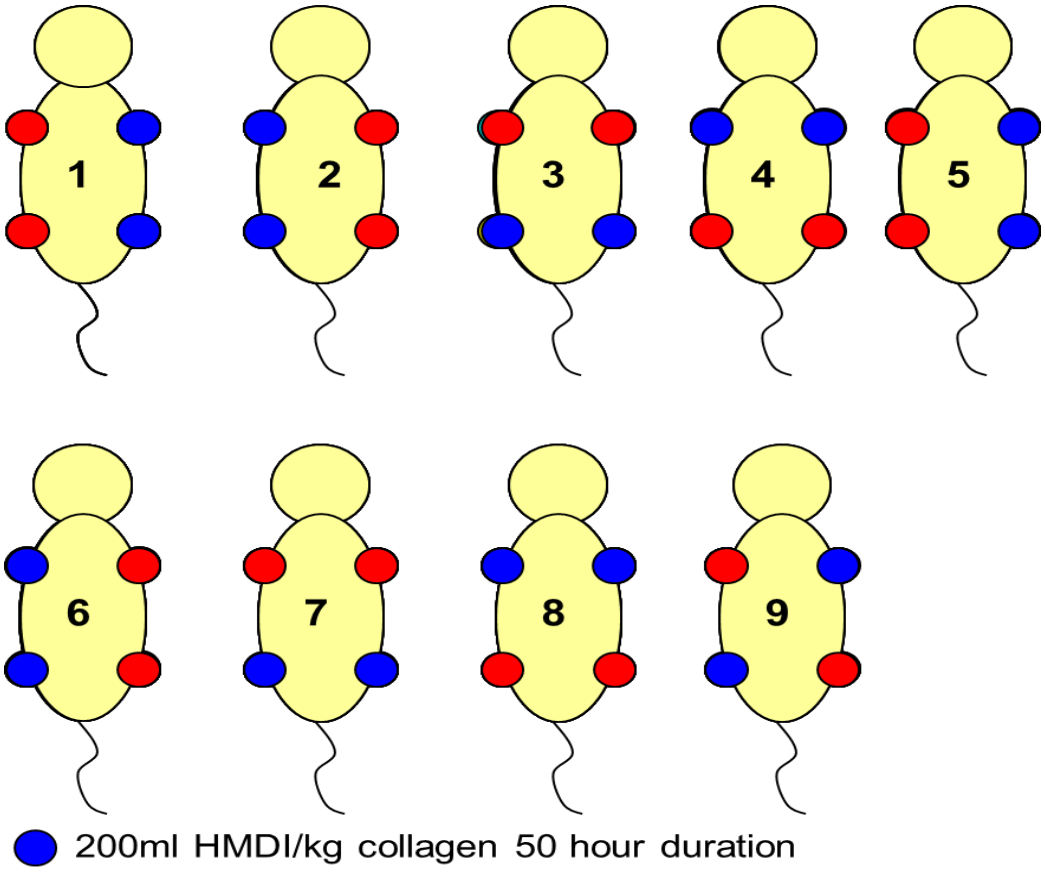

Figure 2.6 Randomised Delivery Schematic for Subcutaneous Implantation of collagen crosslinked with 200ml HMDI/kg collagen for 50 hours. Red circles represent other biological materials that were implanted at the same time, data not included.

Table 2.2 Delivery profiles used for each time point and material.

		Time point (days)			
Material	Schematic (Figure)	2	7	14	28
Non crosslinked	2.5	1, 3, 4, 6, 8, 9	1, 3, 4, 6, 8, 9	1, 3, 4, 6, 8, 9	1, 3, 4, 6, 8, 9
Permacol™	2.5	2, 4, 5, 6, 7, 8	2, 4, 5, 6, 7, 8	2, 4, 5, 6, 7, 8	2, 4, 5, 6, 7, 8
200ml HMDI/kg collagen 50 hours	2.6	1, 2	7, 8	3, 4	5, 6, 9

During *in vivo* incubation animals were maintained in single cages and checked postoperatively on a daily basis following U.K. Home office guidelines for health and maintenance of experimental animals in addition to inspecting the areas of implantation for anomalies such as dehiscence.

Animals were euthanised using asphyxiation by incremental concentrations of carbon dioxide. Death was confirmed by destruction of the vertebral column before dissection to remove biomaterial implants.

2.5 Histological analysis

2.5.1 Embedding

To maintain tissue morphology and antigenicity implanted samples were placed directly into periodate-lysine-paraformaldehyde (PLP) fixative post implantation on a roller for 48 hours at 4ºC.

The PLP fixative was prepared as follows; 0.2M lysine-HCl solution was prepared by dissolving 10.96g of Lysine-HCl (Sigma-Aldrich, UK) in 300mL of ddH_2O. A 0.1M solution of Na_2HPO_4 was prepared by dissolving 0.85g of Na_2HPO4 (Sigma-Aldrich, UK) in 60mL of ddH_2O. These two solutions were combined to result in 360ml of solution with a pH of 7.4. 0.1M Phosphate buffer was prepared by dissolving 0.29g NaH_2PO_4 (Sigma-Aldrich, UK) and 1.34g Na_2HPO_4 (Sigma-Aldrich, UK) in 240mL ddH_2O. 240ml of the 0.1M phosphate buffer was then mixed with 360ml of the solution at pH 7.4 resulting in 600 ml of 0.1M concentration of Lysine-HCl. A solution of 2% (w/v) paraformaldehyde (Sigma-Aldrich, UK) was prepared by dissolving 2g of paraformaldehyde in 100mL of ddH_2O with heating and gentle agitation, 2-5 drops of 1M NaOH (Sigma-Aldrich, UK) were used to raise the pH allowing the paraformaldehyde to completely dissolve. Immediately prior to use, 300mL of 0.1M concentration of Lysine-HCl was combined with 100mL of 2% (w/v) paraformaldehyde and to this was added 0.855g of sodium periodate (Sigma-Aldrich, UK) resulting in a 0.1M solution. The fixative was then chilled to 4ºC prior to use.

PLP fixative was aspirated from the samples and replaced with cold washing solution on a roller for 48 hours at 4ºC. The cold washing solution used was 0.1M phosphate buffer modified to contain 7% sucrose and 40mM NH_4Cl, 21g sucrose

(Sigma-Aldrich, UK) and 0.64g ammonium chloride (Sigma-Aldrich, UK) were added to 300ml of 0.1M concentration of Lysine-HCl, prepared as for the PLP fixative.

After 48 hours, cold washing solution was aspirated and replaced with cold acetone on a roller for up to 7 days 4ºC. The acetone solution was aspirated and replaced a minimum of 3 times during this time to effect complete sample dehydration.

After the final acetone aspiration, implants were immersed in Technovit infiltration solution (TAAB, UK) on a roller for 72 hours at 4ºC.

The implants were then moved to an appropriately sized mould and covered in Technovit embedding solution (TAAB, UK), to exclude moisture a layer of oil was used to cover the Technovit embedding solution. The moulds were then placed in a -50ºC freezer for 4 days.

Following storage at -50ºC samples were moved to a -20ºC freezer for 2 days, after which time the samples were brought to room temperature.

Blocks containing implants were removed from the moulds and 50 serial sections of 7µm thickness were cut on a polycot microtome (Reichert-Jung, USA). The sections were placed onto microscope slides coated with 3-aminopropyl triethoxysilane (APTES).

2.5.2 **Tinctoral staining**

2.5.2.1 Haematoxylin

All steps carried out at room temperature. Samples were rehydrated by immersion for 2-3 minutes in 90% ethanol, 70% ethanol and finally ddH_2O. They were transferred to Harris's haematoxylin (Sigma-Aldrich, UK) for 5 minutes; following this, samples were 'blued' in running tepid tap water for 5 minutes. To differentiate the stain, slides were dipped in 1% acid alcohol (4ml 37% HCl in 396ml ethanol) for 5 seconds. The acid alcohol solution was removed by washing in running tap water for 3minutes. Sections were dehydrated by immersion for 2-3 minutes in 70% ethanol, 90% ethanol and finally 100% ethanol. Slides were cleared for a minimum of 3 minutes in Xylene. DPX mountant (Sigma-Aldrich, UK) was used for cover slipping.

Slides were examined by light microscopy. Using this stain, the nuclei of cells were stained blue enabling cell counting.

2.5.2.2 HandE

All steps carried out at room temperature. Sections were rehydrated by immersion for 2-3 minutes in 90% ethanol, 70% ethanol and finally ddH_2O. They were transferred to Harris's heamatoxylin for 5 minutes; following this samples were 'blued' in running tepid tap water for 5 minutes. To differentiate stain slides were dipped in 1% acid alcohol (4ml 37% HCl in 396ml ethanol) for 5 seconds. Acid alcohol solution was removed by washing in running tap water for 3minutes. Slides were immersed in 1% eosin (1g eosin yellowish (Sigma-Aldrich, UK) made up to 100ml in distilled water) for 3 minutes, followed by 3 minutes in ddH_2O. Sections were dehydrated by immersion for 2-3 minutes in 70% ethanol, 90% ethanol and

finally 100% ethanol. Slides were cleared for a minimum of 3 minutes in Xylene. DPX mountant was used for cover slipping.

Slides were examined by light microscopy. This stain was used to visualise the sample structure with the nuclei of cells stained blue and tissue stained various shades of red, pink and orange.

2.5.2.3 Picro-sirius red

All steps carried out at room temperature. Sections were rehydrated by immersion for 2-3 minutes in 90% ethanol, 70% ethanol and finally ddH_2O. Slides were transferred to 0.1% Picro-sirius red solution (1g Sirius red (Sigma-Aldrich, UK) dissolved in 1000ml saturated aqueous solution of picric acid (Sigma-Aldrich, UK)) for 1 hour. Slides were washed in acidified water (0.5% acetic acid, 5ml glacial acetic acid (Sigma-Aldrich, UK) 1000ml distilled water) for 1 minute. Sections were dehydrated by immersion for 1 minute in 70% ethanol, 90% ethanol and finally 100% ethanol. Slides were cleared for a minimum of 1 minute in Xylene. DPX mountant was used for cover slipping.

Slides were examined by transmitted light and polarised light microscopy. Rotating the slide under polarised light until the poles cross birefringence of the collagen occurs, undamaged mature collagen fibres appeared red – orange and undamaged immature collagen fibres appeared green, damaged collagen appeared black. This stain was used to assess collagen integrity.

2.5.2.4 Naphthol AS-D Chloroacetate

Prior to staining a line was drawn around each section using a Dako pen (Dako, Denmark) to prevent solution run off and slides were equilibrated to 37°C. All

solutions were supplied in Naphthol AS-D Chloroacetate (Specific Esterase) Kit (Sigma-Aldrich, UK).

Naphthol AS-D solution was prepared by mixing, 250µl sodium nitrate and 250µl fast red violet LB base, which was allowed to stand for 2 minutes. Then 10ml ddH_2O at 37°C, 1.25ml TRIZMAL 6.3 buffer concentrate and 250µl Naphthol AS-D chloroacetate solution were added. The solution was mixed well and syringe filtered through a 0.45µm filter. Sections were covered with the naphthol AS-D solution for 20 minutes at 37ºC in the dark. After incubation the slides were rinsed in running ddH_2O for at least 2 minutes and mounted using aqueous mounting media.

Slides were examined by light microscopy. Neutrophils, mast cells and basophils were stained magenta/purple colour.

2.5.2.5 α-Naphthyl Acetate (Non-Specific Esterase)

Prior to staining a line was drawn around each section using a Dako pen (Dako, Denmark) to prevent solution run off and slides were equilibrated to 37°C. All solutions were supplied in α-Naphthyl Acetate (Non-Specific Esterase) (Sigma-Aldrich, UK).

α-Naphthyl acetate solution was prepared by mixing, 250µl sodium nitrate and 250µl fast blue BB base and stood for 2 minutes. 10ml ddH_2O at 37°C, 1.25ml TRIZMAL 7.6 buffer concentrate and 250µl α-Naphthyl acetate solution were added. The solution was mixed well and syringe filtered through a 0.45µm filter. Sections were covered with α-Naphthyl acetate solution for a minimum of 1 hour at 37ºC in the dark. After incubation, slides were rinsed in running ddH_2O for at least 2 minutes and mounted using aqueous mounting media.

Slides were examined by light microscopy. Monocytes, macrophages and histiocytes were stained a dark brown / black colour.

2.5.3 **Immunohistochemistry**

A line was drawn around each section using a Dako pen (Dako, Denmark) prior to staining to prevent solution run off.

A 0.15% trypsin in sodium phosphate buffer pH 7.8, prepared by dissolving 0.028g NaH_2PO_4 (Sigma-Aldrich, UK) and 0.48g Na_2HPO_4 (Sigma-Aldrich, UK) in 190ml ddH_2O, adjusted to pH 7.8 with sodium hydroxide and made up to 200ml with ddH_2O. 10 ml of this solution was filtered and 0.015g of trypsin type III (Sigma-Aldrich, UK) dissolved in it.

Section epitopes were unmasked using 0.15% trypsin in sodium phosphate buffer pH 7.8 for 30minutes at 37°C. Sections were washed three times for three minutes with filtered PBS. Non-specific binding was blocked by incubating sections with rabbit serum; 3 drops diluted in 10ml filtered PBS, for 30minutes at 37°C. Primary antibodies (Table 2.3) were diluted to a working concentration of 1:100 using filtered 1% (w/v) bovine serum albumin (BSA) in PBS (0.1g BSA (Sigma Aldrich, UK) dissolved in 10 ml PBS).

Table 2.3 Primary antibodies used for immunohistological staining

Antigen	Target	Speciation	Reactivity	Clone	Supplier
CD5	T-cells	Mouse	Rat	Ox-19	Serotec, UK
CD68	Activated macrophages	Mouse	Rat	ED1	Serotec, UK
Col-1	Collagen I	Mouse	Rat	Col-1	Abcam, UK
FH-7A	Collagen III	Mouse	Rat	FH-7A	Abcam, UK

Sections were incubated overnight (16-20 hours) at 4°C in the dark, then washed three times for three minutes with filtered PBS. Secondary antibody (biotinylated rabbit anti mouse, E0464) at 1:200 concentration in PBS was added to the samples and incubated for 60 minutes at 37°C in the dark. Samples were washed three times for three minutes with filtered PBS. Alkaline phosphatase enzyme conjugated with avidin (ABC/AP kit from vector labs) was used to label the secondary antibody. Two drops of solution A and B were mixed in PBS, this solution was added to the slides and incubated in the dark at room temperature for 30 minutes. Sections were washed once for three minutes with filtered PBS and twice for three minutes with 200mM TRIS-HCL buffer (4.844g TRIS based dissolve in 200ml with ddH_2O and adjusted pH to 8.2). The VECTOR red alkaline phosphatase substrate kit (VECTOR laboratories, UK) was used for the final colour development step. To 5ml filtered 200mM TRIS-HCL buffer, 2 drops of reagent 1, 2 and 3 were added

along with 1 drop of levamisole (VECTOR laboratories, UK) and mixed well. Sections were incubated with this solution for 20 minutes at room temperature in the dark. Sections were washed three times for three minutes with filtered PBS and mounted with aqueous mounting media. Figure 2.7 is a schematic of the immunohistochemical reaction.

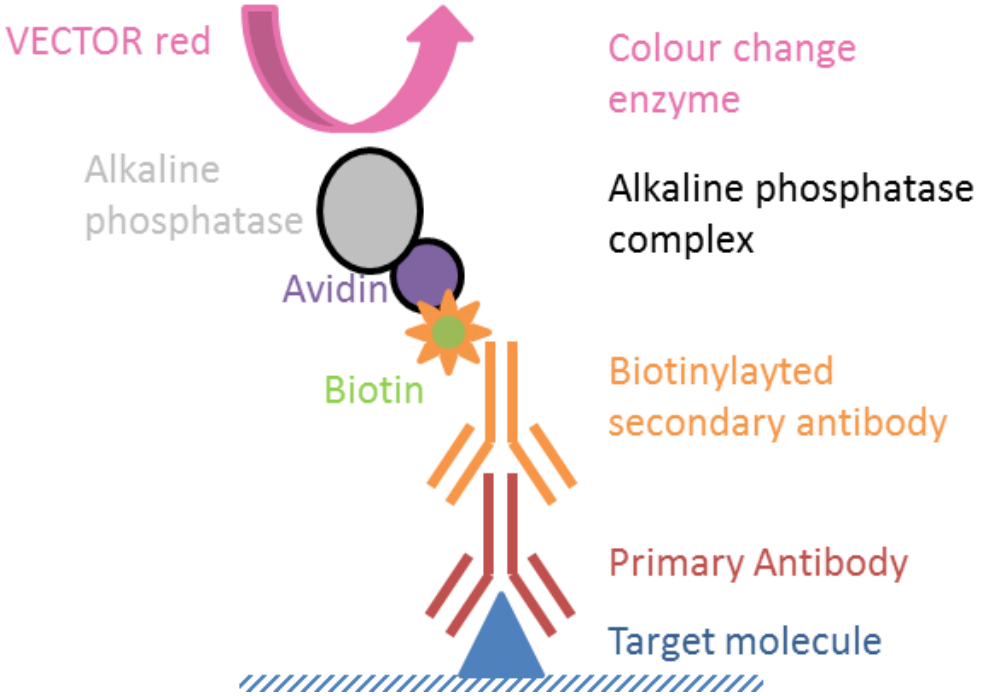

Figure 2.7 Immunohistochemistry schematic

Slides were examined by light microscopy, positive staining was indicated by a pink colouration.

2.6 Image analysis

The cells present in 20 fields of view, 10 at the implant interface and 10 deep and adjacent to these fields (Figure 2.8) were counted. These images were analysed by computer package KS400 (Carl-Zeiss, US). Using the darker colour of the positively stained cells, the software differentiates between non-stained and stained areas. Counting the number of spherical darker patches in each field of view to provide a cell count.

For Naphthol AS-D Chloroacetate the mast cells were identified manually as a separate cell population. These cells were recognised due to their larger size and dark pink staining.

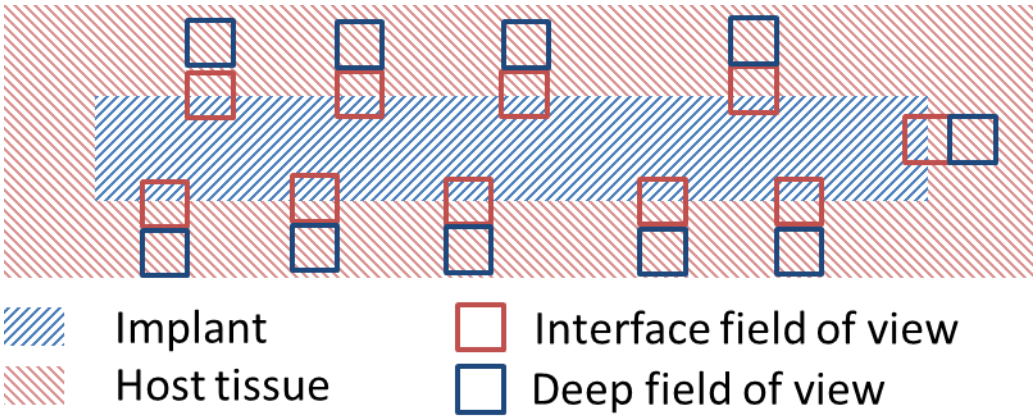

Figure 2.8 Example of where fields of view may be counted for an implant

2.7 Statistical analysis

2.7.1 ANOVA

Analysis of variance was used to determine significant difference between more than 2 groups of data, using Minitab 16. Data was tested at 0.05 significance level. To ascertain the grouping of the data sets, Tukey Post Hoc analysis was utilised.

3 Biomaterial Characterisation

3.1 Introduction

Many collagen based biomaterials are available and can be autogenic, allogenic or xenogenic [9], [60]–[63]. These materials can be tailored to intended applications by varying parameters used in their fabrication including source anatomical origin, tissue processing (decellularisation/delipidation) and cross-linking [62], [64], [65]; with the final aim of producing a biocompatible material capable of restoring normal tissue function.

Most allogenic and xenogenic biomaterials undergo a process to remove cellular material leaving the 3D extracellular matrix (ECM) behind. This matrix is implanted and provides a scaffold for cells to migrate into thereby stabilising the graft and returning mechanical strength to compromised tissue. In this study, porcine dermal collagen was sequentially treated using solvents and enzymatic digestion to remove fats and non-collagenous proteins. Trypsin was used to digest proteins from the collagenous structure leaving collagen intact. In 1972 Oliver and co-workers hypothesised that a crystalline solution of trypsin would eliminate cellular components and antigens from tissue [66].

Cross-links can be added to the ECM structure using a variety of compounds including genipin [34], isocyanates [29] and gluteraldehyde [67]. Cross-linking agents have been shown to provide resistance to enzyme degradation [68] and changes in the materials elasticity, thermal stability, antigenicity and resorption [62]. HMDI was utilised as a crosslinking agent in this study, HMDI reacts with the free amine groups present in the collagen molecules (Figure 3.1) [29].

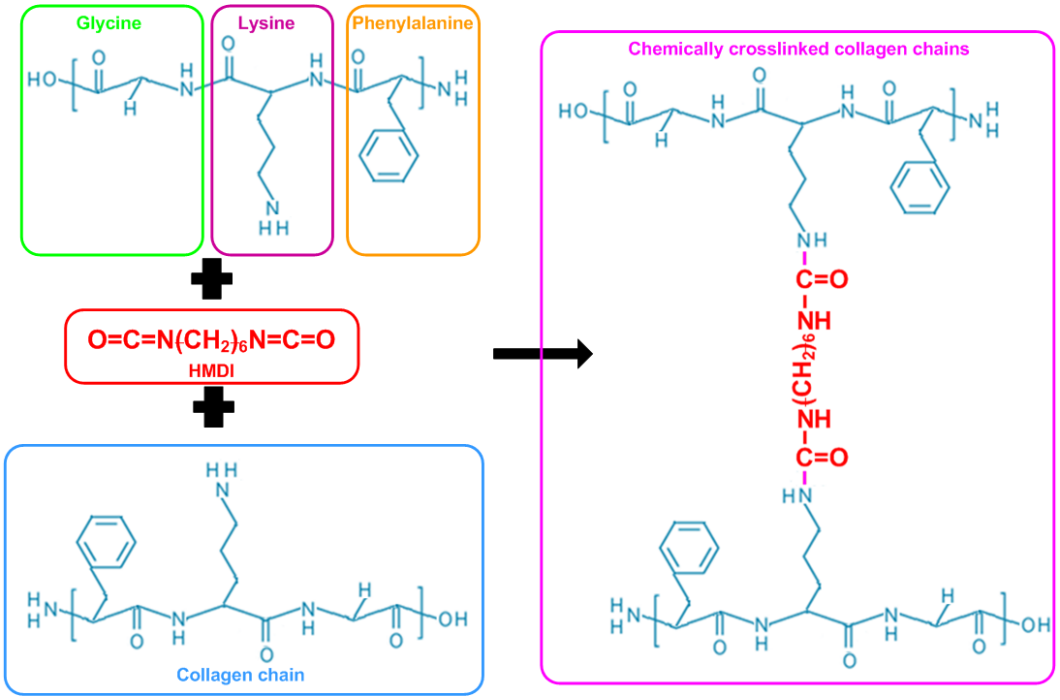

Figure 3.1 Schematic of HMDI reaction with amine groups in collagen molecule.

The acellular porcine dermal collagen material underwent different crosslinking reactions and the effects on the chemical composition, mechanical and physical properties of the biomaterials were determined.

3.2 Aim

The aim of these studies was to investigate how varying the duration and/or quantity of HMDI in the crosslinking reaction altered the level of crosslinking present in the collagen matrix and how this effected the material's biophysical properties.

3.3 Results

3.3.1 Comparison of amino acid composition of crosslinked collagen matrix

When exposed to HMDI, isocyanate groups form bonds with tertiary amines which are present on lysine and hydroxylysine AA in collagen. Collagen matrix samples were analysed to establish their AA composition using HPLC. The crosslinking

parameters used to produce the biomaterials are shown in table 2.1, AA profiles were established for all 23 variants.

AA which formed a bond with HMDI had their structure modified sufficiently that they were distinctly different from their un-bonded form chromatographically. Figure 3.2 depicts an example HPLC chromatogram.

HPLC was able to detect 20 different AA; alanine, arginine, aspartic acid, cysteic acid, cysteine, glutamic acid, glycine, histidine, hydroxylysine, hydroxyproline, isoleucine, leucine, lysine, methionine, phenylalanine, proline, serine, threonine, tyrosine and valine. 2 of which (cysteic acid and cysteine) were not detected in the collagen matrix samples. 5 of the AA (alanine, glutamic acid, glycine and hydroxyproline) peaks were intentionally off scale; this was to enable hydroxylysine to be present in a detectable concentration.

Figures 3.3, 3.4, 3.5, 3.6 and 3.7 show mean values for the 13 AA associated with varying exposure times and HMDI concentrations used in crosslinking reactions. Of these, only lysine and hydroxylysine showed a consistent reduction in concentration with increased HMDI either by concentration or exposure time. Based on this, all subsequent analyses concentrated on lysine and hydroxylysine.

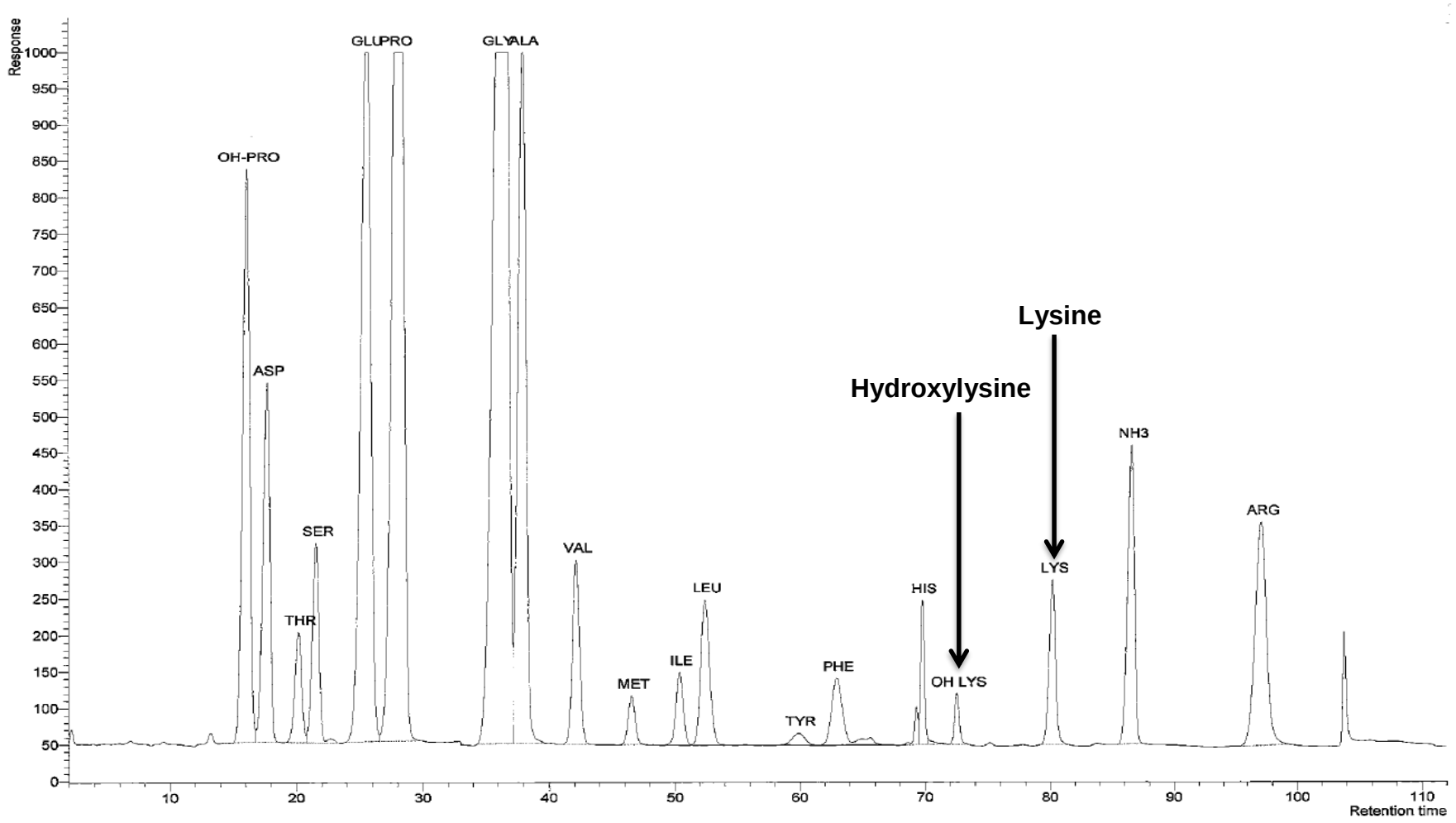

Figure 3.2 Example HPLC chromatogram for AA analysis, glutamic acid, proline, glycine and alanine are all off scale.

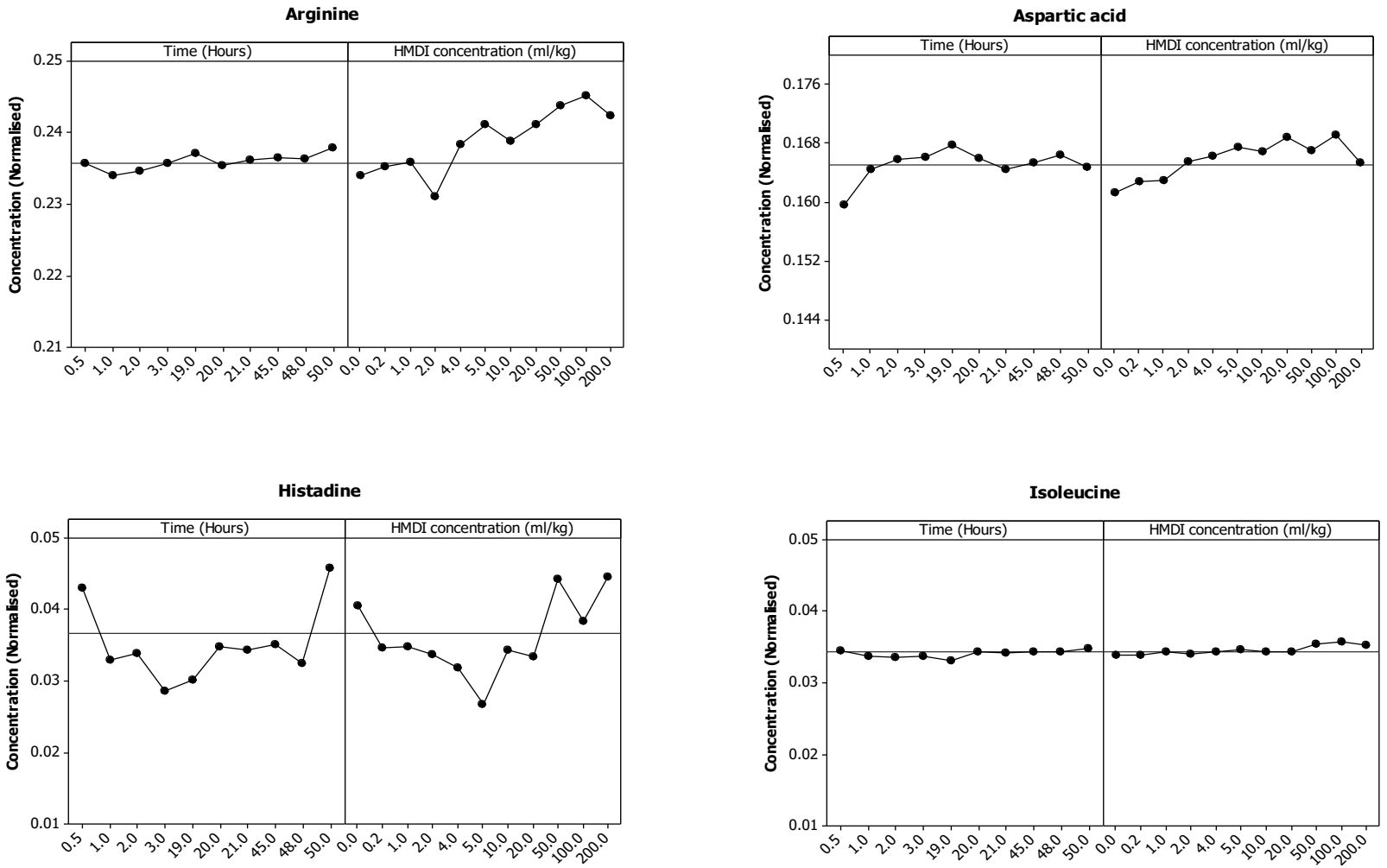

Figure 3.3 Average normalised concentrations for arginine, aspartic acid, histadine and isoleucine across all materials.

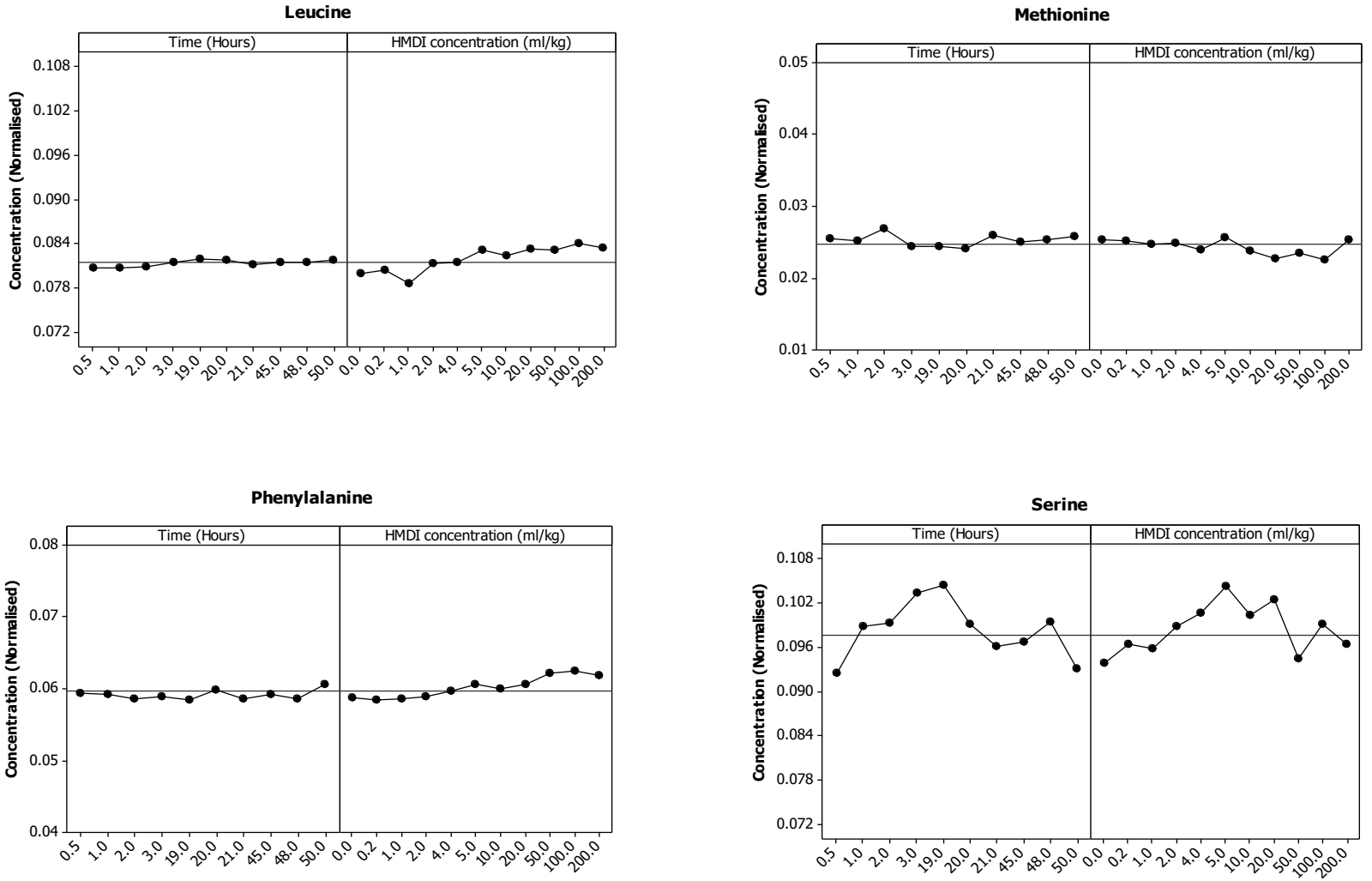

Figure 3.4 Average normalised concentrations for leucine, methioine, phenylalanine and serine detected across all materials.

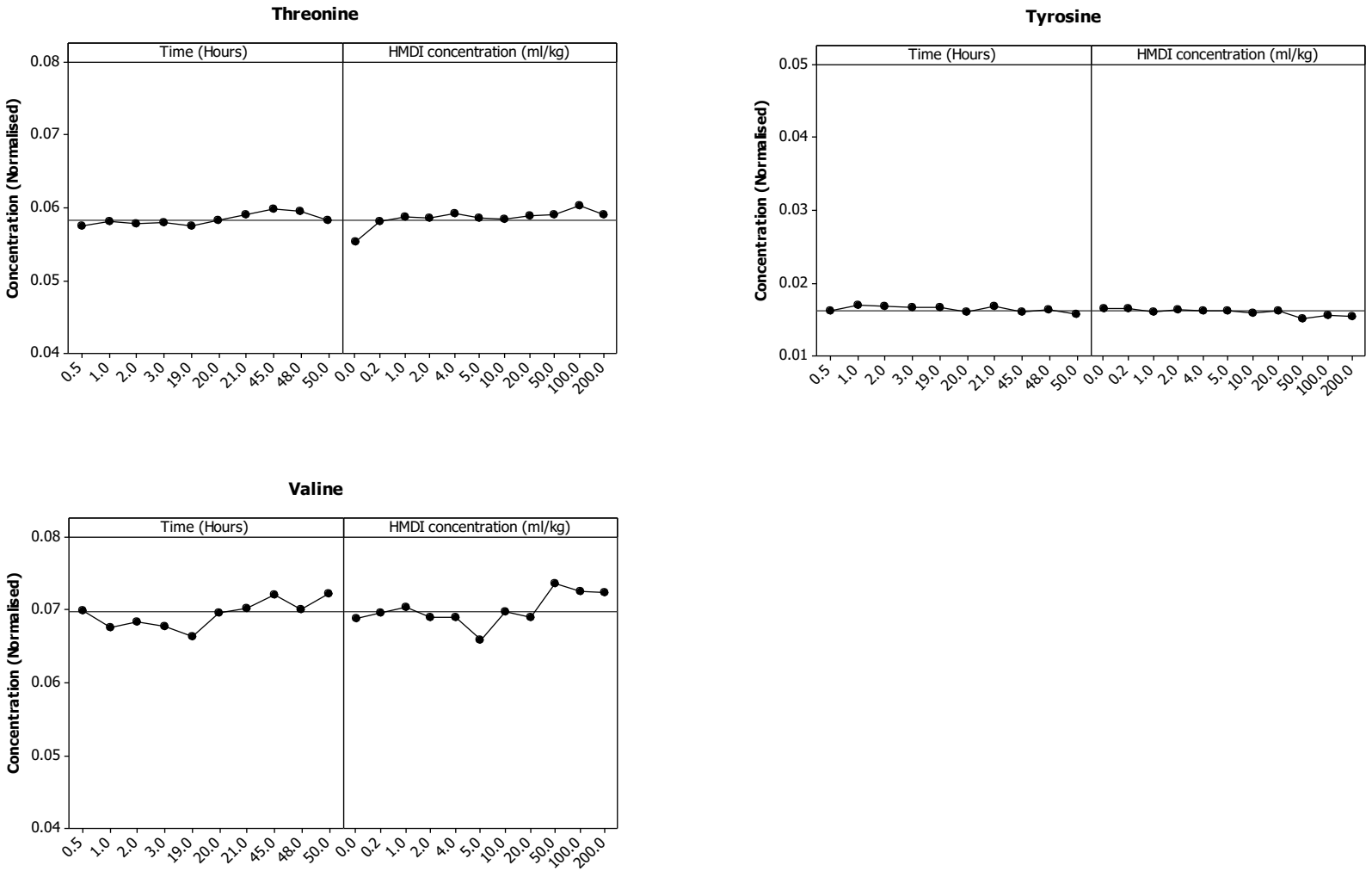

Figure 3.5 Average normalised concentrations for threonine, tyrosine and valine detected across all materials.

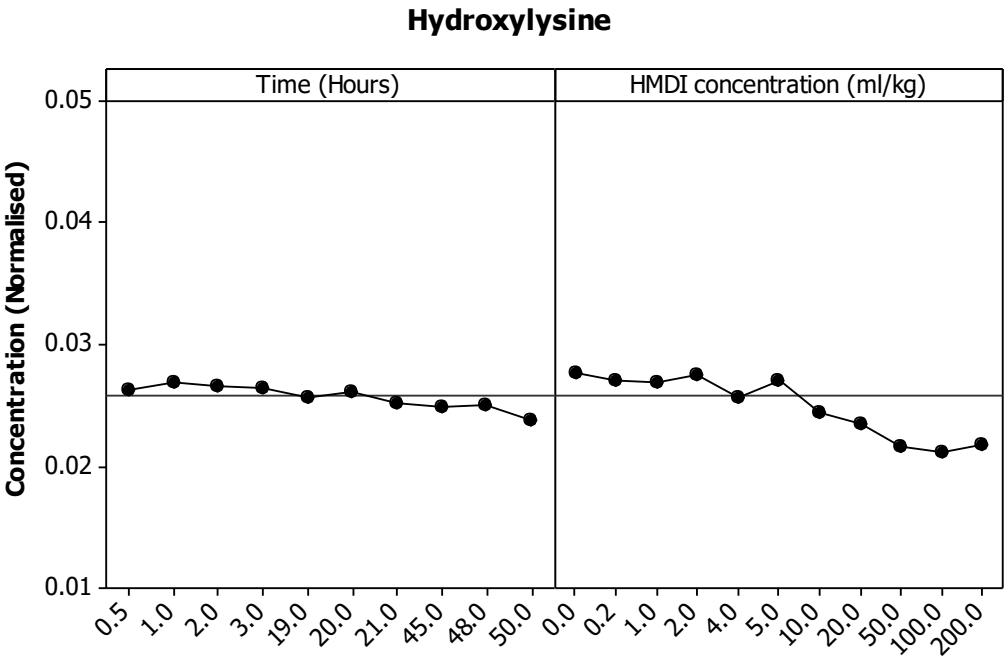

Figure 3.6 Average normalised concentrations for lysine detected in all materials.

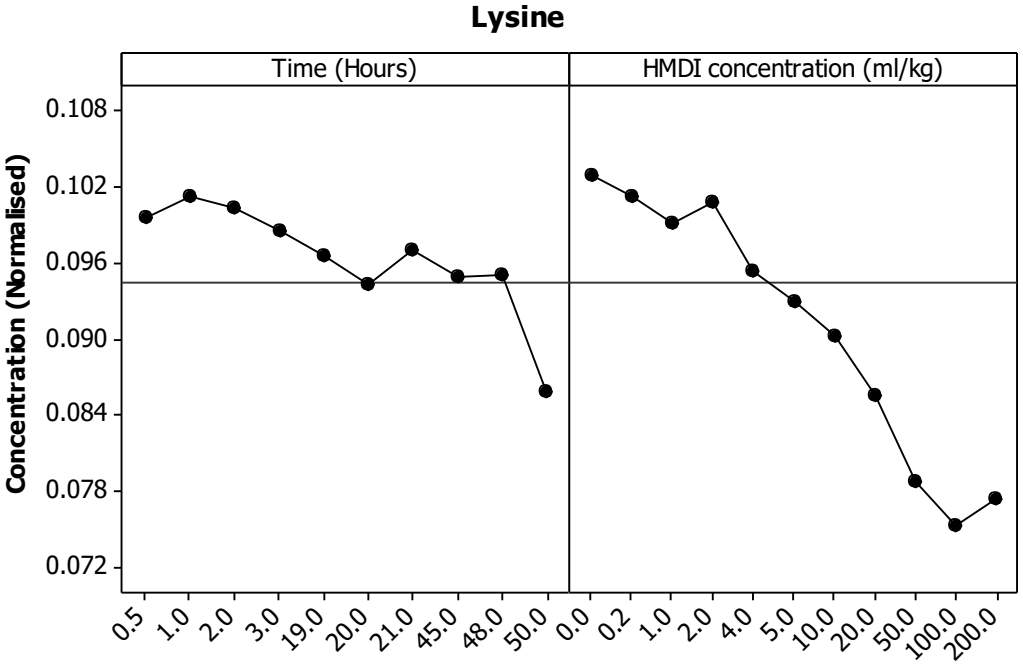

Figure 3.7 Average normalised concentrations for lysine detected in all materials.

Prior to the crosslinking reaction all sheets were marked with a unique identifier, enabling the hide each sample originated from to be identified. To investigate differences between sheets originating from different hides an ANOVA test was conducted. To ensure the most powerful statistical comparison, results were split into 3 tests based on crosslinking parameters;

- 20 hour duration varying HMDI concentration (HMDI)
- 2ml HMDI/kg collagen varying crosslinking duration (time)
- Extreme samples (extreme)
    - 0.5 hours no HMDI
    - 0.5 hours, 200 ml HMDI/kg collagen
    - 50 hours no HMDI
    - 50 hours, 200ml HMDI/kg collagen

The P values were, HMDI 0.958, time 0.099 and extreme 0.997. From the ANOVA results, no statistically significant differences existed between samples arising from different hides. This indicated that observed phenomena were a result of the crosslinking reaction rather than emanating from the originating hide. For subsequent analyses, hides from different source animals were grouped together concentrating on crosslinking variations.

The amount of lysine and hydroxylysine present in the collagen matrices are shown in figures 3.8, 3.9, 3.10 and 3.11. The graphs indicate that as HMDI concentration or crosslinking duration was increased the amount of unbound lysine and hydroxylysine decreased. The relationship was not linear with an initial rapid decrease in lysine and hydroxylysine concentration which plateaued as both duration and HMDI concentration increased. At the levels tested, it does not appear

the reaction had reached completion. Hydroxylysine and lysine decreased at the same rate maintaining the ratio of 3.5 lysine molecules for every 1 hydroxylysine molecule used during crosslinking, this indicated that neither lysine nor hydroxylysine were preferential in the reaction.

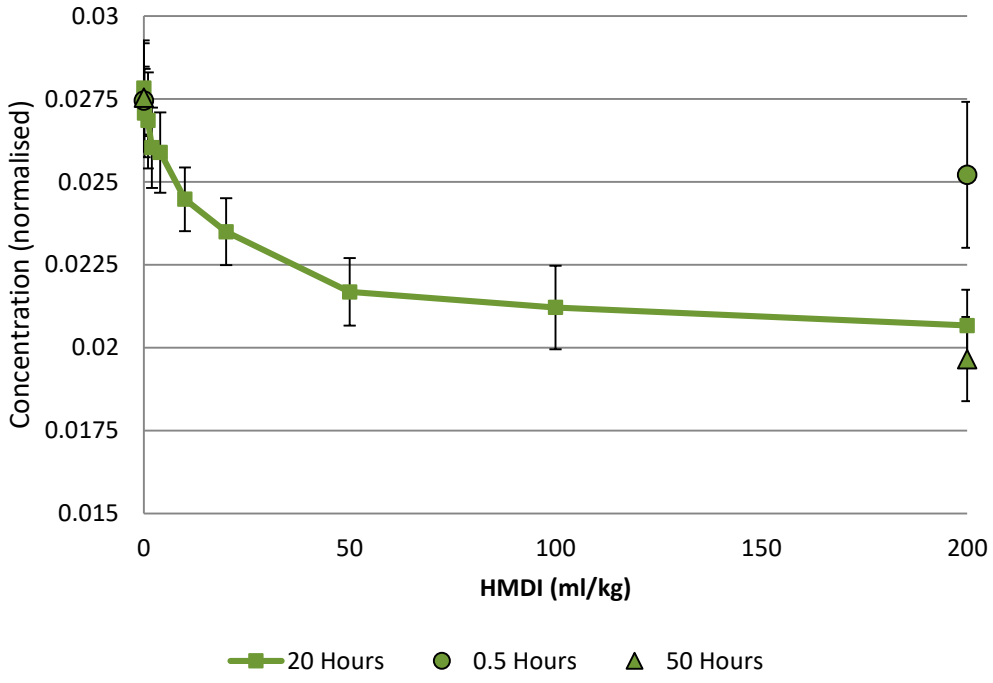

Figure 3.8 Normalised hydroxylysine concentration varying the amount of HMDI added to the reaction, squares 20 hour exposure, circles 0.5 hour exposure, triangle 50 hour exposure, error bars ± standard deviation.

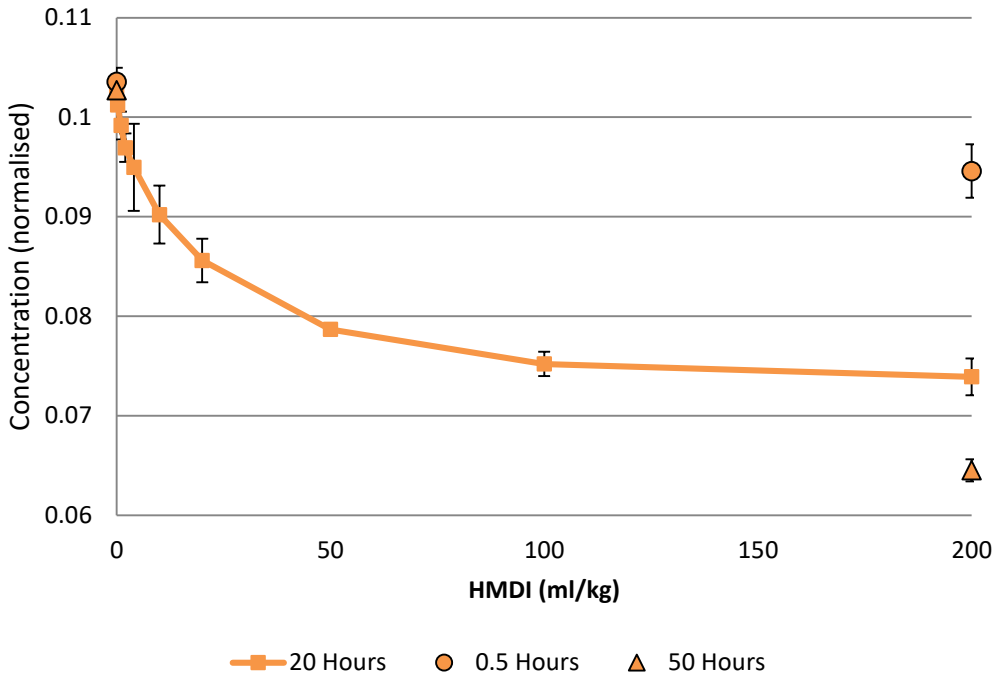

Figure 3.9 Normalised lysine concentration varying the amount of HMDI added to the reaction squares 20 hour exposure, circles 0.5 hour exposure, triangle 50 hour exposure, error bars ± standard deviation.

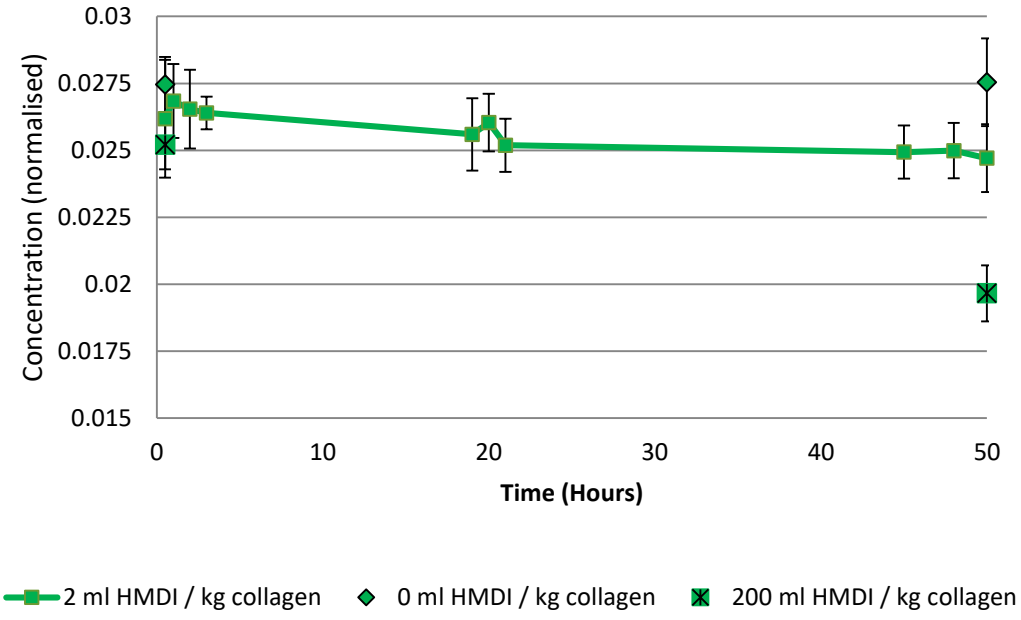

Figure 3.10 Normalised hydroxylysine concentration varying the duration of exposure to HMDI, square 2ml HMDI/kg collagen, diamond no HMDI, cross 200ml HMDI/kg collagen, error bars ±standard deviation.

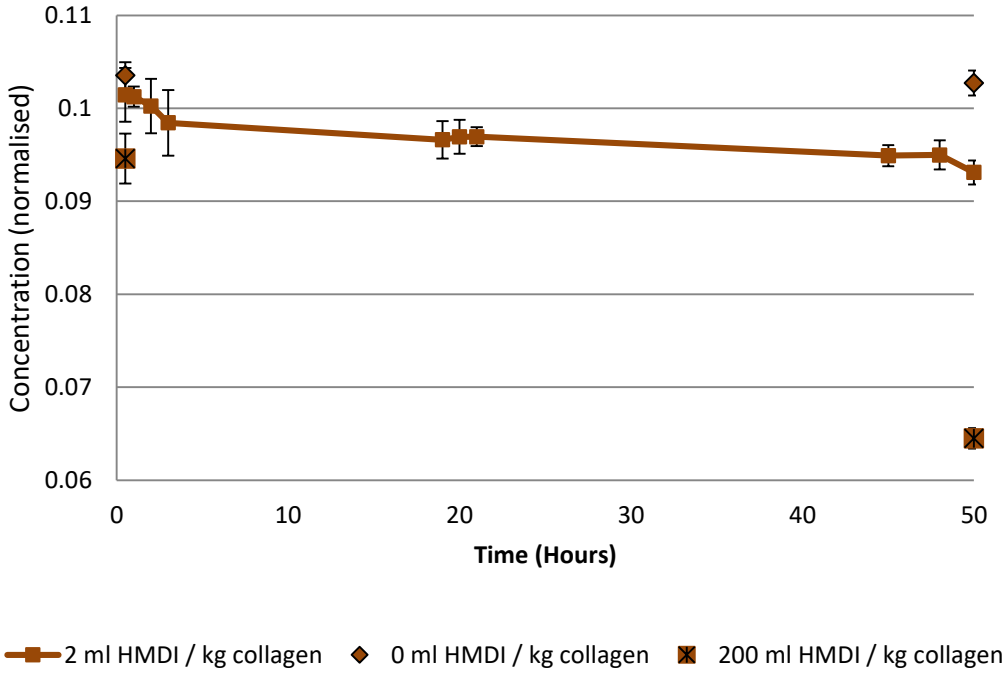

Figure 3.11 Normalised lysine concentration varying the duration of exposure to HMDI: square 2ml HMDI/kg collagen, diamond no HMDI, cross 200ml HMDI/kg collagen, error bars ±standard deviation.

Regression analysis was performed on the lysine and hydroxylysine concentrations to establish if a relationship existed in their utilisation in crosslinking as a function of quantity and duration of exposure to HMDI (Table 3.1).

These relationships were confirmed by regression analysis, ($P<0.05$). The strongest relationship existed between lysine concentration and the concentration of HMDI used in the crosslinking reaction, with an adjusted R^2 of 93%. Hydroxylysine had a weaker relationship than lysine, probably due to natively lower levels present in the biomaterials.

Table 3.1 Relationship of change in lysine / hydroxylysine concentration to HMDI concentration or duration of exposure to HMDI

		Adjusted R sq.	P
Lysine	HMDI concentration	93.38	0.000
	Crosslinking duration	61.57	0.000
Hydroxylysine	HMDI concentration	77.45	0.000
	Crosslinking duration	25.61	0.003

To test for statistical differences between the crosslinking variants a one-way ANOVA was performed. P values for lysine and hydroxylysine were 0.000. A 99.9% confidence level ($p<0.001$) from the ANOVA led to a Tukey's post-hoc test to determine which data sets were statistically different (Table 3.2 and Table 3.4).

Table 3.2 Tukey's post hoc test at 95% level for statistical significance between lysine concentration data sets. Boxes highlighted in red are statistically different means, boxes highlighted in green are statistically similar means.

Concentration (Normalised)	**n**	**Time (Hours)**		**20**										**0.5**	**1**	**2**	**3**	**19**	**21**	**45**	**48**	**50**	**0.5**	**0.5**	**50**	**50**
			HMDI (ml/kg)	**0**	**0.2**	**1**	**2**	**4**	**10**	**20**	**50**	**100**	**200**	**2**									**0**	**200**	**0**	**200**
0.102	6	**20**	**0**																							
0.101	6		**0.2**																							
0.099	6		**1**																							
0.097	13		**2**																							
0.095	6		**4**																							
0.09	6		**10**																							
0.086	6		**20**																							
0.079	3		**50**																							
0.075	3		**100**																							
0.074	6		**200**																							

Table 3.3 (continued) Tukey's post hoc test at 95% level for statistical significance between lysine concentration data sets. Boxes highlighted in red are statistically different means, boxes highlighted in green are statistically similar means.

Concentration (Normalised)	n	Time (Hours)		20										0.5	1	2	3	19	21	45	48	50	0.5	0.5	50	50
			HMDI (ml/kg)	0	0.2	1	2	4	10	20	50	100	200	2									0	200	0	200
0.101	3	**0.5**	**2**																							
0.101	3	**1**	**0.2**																							
0.1	3	**2**	**1**																							
0.098	3	**3**	**2**																							
0.097	3	**19**	**4**																							
0.097	3	**21**	**10**																							
0.095	3	**45**	**20**																							
0.095	3	**48**	**50**																							
0.093	3	**50**	**100**																							
0.104	5	**0.5**	**0**																							
0.095	5	**0.5**	**200**																							
0.103	5	**50**	**0**																							
0.065	5	**50**	**200**																							

Table 3.4 Tukey's post hoc test at 95% level for statistical significance between hydroxylysine concentration data set. Boxes highlighted in red are statistically different means, boxes highlighted in green are statistically similar means.

Concentration (Normalised)	n	Time (Hours)		20										0.5	1	2	3	19	21	45	48	50	0.5	0.5	50	50
			HMDI (ml/kg)	0	0.2	1	2	4	10	20	50	100	200	2									0	200	0	200
0.028	6	20	0																							
0.027	6		0.2																							
0.027	6		1																							
0.026	13		2																							
0.026	6		4																							
0.024	6		10																							
0.023	6		20																							
0.022	3		50																							
0.021	3		100																							
0.021	6		200																							

Table 3.5 (continued) Tukey's post hoc test at 95% level for statistical significance between hydroxylysine concentration data set. Boxes highlighted in red are statistically different means, boxes highlighted in green are statistically similar means.

Concentration (Normalised)	**n**	**Time (Hours)**		20										0.5	1	2	3	19	21	45	48	50	0.5	0.5	50	50
			HMDI (ml/kg)	**0**	**0.2**	**1**	**2**	**4**	**10**	**20**	**50**	**100**	**200**	2									**0**	**200**	**0**	**200**
0.026	3	**0.5**	**2**																							
0.027	3	**1**	**0.2**																							
0.027	3	**2**	**1**																							
0.026	3	**3**	**2**																							
0.026	3	**19**	**4**																							
0.025	3	**21**	**10**																							
0.025	3	**45**	**20**																							
0.025	3	**48**	**50**																							
0.025	3	**50**	**100**																							
0.027	5	**0.5**	**0**																							
0.025	5	**0.5**	**200**																							
0.028	5	**50**	**0**																							
0.02	5	**50**	**200**																							

Altering the concentration of HMDI had a greater influence than contact time on the amount of lysine and hydroxylysine used in crosslinking. This was especially prominent at 2ml/kg collagen HMDI, when altering reaction time from 30 minutes to 50 hours did not derive statistically different data sets (Table 3.2 and Table 3.4). Less distinction was observed in hydroxylysine than the lysine, this was probably due to the lower level of hydroxylysine present in the starting material. Subsequently work focussed on lysine as the greater number of molecules present provided more robust data.

There was no difference between non-crosslinked variants; leaving the collagen matrix in solvent for up to 50 hours did not affect AA composition. When performing the crosslinking reaction for 20 hours no difference was observed between non-crosslinked samples and those crosslinked with up to 2ml/kg collagen HMDI. The crosslinking parameters 20ml/kg HMDI 20 hours and 200ml/kg HMDI 50 hours were statistically different to all the other data sets.

To establish how many AA were involved in crosslinking a full AA profile was established (Table 3.6) for non-crosslinked collagen matrices. These values were recorded as residues/1000 AA (/1000 AA); the approximate chain length of collagen. Diluted samples were analysed to determine the levels of alanine, glutamic acid, glycine and hydroxyproline, all other values were from undiluted samples.

Table 3.6 Non-crosslinked collagen matrix AA break down.

	AA residues/1000	Percentage of total AA
Hydroxyproline	81	8.1
Aspartic acid	49	4.9
Threonine	21	2.1
Serine	36	3.6
Glutamic acid	76	7.6
Proline	126	12.6
Glycine	329	32.9
Alanine	104	10.4
Valine	25	2.5
Methionine	7	0.7
Isoleucine	11	1.1
Leucine	25	2.5
Tyrosine	3	0.3
Phenylalanine	14	1.4
Histidine	11	1.1
Hydroxylysine	6	0.6
Lysine	26	2.6
Arginine	52	5.2

Percentage lysine and hydroxylysine molecules available for crosslinking were determined as Equation 3.1.

Equation 3.1 Percentage of available lysine and hydroxylysine molecules available for crosslinking.

$$\frac{Normalised\ value\ of\ sample}{Normalised\ value\ of\ 0\ ml/kg\ HMDI\ 20\ Hour} X100 = Availalbe\ molecules$$

Equation 3.2 was used to determine the number of lysine and hydroxylysine molecules involved in crosslinking. These 2 values were then added together to establish the total number of AA involved in crosslinking. Table 3.5 shows the

number of lysine and hydroxylysine molecules used in each of the 23 different crosslinking reactions.

Equation 3.2 Determination of molecules used in crosslinking reaction.

$$Amino\ acid\ residues\ per\ 1000 - \left(\frac{Amino\ acid\ residues\ per\ 1000}{100} * Available\ molecules\right) = Molecules\ used$$

Table 3.7 Determination of molecules used in crosslinking reaction.

		Lysine		Hydroxylysine		Total	
Time (Hours)	**HMDI (ml/kg)**	**Available (%)**	**Used (n/1000)**	**Available (%)**	**Used (n/1000)**	**Available (%)**	**Used (n/1000)**
20	**0**	100	0	100	0	100	0
	0.2	98.8	0.3	97.3	0.2	98.1	0.5
	1	96.8	0.8	96.5	0.2	96.7	1.0
	2	94.9	1.3	93.7	0.4	94.3	1.7
	4	92.7	1.9	93.0	0.4	92.9	2.3
	10	88.1	3.1	88.0	0.7	88.0	3.8
	20	83.6	4.3	84.4	0.9	84.0	5.2
	50	76.8	6.0	77.9	1.3	77.4	7.4
	100	73.4	6.9	76.2	1.4	74.8	8.3
	200	72.1	7.2	74.3	1.5	73.2	8.8

Table 3.5 (continued) Determination of molecules used in crosslinking reaction.

		Lysine		Hydroxylysine		Total	
Time (Hours)	**HMDI (ml/kg)**	**Available (%)**	**Used (n/1000)**	**Available (%)**	**Used (n/1000)**	**Available (%)**	**Used (n/1000)**
0.5	**2**	99.0	0.3	94.1	0.4	96.5	0.6
1		98.8	0.3	96.5	0.2	97.6	0.5
2		97.9	0.6	95.4	0.3	96.6	0.8
3		96.1	1.0	94.8	0.3	95.5	1.3
19		94.3	1.5	92.0	0.5	93.1	2.0
21		94.6	1.4	90.5	0.6	92.6	2.0
45		92.6	1.9	89.6	0.6	91.1	2.5
48		92.7	1.9	89.8	0.6	91.3	2.5
50		90.9	2.4	88.8	0.7	89.8	3.0
0.5	**0**	101.1	-0.3	98.7	0.1	99.9	-0.2
0.5	**200**	92.3	2.0	90.6	0.6	91.5	2.6
50	**0**	100.3	-0.1	99.0	0.1	99.6	0.0
50	**200**	63.0	9.6	70.6	1.8	66.8	11.4

The highest number of molecules used during a crosslinking reaction was 67% of the available molecules that equated to 11 AA per 1000. Approximately 2 AA were used in the crosslinking reaction in the production of Permacol™.

3.3.2 **Evaluation of the effect of crosslinking on resistance to enzyme degradation**

Existing literature indicates that introducing crosslinking into collagen can affect resistance *in vivo* to bacterial degradation [68], [69]. This may be due to HMDI blocking the binding sites of the enzymes responsible for *in vivo* degradation. The effect of bacterial degradation was assessed, dermal collagen materials were exposed to bacterial collagenase at 37°C for 20 hours and the weight of collagen remaining measured (Figure 3.12 and Figure 3.13).

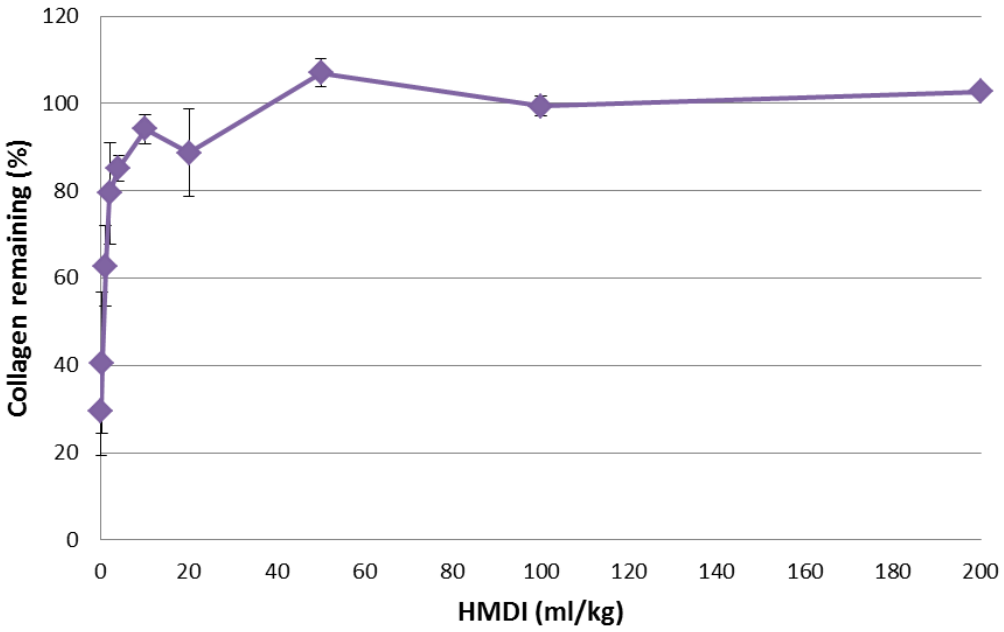

Figure 3.12 Collagenase resistance assay, collagen remaining after enzyme digestion, varying the quantity of HMDI, duration of the crosslinking reaction 20 hours, error bars ± standard deviation.

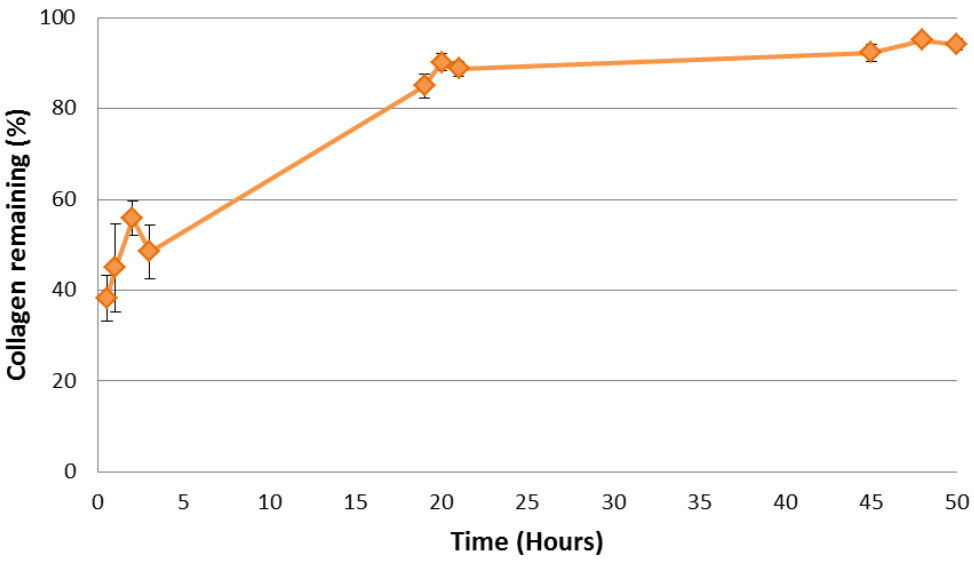

Figure 3.13 Collagenase resistance assay, collagen remaining after enzyme digestion, using 2 ml of HMDI per kg of collagen, varying the duration of the crosslinking reaction error bars ± standard deviation.

When the amount of HMDI or the duration of crosslinking was increased, resistance to degradation by bacterial collagenase also increased. The increase in resistance to collagenase digestion happened rapidly. After 20 hours digestion, non-crosslinked material had 29% mass remaining; adding 10ml/kg HMDI and crosslinking for 20 hours increased the mass remaining to approximately 95%. Little change was observed in the mass remaining above 10ml/kg HMDI. Crosslinking for a short duration (0.5-3hours) slightly increased resistance to degradation. After 19 hours digestion 85% collagen remained. Extending the crosslinking duration to 50 hours increased the mass remaining to 94% for the same digestion time. Figure 3.14 shows how resistance to enzyme degradation relates to the number of crosslinks per collagen molecule.

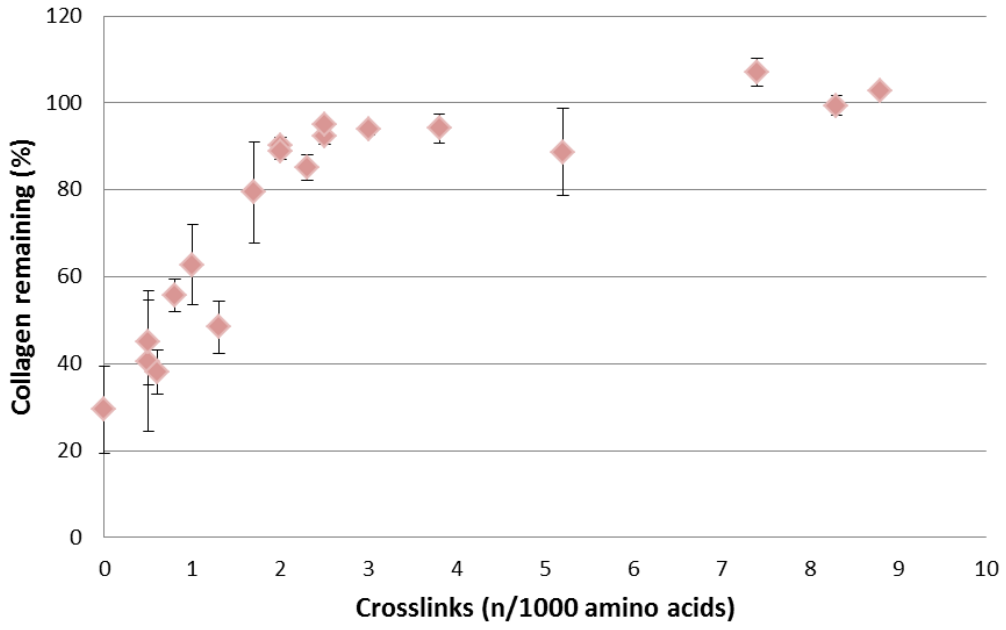

Figure 3.14 Collagenase resistance assay, collagen remaining after enzyme digestion, number of crosslinks present in the material per 1000 AA, error bars ± standard deviation.

A relationship existed between the number of crosslinks present in the material and its resistance to degradation by collagenase: as crosslinks increased, resistance to enzymatic degradation increased.

3.3.3 **Evaluation of the effect of crosslinking on denaturation temperature.**

The addition of crosslinks into collagen materials has previously been shown to alter denaturation temperature [34], [70]. The amount of energy required to denature the materials was measured by DSC. Figures 3.15 and 3.16 illustrate that as the amount of HMDI added or reaction duration was increased the material denaturation temperature increased. Table 3.6 and figure 3.17 show the denaturation temperature in relation to the number of crosslinks per collagen molecule. The denaturation temperature of sliced porcine dermal collagen prior to removal of lipids and cells was 65°C and represented on figures 3.15 and 3.16 as a green reference line.

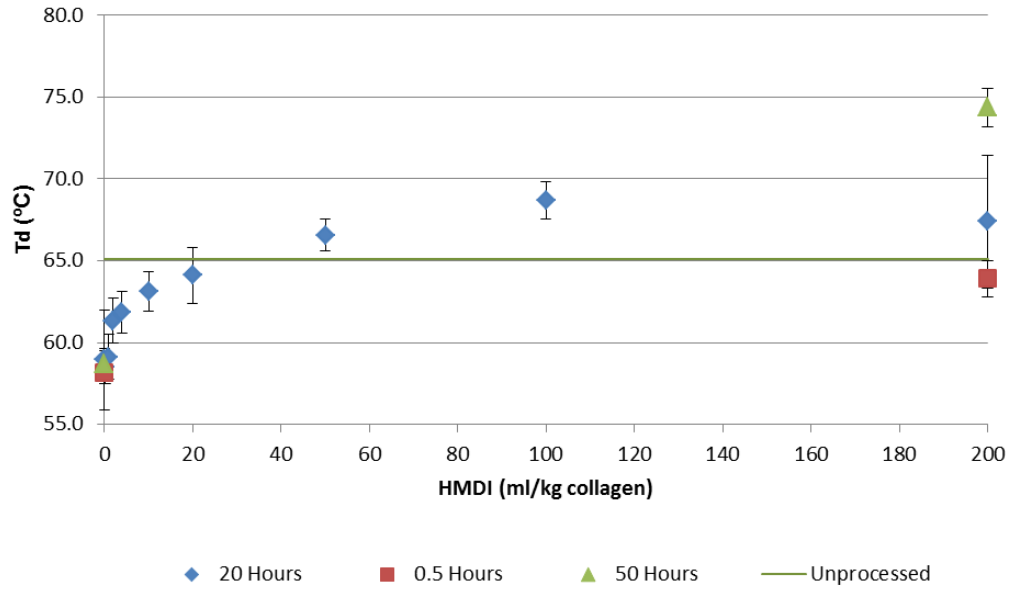

Figure 3.15 Collagen denaturation temperature, varying the quantity of HMDI, duration of the crosslinking reaction; diamonds 20 hour exposure, squares 0.5 hour exposure, triangle 50 hour exposure, green line unprocessed collagen, error bars ± standard deviation

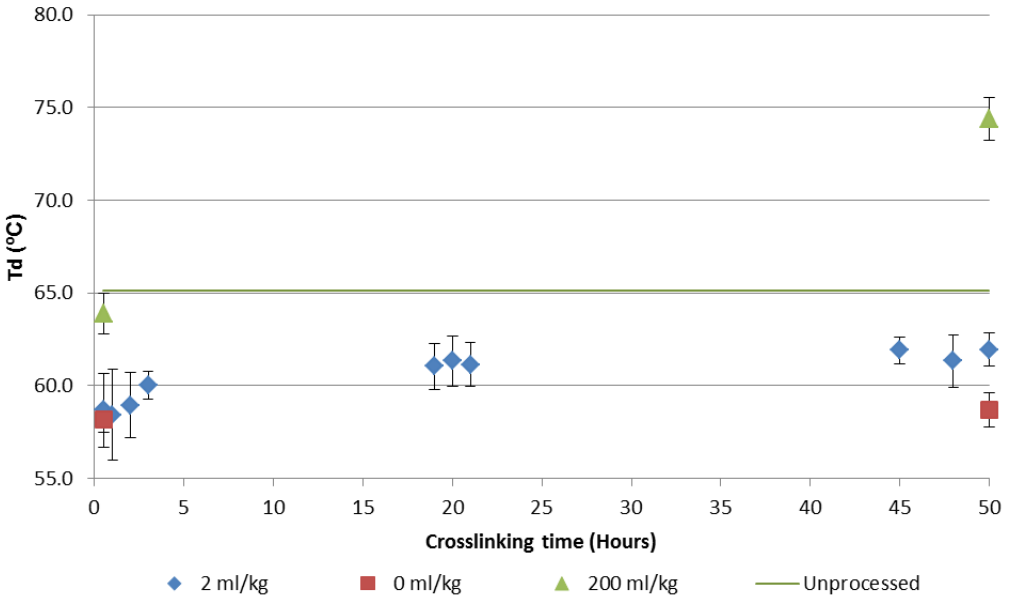

Figure 3.16 Collagen denaturation temperature, using 2 ml of HMDI per kg of collagen, varying the duration of the crosslinking reaction; diamonds 2ml HMDI/kg collagen, squares no HMDI, triangle 200ml HMDI/kg collagen, error bars ± standard deviation.

Table 3.8 Collagen denaturation temperature for varying crosslinking levels.

	Denaturation temperature (°C)	
Crosslinks (n/1000 AA)	**Average**	**SD**
0	58.9	2.6
0.5	58.5	1.6
0.6	58.7	2.0
0.8	58.9	1.8
1	59.1	1.4
1.3	60.0	0.7
1.7	61.3	1.4
2	61.1	1.2
2.3	61.8	1.3
2.5	61.6	1.1
2.6	63.9	1.1
3	62.0	0.9
3.8	63.1	1.2
5.2	64.1	1.7
7.4	66.6	1.0
8.3	68.7	1.1
8.8	67.4	4.0
11.4	74.4	1.2
Unprocessed	65.1	0.7

Increased duration of the crosslinking reaction or HDMI concentration caused an initial sharp increase in the denaturation temperatures of the collagen matrices (figure 3.15 and 3.16). The relationship between denaturation temperature and number of crosslinks present per collagen molecule had a more linear relationship

with an adjusted R^2 95% (figure 3.17). The denaturation temperatures ranged from 58°C-74°C (unprocessed dermal collagen 65°C).

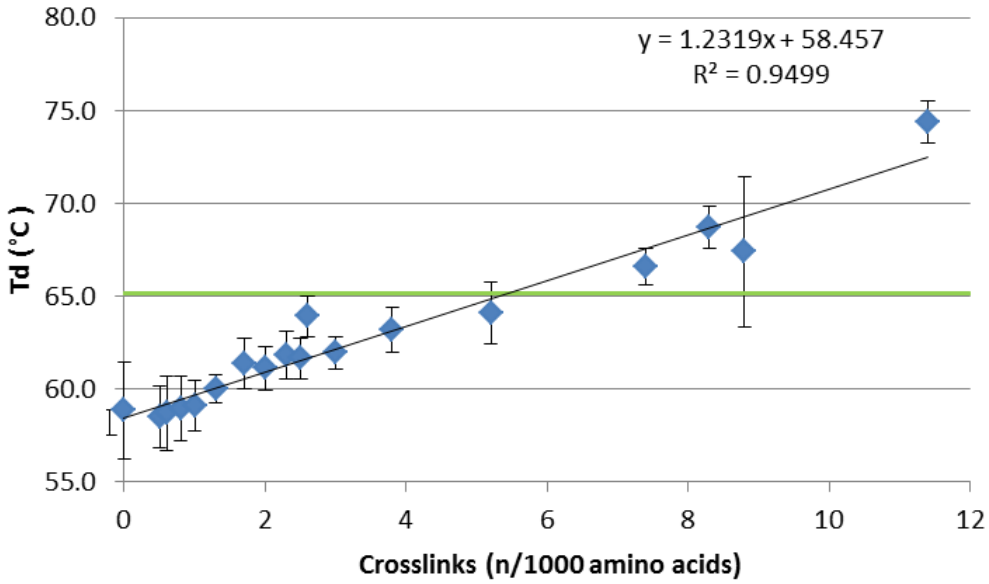

Figure 3.17 Collagen denaturation temperature v's number of crosslinks present in material per 1000 AA, error bars ± standard deviation.

Varying the Permacol™ cross-linking process affected the denaturation temperature of the dermal porcine collagen, most of the processed and crosslinked materials had a lower denaturation temperature than unprocessed porcine dermal collagen. Rearranging the trend line in figure 3.17, equation 3.3 established that 5.3 (65-58.501)/1.2283= 5.3 AA would need to be involved in the crosslinking reaction to produce a biomaterial with equivalence to non-processed porcine dermal collagen.

Equation 3.3 Linear regression equation for collagen denaturation temperature v's number of crosslinks in material per 1000 AA.

$$\frac{y-58.501}{1.2283} = x \qquad \frac{65-58.501}{1.2283} = 5.3$$

Statistical differences between the denaturation temperatures of crosslinking variables were analysed using a one-way ANOVA which returned a P value of 0.000. A 99.9% confidence level ($p<0.001$) from the ANOVA led to a Tukey's 'post-hoc' test to determine which data sets were statistically different, table 3.7 depicts the results.

Table 3.9 Tukey's post hoc test at 95% level for statistical significance between the denaturation temperature by the number of crosslinks per collagen molecule. Boxes highlighted in red are statistically different means, boxes highlighted in green are statistically similar means.

Td (°C)	n	Crosslinks (n/1000 AA)	Unpro-cessed	0	0.5	0.6	0.8	1	1.3	1.7	2	2.3	2.5	2.6	3	3.8	5.2	7.4	8.3	8.8	11.4
65.1	6	**Unprocessed**																			
58.9	6	**0**																			
58.5	6	**0.5**																			
58.7	13	**0.6**																			
58.9	6	**0.8**																			
59.5	6	**1**																			
60.3	6	**1.3**																			
61.2	3	**1.7**																			
60.9	3	**2**																			
61.8	6	**2.3**																			
61.7	3	**2.5**																			
63.9	3	**2.6**																			
62	3	**3**																			
63.1	3	**3.8**																			
64.1	3	**5.2**																			
66.6	3	**7.4**																			
68.7	3	**8.3**																			
67.4	3	**8.8**																			
74.4	3	**11.4**																			

The Tukey's post hoc test showed that 4 crosslinking variants (2.6, 3.8, 5.2 and 7.4 crosslinks/1000 AA) were similar to unprocessed porcine dermal collagen. The addition of HMDI to the porcine dermal collagen matrix affected the denaturation temperature. As duration and/or concentration of exposure to HMDI increased denaturation temperature also increased.

3.3.4 **Tensile Testing**

The tensile strength and stiffness of crosslinked variants was measured using a ball burst rig. Using this method, the orientation of the sample was no longer important, due to the anisotropic nature of collagen. The ultimate tensile strength of the material was used as an indication of strength and Young's modulus was used as an indication of material stiffness or elasticity. Figure 3.18 represents a typical stress strain curve.

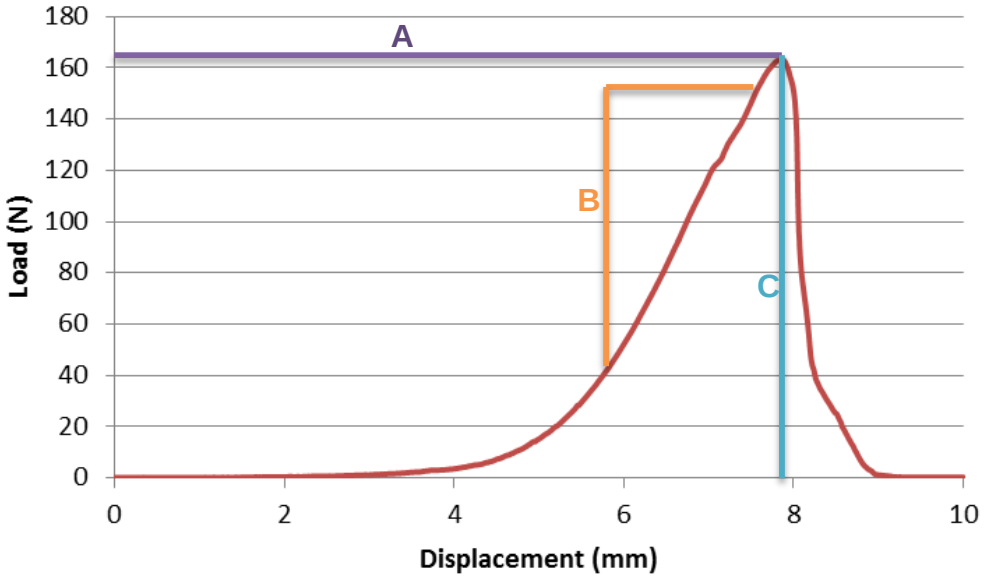

Figure 3.18 Graphical representation of stress strain curve. Line A represents ultimate tensile strength, the slope between points B is Young's modulus and C represents extension at maximum load.

Table 3.8 lists the average values and standard deviations for ultimate tensile strength, Young's modulus and the extension at maximum load for each crosslinking level (figure 3.19, 3.20 and 3.21).

Table 3.10 Crosslinking variants tensiometry results

	Ultimate tensile strength (N)		**Young's modulus (N/mm)**		**Extension at maximum load (mm)**	
Crosslinks (n/1000 AA)	**Average**	**SD**	**Average**	**SD**	**Average**	**SD**
-0.2	184.9	18.6	40.7	9.7	7.3	1.2
0	159.5	31.1	53.7	9.2	6.8	1.8
0.5	155.7	50.2	50.2	8.7	7.3	2.6
0.6	151.9	18.0	45.3	3.5	6.5	0.0
0.8	169.9	51.5	53.9	4.8	6.8	0.9
1	169.2	30.4	58.1	15.3	6.2	1.6
1.3	171.1	48.7	52.9	4.1	6.1	1.6
1.7	221.4	54.5	60.8	17.8	7.0	0.8
2	198.9	41.8	46.6	9.7	8.4	1.0
2.3	199.2	38.8	57.5	15.1	7.0	1.6

Table 3.8 (continued) Crosslinking variants tensiometry results

	Ultimate tensile strength (N)		**Young's modulus (N/mm)**		**Extension at maximum load (mm)**	
Crosslinks (n/1000 AA)	**Average**	**SD**	**Average**	**SD**	**Average**	**SD**
2.5	173.8	20.9	59.9	5.0	6.7	0.9
2.6	175.8	20.4	34.5	9.7	7.3	1.0
3	179.7	82.4	47.2	5.1	7.1	1.8
3.8	169.2	25.3	54.2	11.5	6.6	1.3
5.2	172.8	25.2	55.3	15.0	5.7	1.2
7.4	161.0	15.7	60.3	14.6	5.4	0.7
8.3	150.6	25.6	53.4	13.1	5.1	0.2
8.8	217.9	40.6	63.3	13.2	7.1	1.2
11.4	228.4	38.8	62.8	4.2	6.9	0.8

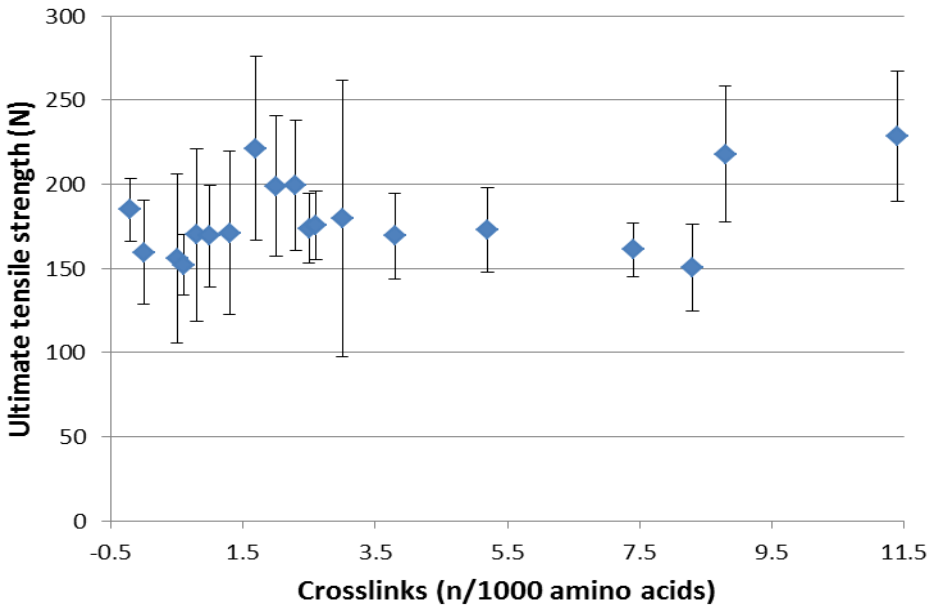

Figure 3.19 Ultimate tensile strength varying the number of crosslinks present in the material per 1000 AA. Error bars ± standard deviation.

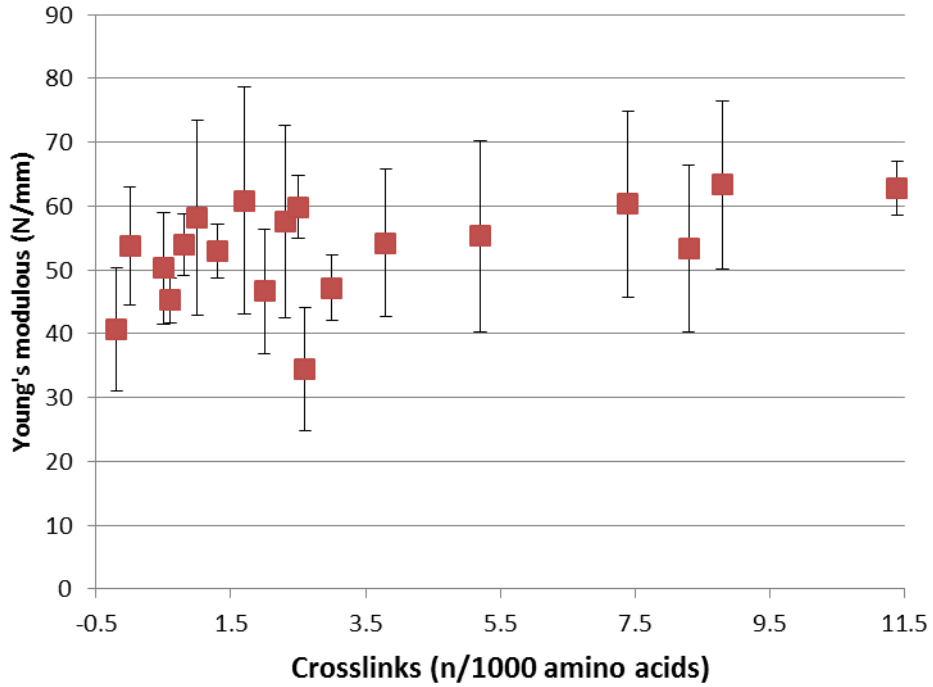

Figure 3.20 Young's modulus varying the number of crosslinks present in the material per 1000 AA. Error bars ± standard deviation.

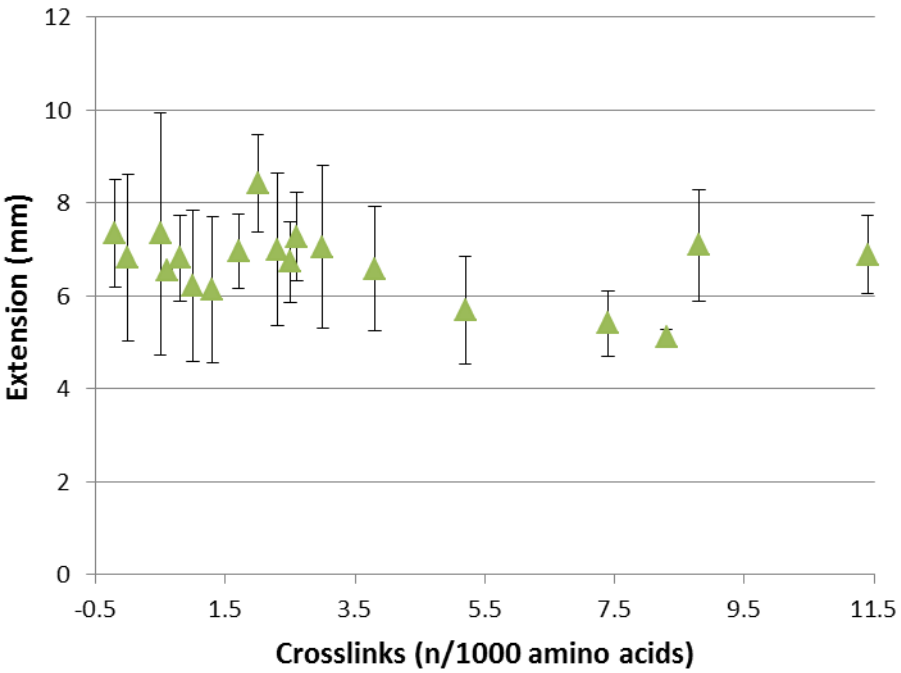

Figure 3.21 Extension at maximum load varying the number of crosslinks present in the material per 1000 AA. Error bars ± standard deviation.

There were no significant differences or trends observed in the tensile properties of the 23 different biomaterials.

3.4 Discussion

For surgeons to make an informed decision about which prosthesis will be most efficacious at a patient by patient level, materials need to be characterised. The requirement for biological meshes to undergo processing prior to implantation to produce an acellular matrix has been well established. Much conjecture still surrounds the effect of the addition of chemical crosslinks to biological meshes.

In this study, materials were fabricated with varying degrees of crosslinking. Crosslinking was altered by either varying the length of time the collagen was exposed to 2ml/kg HMDI, or by varying the concentration of HMDI with a fixed 20 hour exposure. To establish subsequent effects the materials were evaluated for AA composition, collagenase resistance, denaturation temperature and tensile properties.

Addition of HMDI to acellular dermal collagen affected the AA composition of collagen, binding to primary amines on lysine and hydroxylysine (figure 3.1). Previously studies concerned with the effect of crosslinking collagen via primary amines have used ninhydrin or trinotrobenzensulfonic acid (TNBS) calorimetric tests to determine the level of free amines remaining [29], [32], [34], [69], [71], [72]. A pilot study was carried out on the crosslinking variants produced in these studies using the ninhydrin and TNBS assays previously reported (data not shown). The degree of overlap between the crosslinking variants meant no clear differences were observed in the readings at the lower crosslinking levels. To overcome this issue an alternative HPLC based methodology was employed to determine the degree of crosslinking achieved by the different processing parameters.

Using HPLC analysis it was determined that as either the duration of exposure or concentration of HMDI increased, the number of AA used in crosslinking increased (figures 3.8, 3.9, 3.1 and 3.11). This was translated into a value of crosslinks/1000 AA (approximately the length of one collagen molecule). Material that had not been exposed to HMDI was used to establish a base level of free AA in the acellular dermal collagen matrix are attributed a value of 0 crosslinks/1000 AA. The level of AA used in the reaction varied from 0.5–11.4 per 1000 AA (Table 3.7). The percentage of lysine in collagen was greater than hydroxylysine, with a ratio of 3.5:1. The ratio remained constant as the degree of crosslinking varied; showing crosslinking was not biased to the hydroxylated or unhydroxylated form of lysine. No other AA demonstrated a trend in relation to the crosslinking reaction.

As either exposure time or HMDI concentration increased, collagen became more resistant to degradation by collagenase. A sharp rise in resistance to enzyme degradation was observed as the level of HMDI added increased. Non-crosslinked acellular dermal collagen had 22% collagen remaining after digestion, with the addition of 2 ml HMDI /kg collagen this value rose to 69% and by 10ml HMDI/kg collagen there was almost no collagen degradation observed (96% recovery). Increased exposure time increased degradation resistance with 90% achieved at 20 hours. When looking at enzyme resistance as a function of number of crosslinks present, a sharp increase in resistance was observed, levelling off at 3 crosslinks/collagen molecule. This is in line with another study which noted non-crosslinked collagen matrix after 7 hours was no longer visible whereas the HMDI crosslinked collagen matrix was still visible [69]. Collagenase resistance has also been noted in collagen matrices and gels crosslinked with formaldehyde [73], genipin [34] and oleuropein [72].

The ability to resist digestion could be beneficial if collagenase-forming bacteria are present at the implant site [74]. This attribute could be invaluable in contaminated implant sites, allowing the contaminated site to be decontaminated with the implant retaining functionality allowing the site to repair. Evidence to support this theory is currently limited but every year more case studies are being reported and clinical data gathered and analysed. Much of this data groups crosslinked and non-crosslinked biological implants together, one such systematic review was carried out on the literature available up to 2013, data to support the use of biological implants over synthetic in ventral hernia repair could not be established, though there are two further randomised trails running which may help clarify the effects [75]. A review of literature relating to biological implants carried out in 2008 listed crosslinking and field infection status as parameters affecting success and reoccurrence [76]. From this review 11 % of the implants were crosslinked with a recurrence rate of 5 % compared to 10 % for non-crosslinked implants. Of these, 14 % of the crosslinked implants and 26 % of the non-crosslinked implants were in infected fields with a recurrence rate of 4 % and 18 % respectively, these studies are a small cohort supporting the hypothesis that crosslinking improves patient outcome. Saettele *et al.* reported a case study where Permacol™ successfully replaced a failed synthetic mesh hernia repair in a contaminated field [77]. Permacol™ has also been successfully used to reconstruct the contaminated abdominal wall of a 105-year-old woman [78].

After performing a Tukeys post hoc analysis (table 3.3) on the AA concentration data it was demonstrated that changing the quantity of HMDI added to the reaction from 0ml/kg collagen to 4ml/kg collagen did not produce statistically different data sets. However this range was critical in achieving resistance to enzyme

degradation. Increasing the concentration of HMDI above 50ml/kg collagen gave data sets that were not statistically different, indicating that lysine consumption in crosslinking had plateaued. Changing exposure time to HMDI had less of an effect than altering the concentration, with only extreme data sets being statistically different. When comparing exposure time to concentration, the longest exposure times 45–50 hours showed equivalence to 20 hours with 10ml HMDI/kg collagen for lysine.

The lysine concentration of collagen produced using the Permacol™ parameters showed equivalence between 0.1ml-4ml HMDI/kg collagen at 20 hour exposure and 2ml HMDI/kg collagen at 0.5-50 hours.

The extreme crosslinked samples showed that exposure time to HMDI could be significantly decreased (from 20 hours to 0.5 hours) if HMDI concentration was increased 100 fold. The degree of crosslinking was similar to the commercially available Permacol™ surgical implant.

DSC data examining the denaturation temperature of the materials had an inverse relationship to the AA data. As crosslinking increased, denaturation temperature increased. The range of denaturation temperatures observed for the acellular dermal collagen matrices was 58 - 67°C. Liang *et al* demonstrated a similar trend with bovine pericardium crosslinked with genipin which showed an increase in denaturation temperature from 62°C to 77°C depending on crosslinking level [34]. The denaturation temperature of the material prior to processing was measured at 65°C. This would indicate a change in material composition, during processing to remove cells and fats. This processing could also have broken some of the natural crosslinks / structure present in the starting dermal material..

At the maximum duration (2ml HMDI, 50 hours) the denaturation temperature was equivalent to 2–10 ml HMDI for 20hrs. The denaturation temperature of standard commercially available Permacol™ showed equivalence to using a concentration between 0.1ml and 10ml HMDI/kg of collagen for 20 hours and exposing the collagen for 3–50 hours to 2ml HMDI/kg of collagen.

Addition of crosslinks to the matrices did not have a significant effect on tensile or elastic material properties. The dermal collagen used was a natural product and a large variation was observed within each data set.

It is well established that the addition of crosslinks to collagen biomaterials increases resistance to degradation by collagenase [62], [73], [79] and increases the materials denaturation temperature [33], [34], [70]. The data in this chapter supports the previous findings that if exposure to HMDI was increased, the resistance of collagen to degradation by collagenase was increased, free lysine / hydroxylysine concentration decreased and denaturation temperature increased. Previous studies comparing non-crosslinked and crosslinked biomaterials only looked at a few variants [33], [69], [80], [81], Liang *et.al* reported the most with 4 crosslinking variants characterised [34]. In the studies reported in this thesis, over 20 crosslinking variants, from non-crosslinked to 11.4 crosslinks per 1000 AA, were produced and characterised. Characterising a large range of crosslinking levels has enabled a better understanding of the dynamics of how collagenase resistance and denaturation temperature increases in relation to crosslinking level. With only a few crosslinks required to impart significant collagenase resistance and maximal resistance achieved with only 3 crosslinks per 1000 AA. The relationship between crosslinking and denaturation temperature was linear allowing a linear

regression equation to be established, using the denaturation temperature this equation could quickly establish the level of crosslinking present within materials prepared via the proprietary Permacol™ process.

4 Effect of crosslinking on leukocyte activation

4.1 Introduction

Leukocytes play an important role in would healing by producing cytokines, reactive oxygen species (ROS) and enzymes, which direct the way in which a damaged tissue returns to a normal homeostatic state. Leukocytes can be activated by a range of stimuli including damaged tissue, cell debris, microorganisms, pattern recognition receptors (PRRs) and foreign bodies [82]. This series of experiments investigated the influence of crosslinks in acellular porcine dermal matrices on leukocyte activation.

Cytokines and other small molecules released by leukocytes signal in both endocrine and paracrine fashions to a plethora of immune cells including B-cells, T-cells and monocytes to progress inflammation and ultimately resolve wound healing. Nicotinamide adenine dinucleotide phosphate-oxidase (NADPH oxidase) is a multimeric membrane bound enzyme resident on the surface of leukocytes. This enzyme is fundamental in leukocyte signalling and host defence through generation of ROS in a process called the respiratory burst[83], [84], (figure 4.1). ROS play an integral role in inflamation by stimulating production of cytokines, acting as cell signal molecules and recruting neutrophils and macrophages to the site of tissue damage or infection [85], [86]. Excessive or quenched ROS production at an implantat site will impact device efficacy, integration and longevity. Excessive ROS could lead to chronic inflamation, poor wound healing, and damage to otherwise healthy native tissue [39], [87], [88]. If ROS are supressed, signaling pathways to recruit cells required for healthy wound healing may be inhibited, possibly leading to infection, poor angiogenesis, unstable device integration and ultiamtely, implant faliure.

Leukocytes are critical in a healthy inflammatory response and the foreign body interrogation. Leukocyte response to implantable biomaterials plays an important role in implant efficacy and subsequent return to full activity of the patient. *In vitro* chemilluminescence tests can be employed to assess whole blood leukocyte ROS production in the presence of crosslinked and non-crosslinked biomaterials. The ability to test for leukocyte activation prior to surgery could aid in implant selection by personalising graft selection. This would allow an individual to receive the most appropriate implant for them specifically, based on a simple pre-operative screen to assess the influence of a panel of prospective implants on this fundamental component of their acute inflammatory reaction.

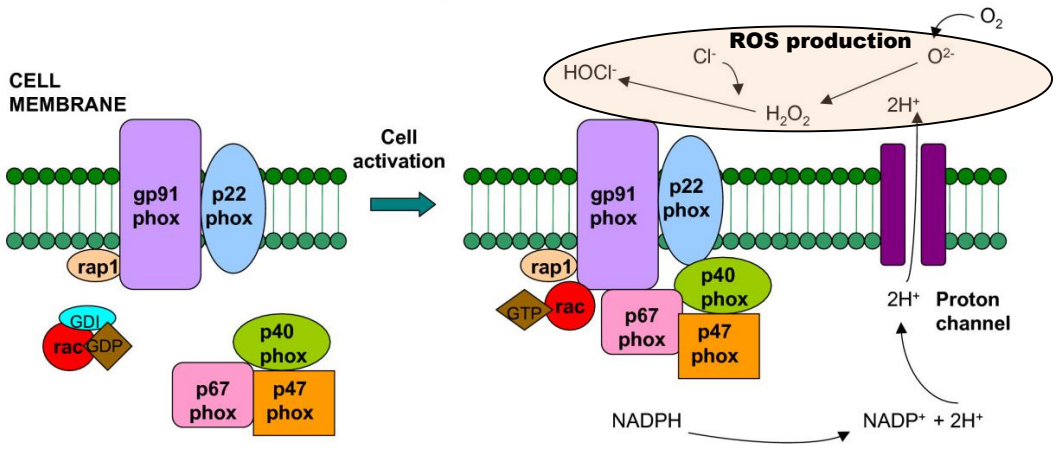

Figure 4.1 The role of NADPH oxidase in ROS production[89].

4.2 Aim

These studies aimed to investigate how altering the extent of crosslinking in porcine dermal collagen affected ROS productionby healthy human peripheral blood leukocytes.

4.3 Results

4.3.1 Material stimulated Leukocyte activation

ROS release in response to materials was quanitified using Pholasin® a luminescent photoprotein derived from *Pholas dactylus*, a marine mollusc, which emits measurable photons in the presence of ROS. Light emission (RLU) was measured over a 130 minute period to asses the influence of materials on leukocyte respiritory burst. RLU measured during this period were combined to get a "total RLU" for each sample. At 130 minutes formyl-methionyl-leucyl-phenylalanine (fMLP) was added to the reaction as a positve activation control of NADPH oxidase. At 160 minutes phorbol-myristate-acetate (PMA) was added causing degranulation of the cells to release total ROS remaining in the population. Figure 4.2 shows a typical RLU profile produced by the assay, readings were taken from each well approimately every 30 seconds, 3 wells were used for each material, points have been plotted as a continuous line.

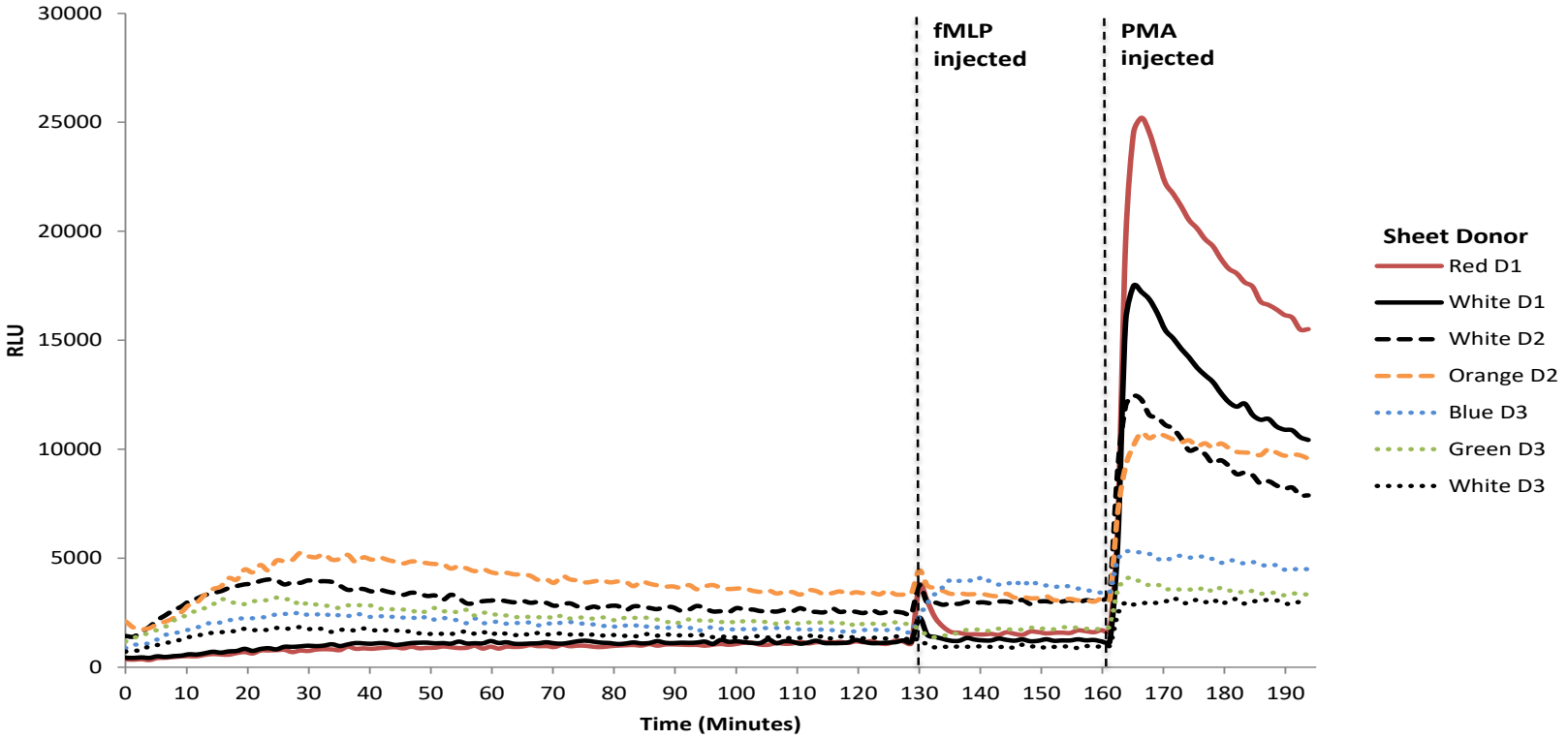

Figure 4.2 Leukocyte ROS production in response to acellular porcine dermal matrix with a crosslinking level of 1.7 crosslinks per 1000 AA. Each line represent mean RLU production n=3, for donors 1-3 (D1, D2 and D3) response to different sheets (red, white, orange, blue and green)

Initially, ROS production from 3 different donors' (D1, D2 and D3) whole blood to a range of crosslinking and source tissue sheets was examined. The initial sheet of dermis used to manufacture the materials was tracked by color (red, white, orange, blue and green), to establish if differences were due to crosslinking level or sheet origin.

In figure 4.3 the mean total RLU production for each sheet / donor combination (n=3) and mean ROS production for each crosslinking level. Donors 1 and 3 have similar total ROS generation all below 20000 RLU, whereas donor 2 were all above 30000 RLU. ANOVA analysis on the 3 donors total RLU values ($P<0.000$), indicated that this difference was significant. This was investigated further using Tukey Post Hoc ranking which confirmed the responses of donors 1 and 3 were statistically comparable however donor 2 was significantly different.

When examining the relationship between total RLU and crosslink number no clear correlations could be made. Figure 4.4 shows the total RLU production for donor 3 to crosslinked materials, 14 out of 22 error bars lie across the average line depicted, including the highest and lowest crosslinking levels.

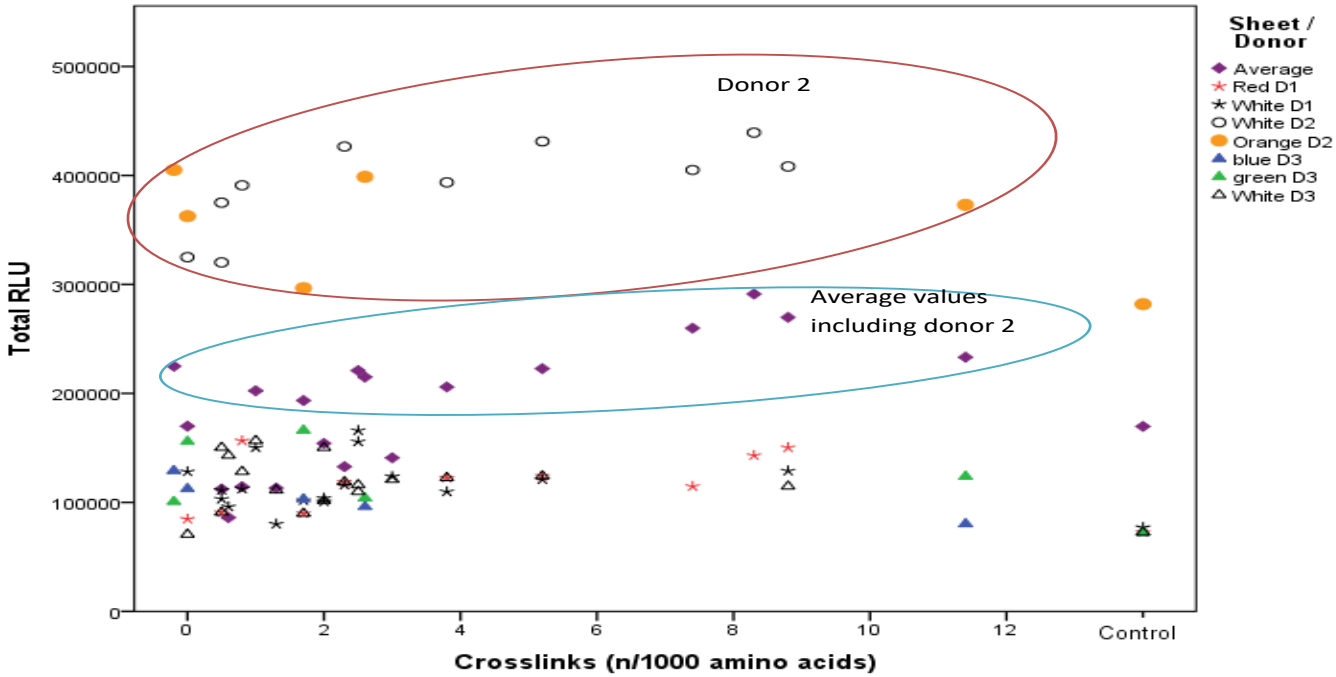

Figure 4.3 Mean total RLU, 3 donors, varying levels of crosslinked material and the average total RLU production for all 3 donors. Each point (except the average, purple diamonds) represent mean RLU production n=3, for donors 1-3 (D1, D2 and D3) response to different sheets (red, white, orange, blue and green)

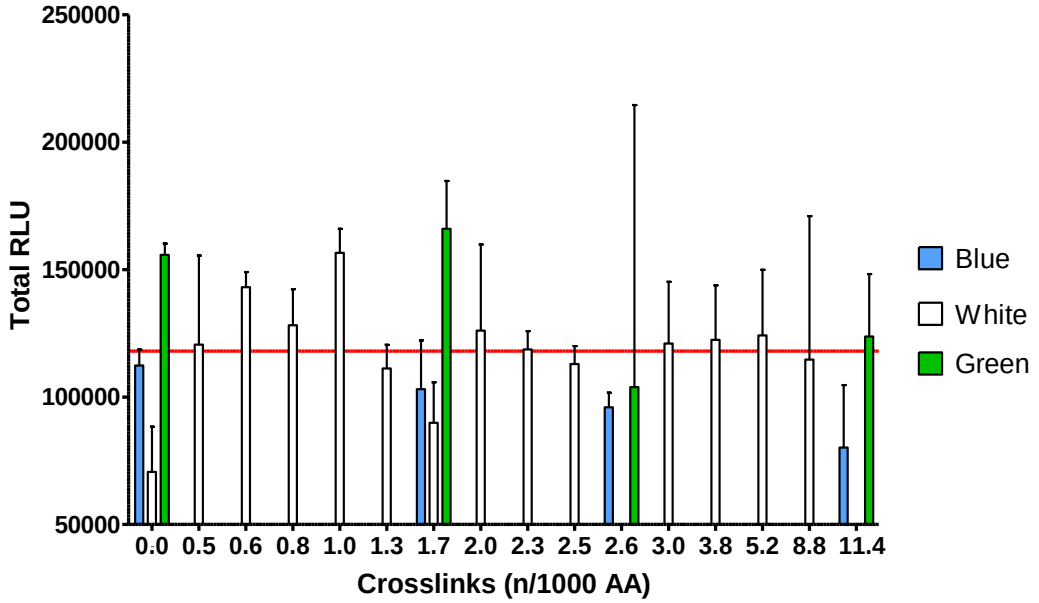

Figure 4.4 Mean total RLU production for donor 3, green blue and white sheets with varying crosslinking levels (n=3), red line represents average RLU across all materials, error bars +standard deviation.

To establish if changes in ROS were material or donor specific, further assays were performed using the orange sheet set of samples with -0.2, 0, 1.7, 2.6 and 11.4 crosslinks per 1000 AA. The assay was repeated using donors 1, 2 and 3 and an additional 4th donor.

Figure 4.5 shows total RLU from the first experiments and subsequent tests on the orange sheets. The control samples showed the total RLU from blood solely exposed to tissue culture plastic (TCP). The first time blood from donor 2 was exposed to the orange sheets total RLU was approximately double the total RLU expressed on the subsequent analysis. On the second analysis, the response of donor 2 to the material was comparable with the remaining donors. The validity of

donor 2's first set of data remained, biological systems change so the results obtained on a day-to-day basis can vary. Performing an ANOVA analysis on average results, no significant differences were reported.

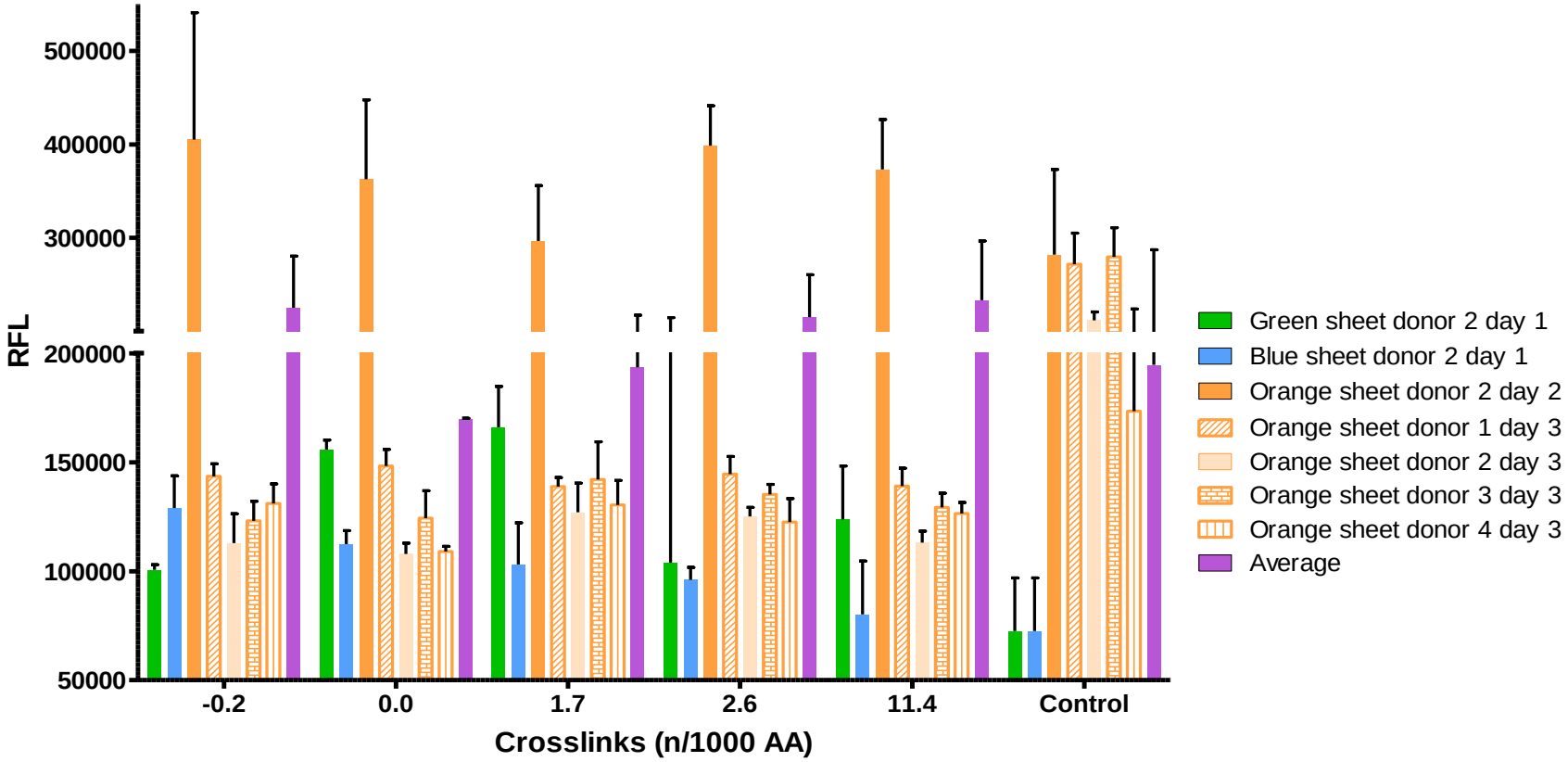

Figure 4.5 Mean total RLU production for 4 different donor's whole blood to material with -0.2, 0, 1.7, 2.6 and 11.4 crosslinks per 1000 AA (n=3), error bars + 1 standard deviation from the mean.

A more extensive study with 10 healthy volunteers compared three crosslinking levels:

- Non-crosslinked (0.0 crosslinks per 1000 AA),
- Permacol™ (1.7 crosslinks per 1000 AA)
- Highest crosslinking level recorded (11.4 crosslinks per 1000 AA)

9 out of the 10 donors had the highest ROS production associated with the highest crosslinking level (figure 4.6). Using an ANOVA test no significant difference was observed between the non-crosslinked and Permacol™ variants; however the highest crosslinking levels did induce significant differences ($P < 0.001$) in cell response compared to lower crosslinking levels.

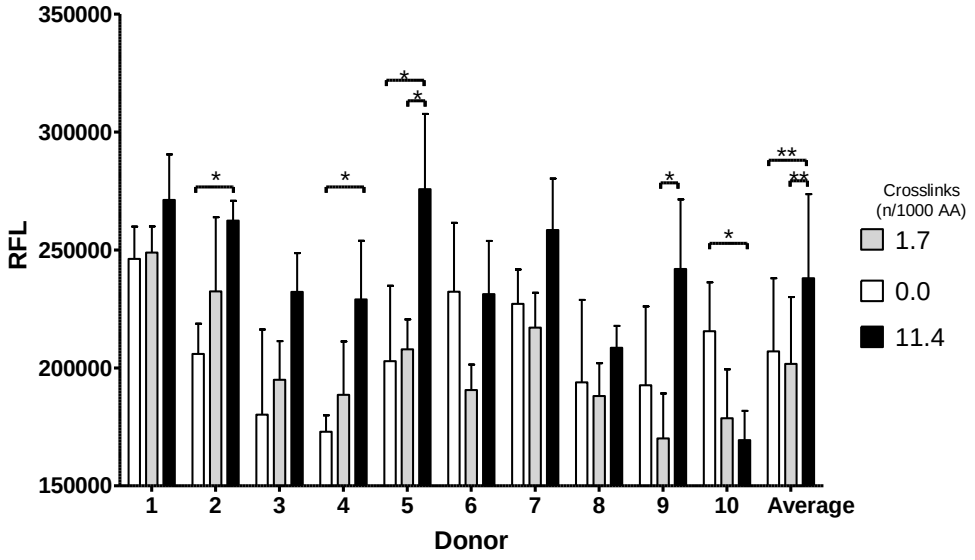

*Figure 4.6 Mean ROS production from 10 donor's whole blood to materials with 0.0, 1.7 and 11.4 crosslinks per 1000 AA (n=3) and the combined mean of all 10 donors (n=30). * P<0.05 ** p<0.01, error bars + standard deviation.*

Concurrently the 10 donor's blood was assessed against 3 other commercial collagen based implants comprising both different species (human and porcine) and different source tissues (dermis and small intestinal submucosa):

- Strattice® firm (LifeCell corp., US), an acellular porcine dermal matrix not chemically crosslinked [90].

- Alloderm® (LifeCell corp., US), acellular cadaveric human dermal collagen, not chemically crosslinked [91].

- Surgisis® (Cook medical, US), porcine small intestinal submucosa, not chemically crosslinked, 4 or 8 layers laminated [92].

Figure 4.7 shows the mean ROS production from the 10 donors when exposed to 4 commercially available biomaterials. The 3 biomaterials derived from dermal collagen (Permacol™, Alloderm and Strattice) exhibited no statistical differences in the donor responses. However for eight out of the ten donors Surgisis® elicited a greater leucocyte reaction when compared to at least one of the other commercially available implants.

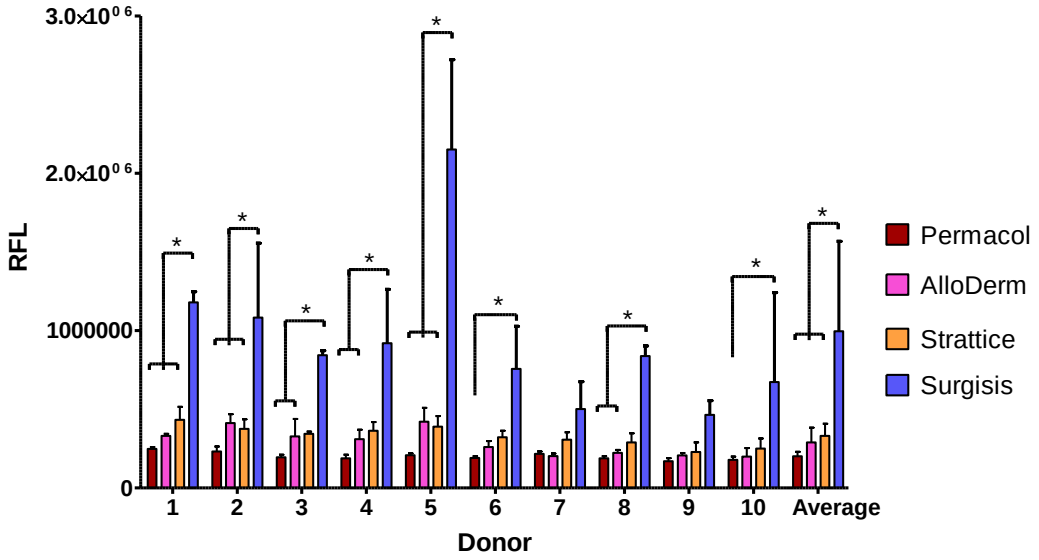

*Figure 4.7 Mean ROS production from 10 donor's whole blood to commercialy available materials, Permacol™, AlloDerm, Strattice and Surgisis® (n=3) and the combined mean of all 10 donors (n=30). * P<0.05, error bars + standard deviation.*

Figure 4.8 shows the total RLU for all 10 donors. Boxes represent upper and lower quartile range; whiskers extend to highest and lowest data points with outliers represented by stars (greater than ± 2 residual values, calculated by Minitab). The control box shows the total RLU from blood solely exposed to TCP.

There were no differences between the donors total RLU profiles to all materials (P<0.243). However, considering the 7 materials (6 collagen based and tissue culture plastic) P<0.000, signifying a statistical significance exists in the data. To establish which groups were statistically different a Tukey Post Hoc test was used, grouping all the materials together with the exception of Surgisis®.

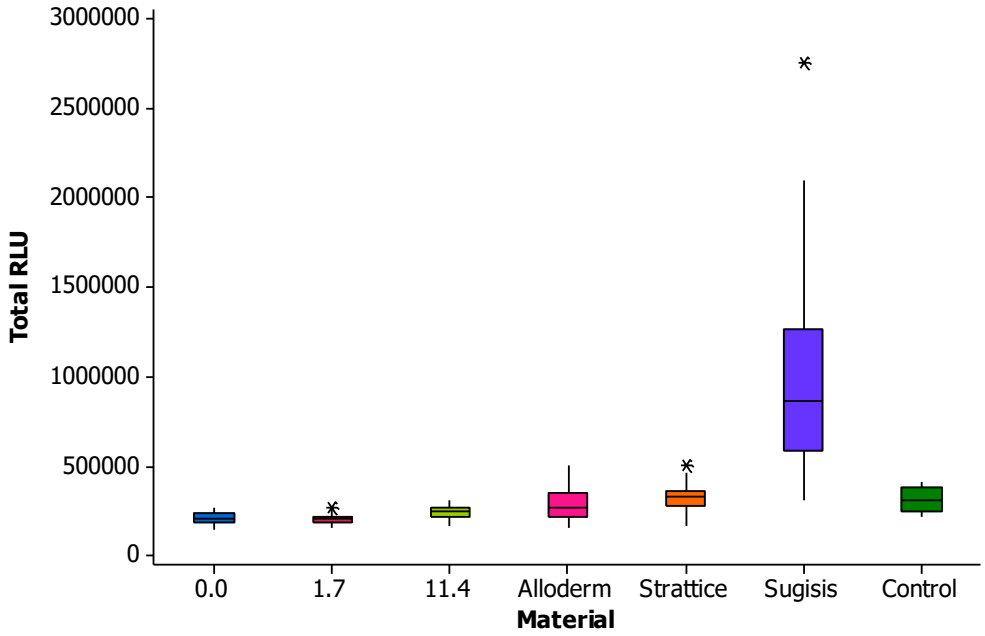

*Figure 4.8 Box and whisker plot of total RLU for 10 donors blood(n=30) to material with 0.0, 1.7 and 11.4 crosslinks per 1000 AA, Alloderm, Strattice, Surgisis® and tissue culture plastic. * indicates outlier greater than ± 2 residual value away from the median value.*

Data from the 3 sets of experiments was combined (excluding donor 2 day two) (figure 4.9). Donor 2 day two was excluded from this set as not every crosslinking level was assessed in that experiment, any points included skewed the data. Figure 4.9 shows no correlation exists between crosslinking and ROS production *in vitro.* Average value for 15 out of the 19 data sets had lower leukocyte activation than when the cells were exposed only to TCP (dashed line on figure 4.9).

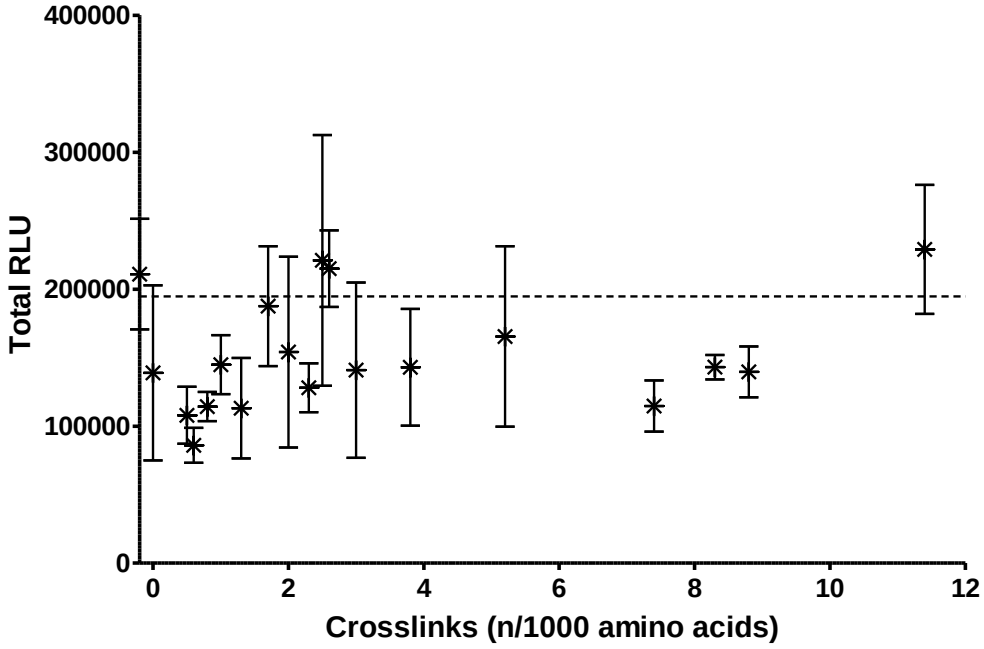

Figure 4.9 Average total RLU for the crosslinking variants (excluding donor 2 day 2), error bars ± 1 standard deviation from the mean, dashed line represents control cells exposed to TCP.

No clear relationship was seen between the number of crosslinks and *in vitro* ROS production.

4.4 Discussion

All implanted biomaterials will elicit an acute inflammatory phase, from the host cellular response to the implanted material and to the surgical trauma during implantation. The level of this response will influence the efficacy of the repair and wound maturation, the ability to asses leukocyte activation via ROS production could be a useful evaluation tool.

The initial assessment of ROS production to material with varying degrees of crosslinking (figure 4.3) considered 3 healthy donors. 2 of the donors had similar ROS production across the differing crosslinked materials. Donor 2 produced significantly more ROS.

To understand if this was an isolated incident, another donor was recruited. All 4 donor's ROS production against the same 5 fabrication variants (-0.2, 0.0, 1.7, 2.6 and 11.4 crosslinks per 1000 AA) were tested on the same day (figure 4.4). No differences were observed in ROS production between donors or materials. Control wells of no material (whole blood exposed to TCP) were run on each experiment, on both occasions donor 2's ROS production elicited by TCP were similar. This indicated that increased ROS production was a specific material mediated response as opposed to the donor having raised ROS activity on that day due to unforeseen physiology.

A 10-donor study was carried out on a single day. In the experiment, donor's whole blood was exposed to 6 biomaterials (0.0, 1.7 and 11.4 crosslinks per 1000 AA, Strattice firm, Alloderm and Surgisis). All materials apart from Alloderm, an allograft, were xenografts of porcine origin. Surgisis® was the only implant not made from dermal collagen instead being manufactured from layers of small

intestinal submucosa. Figure 4.6 shows total RLU production for each material across all 10 donors. Porcine dermal materials, crosslinked or non-crosslinked, were grouped together without inter-material statistical differences. Total RLU elicited by Surgisis® however was significantly higher than all the other materials. Surgisis® also had the greatest spread in data points with some points almost being 10 times higher than the lowest indicating a substantial inter-donor variation in response to this material vs. the remaining materials tested.

The variations observed in ROS production for the 10-donor study was interesting. This study highlighted the different effects biomaterials could have on a patient's response and ultimate recovery from surgery. Limited differences were observed between the three commercially available biomaterials derived from dermal collagen (Permacol™, Strattice and AlloDerm), the biomaterial derived from SIS caused a significantly greater response from the donor leukocytes in 8 donors. The increased response observed towards the SIS implant may partly be caused by it being a laminated material (8 layers of SIS bonded together), as on separating these layers offer a larger surface area of the material to cells than single layer materials [39]. The presence of the bonding agent may also increase the response compared to SIS alone. A simple test such as the leukocyte activation assay carried out in these studies could be utilised prior to surgery to establish which material would be most appropriate for the individual patient. This type of testing could help understand the variability of patient response not apparent on clinical examination [93].

Taking all ROS data across the crosslinking variants (figure 4.6) no relationship was present between leukocyte activation and the number of crosslinks present.

When adding a linear regression line to the data an R^2 value of 0.05 was returned. Large standard deviations also exist, with many of the data sets overlapping.

A study previously published by Bryan *et al.* [39] used the same methodology to asses synthetic hernia meshes. The textiles were made from polypropylene (PP), polyethyleneterephthalate (PET), polyglycolic acid (PGA) and were knitted from either monofilament or multifilament yarns. ROS production from 'cells without textile' or cells response to tissue culture plastic (TCP) were in line with levels observed in my experiments (figure 4.5), allowing a direct comparison between studies. None of the materials tested by Bryan *et al.* could be grouped with 'cells without textile' with all the fabrics stimulating greater ROS production from leukocytes than the TCP, based on a Waller-Duncan post hoc analysis $P<0.05$. Multifilament yarns produced the greatest response, with PGA being the most reactive material. In my studies, all biomaterials tested with the exception of Surgisis® had similar ROS production from leukocytes when compared to TCP. Bryan *et al.* concluded that 'yarn confirmation – monofilament vs multifilament – plays a greater role in cellular activation that the polymer chemistry'. Multifilament yarns have a greater surface area when compared to monofilament yarns, supporting the theory that the surface area of Surgisis® contributed to its higher leukocyte activation. Comparing average leukocyte activation in figure 4.9 15 of the 19 crosslinking variants tested were lower than TCP in the Bryan *et al.* study. All of the average leukocyte activation for the synthetic materials were greater than TCP. This indicated that synthetic materials have a greater capacity to activate leukocytes than biomaterials derived from dermal matrices.

Liu *et al.* carried out two *in vivo* studies using bioluminescence to measure ROS production [94]. The first experiment subcutaneously implanted polystyrene beads (synthetic), PBS (control) and untreated (background) and bioluminescence was measured indicating the level of ROS production over 60 minutes. In this study, an initial burst of ROS production was observed peaking at 20 minutes in all 3 groups, the *in vitro* work carried out by these groups showed a peak at 30 minutes (figure 4.2). Control levels increased slightly over background for 40 minutes and then converged for the remaining 4 time points. Synthetic implants induced a much stronger ROS production. The second study measured ROS production periodically over a 28-day time course in relation to subcutaneously implanted polystyrene beads (synthetic), alginate (biological) implants and PBS (control). Liu *et al.* findings support the *in vitro* data reported in this thesis with biological and control samples having similar ROS levels at the first time point (1 day) and synthetic implants eliciting a greater ROS response from the host.

Surgeons could use leukocyte activation testing preoperatively to help inform their choice of surgical implant. Testing could provide additional information regarding the patient's response to the proposed implant material. An elevated response could be an indication that the implant may be 'rejected' by the patient resulting in poor integration and not recovering full site integrity.

Considering the leukocyte activation observed throughout these experiments, the number of crosslinks present in a material did not significantly influence the host's respiratory burst. The commercially available collagen based hernia implants, designed to have minimal antigenicity, showed that harvest location and processing of implant material have an impact on leukocyte activation with submucosa having

a significantly higher ROS response than dermal collagen [85]. On average, the biomaterials tested showed lower leukocyte activation when compared to synthetic hernia fabrics tested by Bryan *et al* [39].

5 Effect of Crosslinking on Immune Response

5.1 Introduction

Biomaterials have been used extensively in soft tissue repair but the inflammatory response of these materials is not fully understood, especially the effects caused by the addition of chemical crosslinks.

A large proportion of literature comparing crosslinked versus non-crosslinked biomaterials use materials which have undergone different manufacturing processes [63], [95]–[107]. Making it difficult to establish if differences observed in response to implanted biomaterials are due to the presence of crosslinks, other manufacturing processes, harvest location or species.

Animal models have been used to study biomaterial characteristics and interactions[108]. Selection of an appropriate animal model is critical in being able to answer the research question being posed. Selection criteria should include ethics, species, strain and anatomy. Currently small animal (rodents[80], [109], [110] and rabbits [111]–[114]) and large animal (sheep [115], [116] and pigs[66], [95], [101], [102], [117]) are used for studying biomaterial behaviour.

Rodents are the most common species for the assessment of inflammation, immune response, integration and angiogenesis. Partly due to their size and behaviour making them easy to handle and requiring less space and resources over the study. More recently the ability to produce genetically modified strains to help mimic disease states and knock out gene functions has increased rodent use [118]. Acute and chronic inflammation phases can be studied post subcutaneous implantation as this technique causes minimal trauma to the surrounding tissue and does exert load

onto the implant. Resultant histological and morphological features observed can be due to the host cellular interactions with the implanted material. To bring mechanical properties of the host and biomaterial into the experimental design an abdominal wall defect model would be used.

Acute and chronic host response to subcutaneously implanted biomaterial can be measured by macroscopic observations and microscopically by type and frequency of host cells surrounding and entering the implanted biomaterial.

5.2 Aim

The aim of these studies was to investigate how altering the extent of crosslinking in porcine dermal collagen affected the immune response in a sub cutaneous implantation *in vivo* rat model.

5.3 Results

From the data provided in the previous studies three materials were selected for implantation. Non-crosslinked, Permacol™ (1.7 crosslinks / 1000 AA) and highly-crosslinked (11.4 crosslinks / 1000 AA).

All animals survived the surgery and implantation terms. Animals were euthanised after 2, 7, 14 and 28 days *in vivo* incubation. Skin was dissected away from underlying tissues exposing implants. Macroscopic observations of implants prior to removal were made noting the presence or absence of key features. These features were seromas / haematomas, implant degradation, vasculature and attachment to underlying musculature.

After recording macroscopic features, the implant including surrounding tissue and underlying tissue was dissected and fixed in NBF. Implants were dehydrated and embedded in resin as described in 5.2.1. 7µm sections were cut form all samples and tinctoral and immunohistochemical staining was performed.

Haematoxylin and eosin (H&E), Van Geison and picro sirius red were used for semi-quantitative histological scoring. Semi-quantitative histological scoring criteria were established and sections were examined for the features in table 5.1.

Table 5.1 Semi-quantitative histological scoring criteria, units per field view.

	Level				
Criteria	**Absent - 0**	**Slight - 1**	**Moderate -2**	**Marked - 3**	**Severe - 4**
Granulocytes - Neutrophils, eosinophil and basophils. (Cells)	0	1-5	5-20	21-50	> 50
Lymphocytes - T cells, B cells and natural killer cells. (Cells)	0	1-2	3-4	5-10	> 10
Fibroblasts (Cells)	0	1-5	5-20	21-50	> 50
Macrophages (Cells)	0	1-2	3-4	5-10	> 10
Giant cells (Cells)	0	1-2	3-4	5-10	> 10
Material residue - Integrity of the implant and its disappearance (implant remaining)	0%	1-33%	34-66%	67-90%	> 90%
Degradation - Evaluation of physical degradation of the implant. (Implant remaining)	> 90%	67-90%	34-66%	1-33%	0%
Fibroplasia - Non-homogeneously orientated collagen, with neo / vascularisation. (Interface)	0%	1-33%	34-66%	67-90%	> 90%
Fibrosis [77] - Organised and orientated mature collagen, lacking vascularisation. (Interface)	0%	1-33%	34-66%	67-90%	> 90%

Table 5.1(continued) Semi-quantitative histological scoring criteria, units per field view.

	Level				
Criteria	**Absent - 0**	**Slight - 1**	**Moderate -2**	**Marked - 3**	**Severe - 4**
Integration - Continuity between native tissue and tissue colonising the implant. (Integration)	0%	1-33%	34-66%	67-90%	> 90%
Colonisation - Penetration of cells / ECM into the implant. (Penetration)	0	1-12%	12-25%	25-40%	> 40%
Neo-vascularisation - Formation of new vasculature. (Vessels)	0	1-5	6-10	11-15	> 15
Encapsulation - Concentrical organisation of mature collagen deposits that isolate the implant from host tissue. (Implant isolated)	0%	1-33%	34-66%	67-90%	> 90%
Oedema - Fluid build-up. (implant isolated)	0%	1-33%	34-66%	67-90%	> 90%
Haemorrhage - Presence of red blood cells outside of vessels. (Haemorrhage)	0	1-2	3-4	5-10	> 10
Necrosis - Amorphous fibrin like material. (interface)	0%	1-33%	34-66%	67-90%	> 90%

Haematoxylin, naphthol AS-D chloroaceate (ASD), α-Naphthyl Aceate (αASD) and immunohistochemistry were used for quantitative histological scoring. Stains with associated cell types are listed in table 5.2.

Table 5.2 Stains used for quantitative histological scoring, tinctoral or immunohistochemistry and cell type identified by stain.

	Stain / Antibody	Cell type
Tinctoral	Haematoxylin	All cell nuclei
	ASD	Neutrophils, mast cells and basophils (mast cells pulled out as a separate population)
	αASD	Monocytes, macrophages and histiocytes
Immunohistochemisty	CD5	T-cells
	CD68	Activated macrophages
	Col-1	Collagen I (area not cell count)
	FH-7A	Collagen III (area not cell count)

Light microscopy was used to examine the sections in bright field. Picro sirius red stains were examined with and without a polarising filter (figure 5.1).

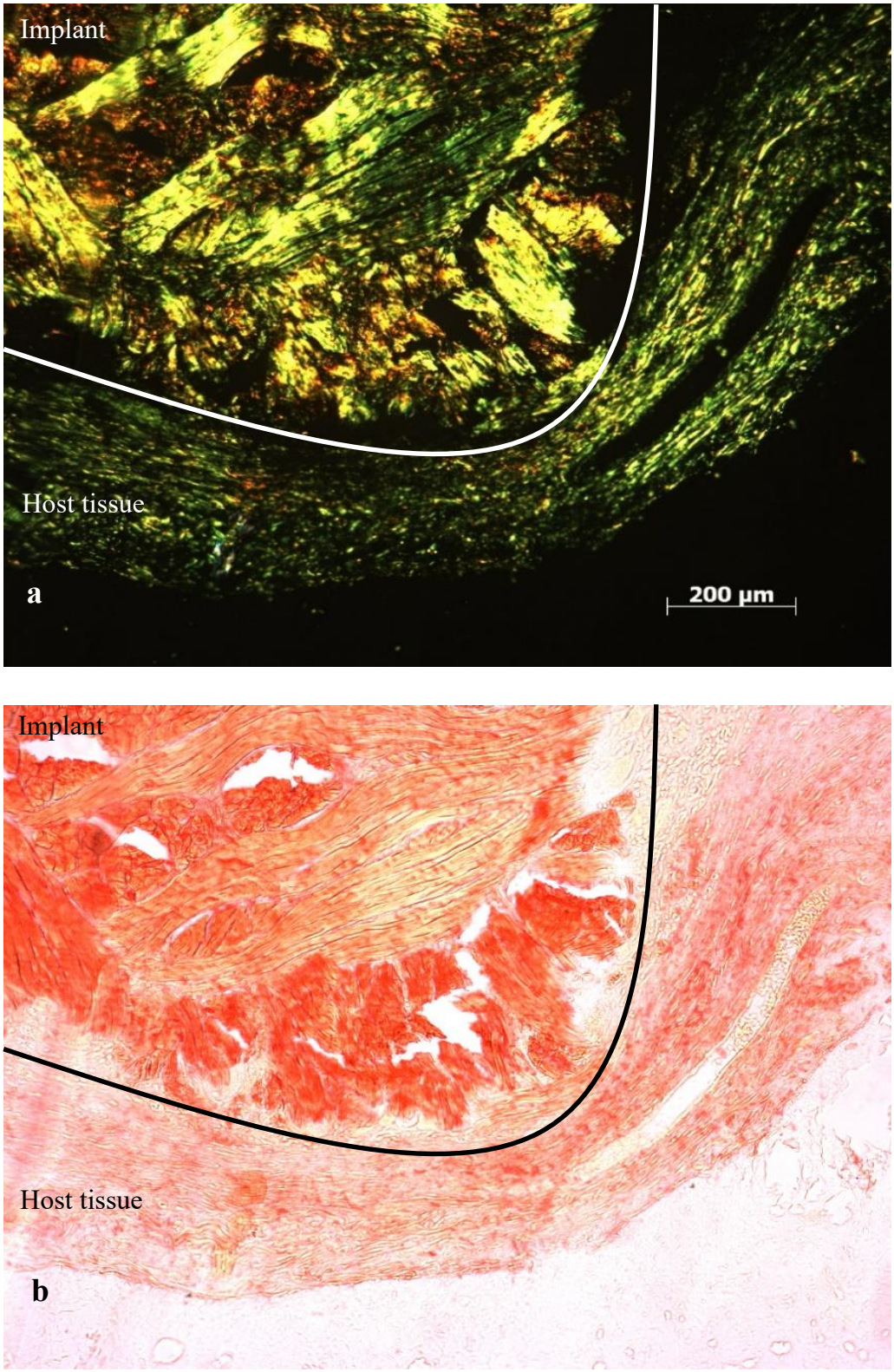

Figure 5.1 Pico sirus red stain of Permacol™ 14 days post implantation, a) with polarising filter b) without polarising filter (20X magnification). Host / implant interface highlighted by white line in image a and black line in image b

5.3.1 **Day 2 implant observations**

After 2 days *in vivo* incubation a layer of fascia had formed over all implants and implants had adhered to the underlying musculature. Several seromas / hematomas were observed across all crosslinking levels. No association between crosslinking level and seroma / hematoma frequency could be established. Figure 5.2 shows a hematoma after 2 days *in vivo* incubation. The seromas may partly be due to surgical trauma or angiogenesis, were cells are pooling at the ends of blood vessels forming over the implant. No macroscopic inflammatory differences were observed between the different crosslinking levels.

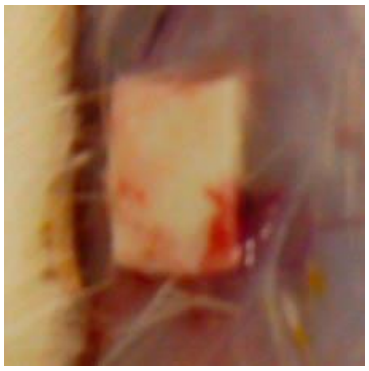

Figure 5.2 Implant images, Permacol™ 2 days post implantation, with a hematoma.

No degradation of the implants was noticeable; all implants were attached to the underlying musculature. From the macroscopic observations no clear differences were observed between the different crosslinking levels, see figure 5.3 for frequency of macroscopic observations.

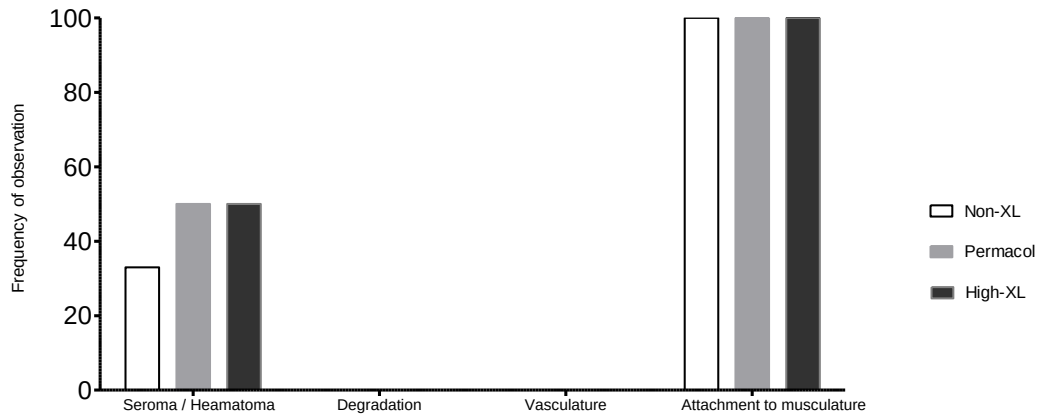

Figure 5.3 Macroscopic implant observations for day 2 implants.

Histological analysis of implants confirmed an inflammatory response was present for all implants. Cells accumulated at the host / biomaterial interface see figures 5.4 and 5.5. The interface is clearly visible between host tissue and implant. Connective tissue can be seen forming between the host tissue and implant, backing up the macroscopic observations that the implants were all attached to the underlying musculature.

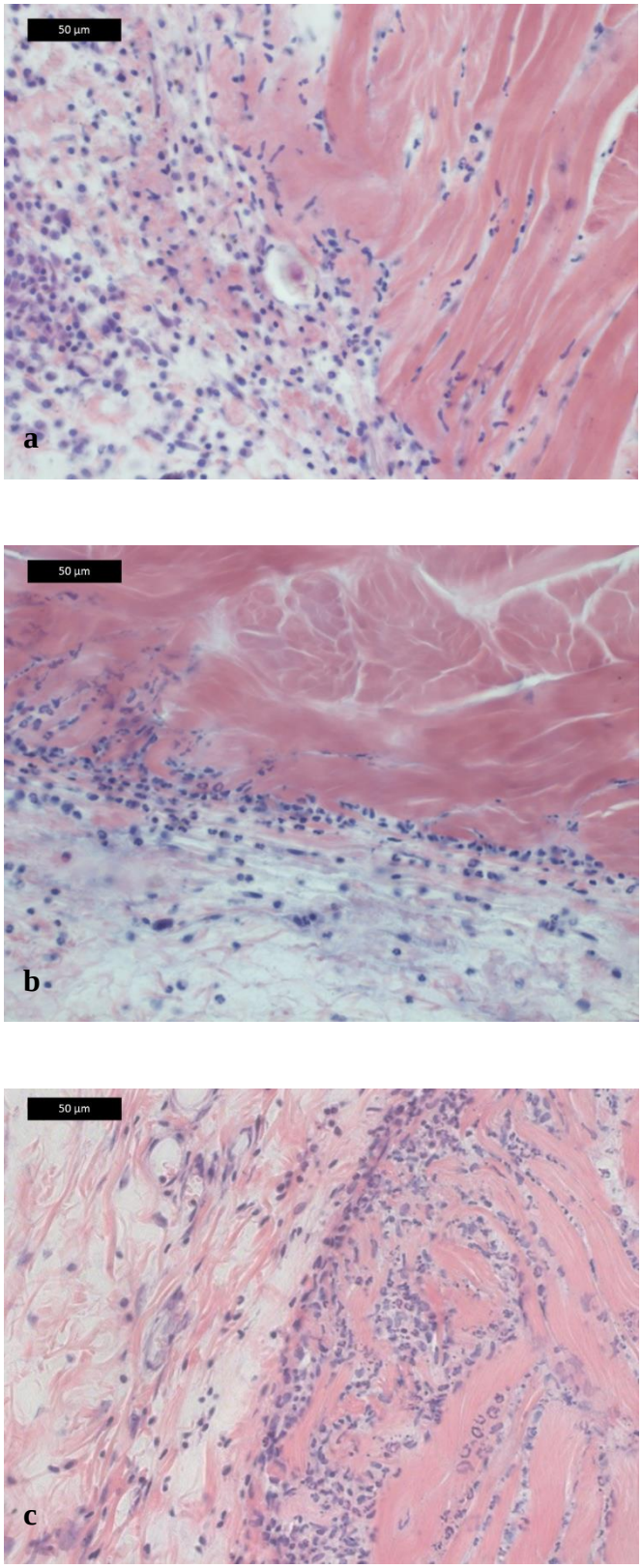

Figure 5.4 Day 2 implants, a) non-crosslinked b)Permacol™ c) highly-crosslinked H&E 40X magnification

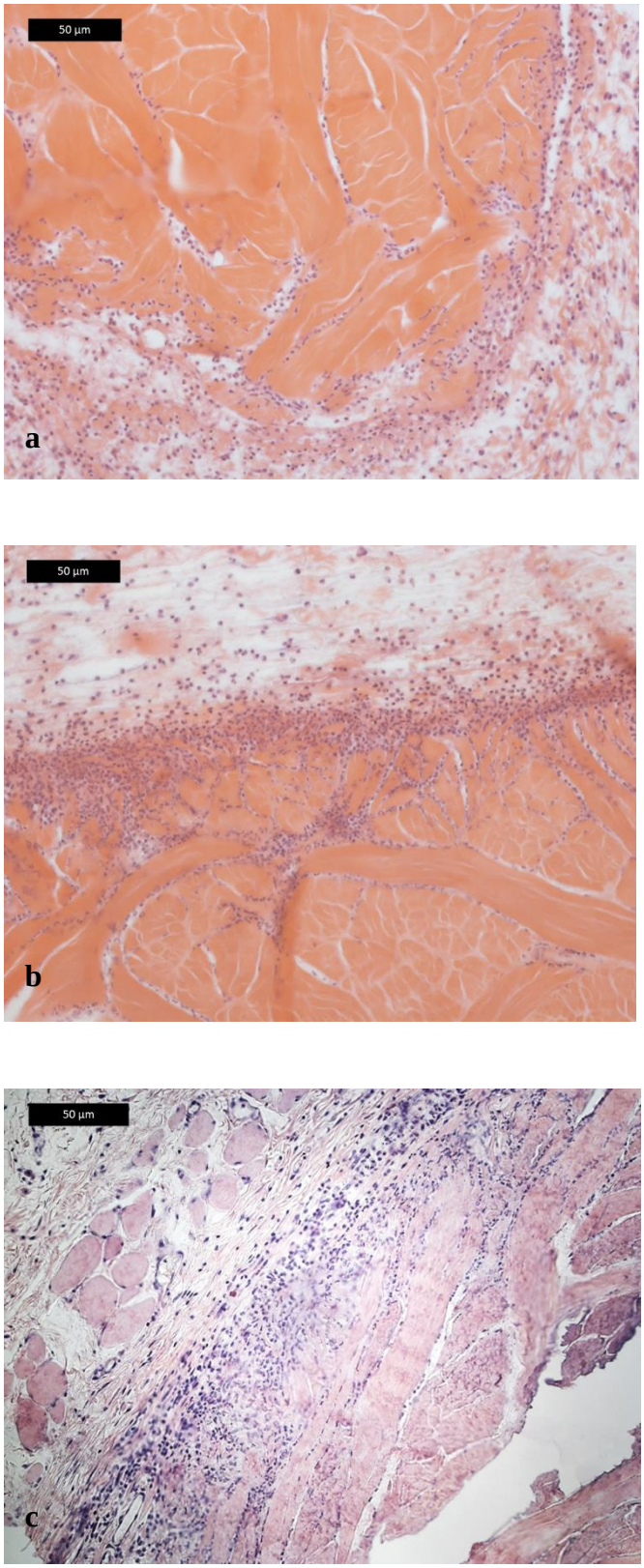

Figure 5.5 Day 2 implants, a) non-crosslinked b)Permacol™ c) highly-crosslinked H&E 20X magnification

Histological scores for the range of measured characteristics are summarised in figure 5.6. All implants remained intact maintaining 3D collagen structure with minimal degradation, confirmed by examining pico sirus red stained implants under polarised light.

As crosslinking levels increased the number of granulocytes present also increased. This difference was significant ($p < 0.99$) between the non-crosslinked and the highly-crosslinked groups. Cells of granulocytic lineage were the only group to show this trend; lymphocyte, fibroblast, residue, fibroplasia, integration and neovascularisation scores all showed a decrease in score from low to high crosslinking levels, none of these were significant.

Macrophages were most prevalent in the Permacol™ group followed by the non-crosslinked group and the least number of macrophages were observed in the highly-crosslinked group. The difference between the number of macrophages observed in Permacol™ and highly-crosslinked groups was significant with a p value of > 0.095.

No significant difference was observed in the colonisation of the implants. Between the non-crosslinked and Permacol™ groups a slight increase in cell penetration into the implants was observed. However this dropped back slightly in the highly-crosslinked group, but remained higher than the non-crosslinked group. The majority of the cell penetration into the implants followed the collagen fibres (see figures 5.4 and 5.5)

No giant cells, oedema or necrosis were observed in any of the implants.

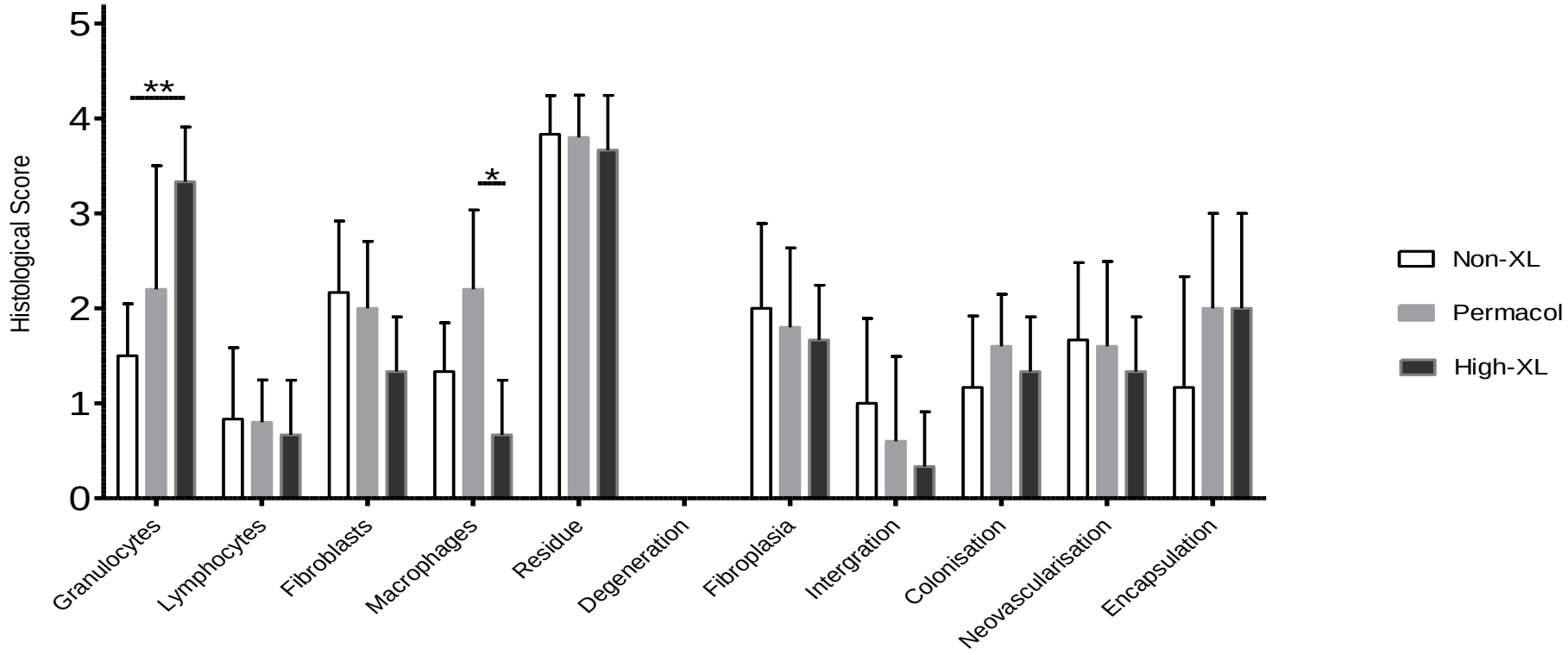

Figure 5.6 Semi-quantitative histological scores for day 2 non-crosslinked, Permacol™ and highly-crosslinked implants, error bars + 1 SD from the mean, n= 6 for non-crosslinked and Permacol™ and n=4 for highly-crosslinked.

Non-crosslinked and Permacol™ implants had similar total cell numbers, an increased total cell count was observed for highly-crosslinked implants (figure 5.7).

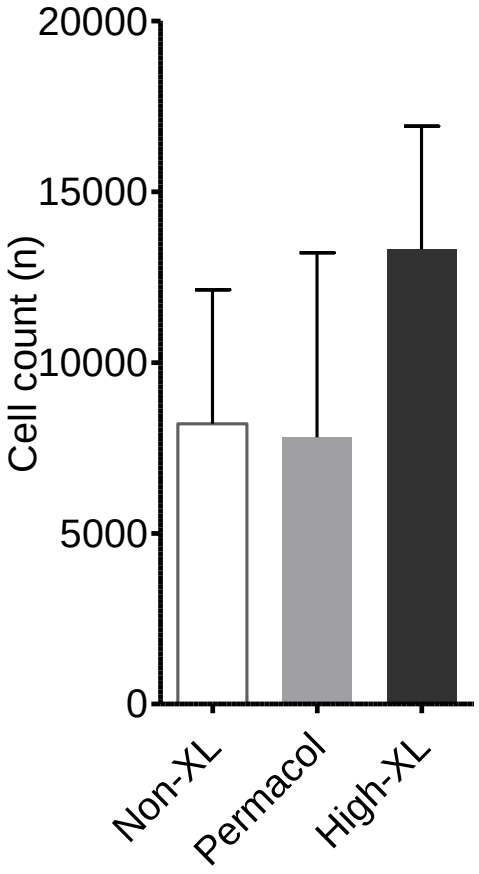

Figure 5.7 Quantitative cell count for day 2 non-crosslinked, Permacol™ and highly-crosslinked implants, error bars + 1 standard deviation from the mean, n= 6 for non-crosslinked and Permacol™ and n=4 for highly-crosslinked.

Approximately the same percentage of granulocytic cells were present in each of the 3 crosslinking levels (figure 5.8). Due to the higher total cell count for highly-crosslinked implants, more granulocytes were observed in the semi-quantative analysis (figure 5.6). ASD staining in figure 5.9 shows granulocytes in the host tissue surrounding the implant and interrogating the interface.

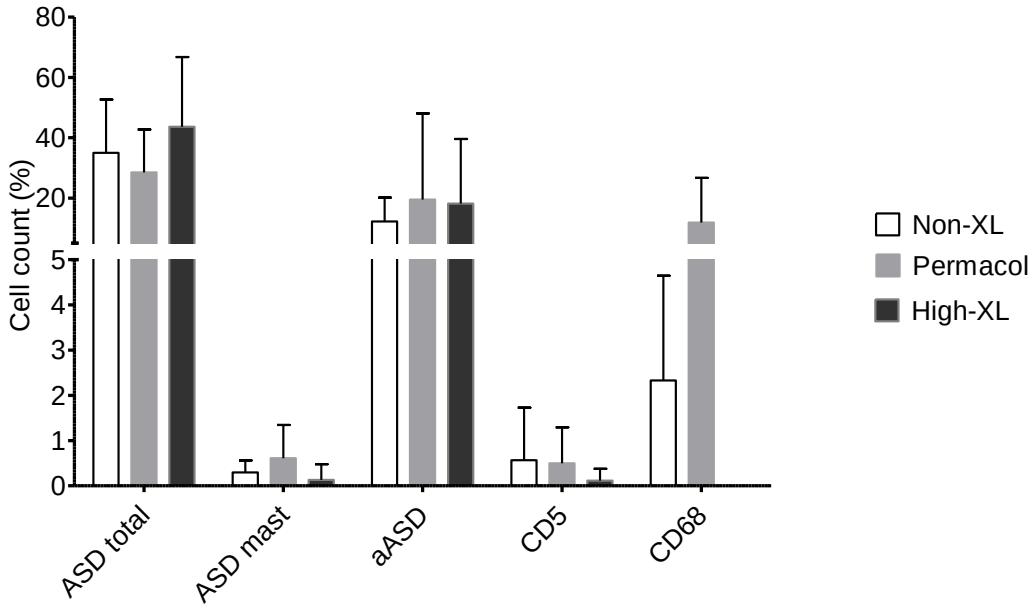

Figure 5.8 Quantitative cell percentages for day 2 non-crosslinked, Permacol™ and highly-crosslinked implants, error bars + 1 standard deviation from the mean, n= 6 for non-crosslinked and Permacol™ and n=4 for highly-crosslinked.

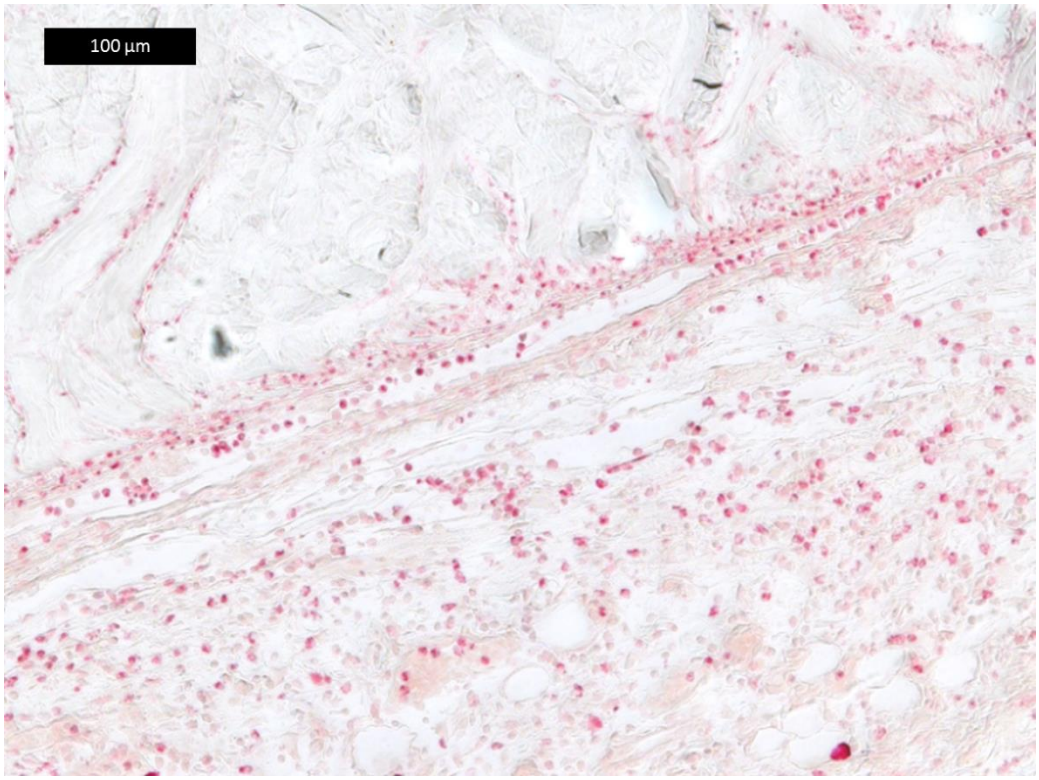

Figure 5.9 ASD staining of granulocytes, day 2 implants 20X magnification

Similar numbers of lymphocytes were observed across the different crosslinking levels and were present in quantities expected at this stage of wound healing. Fibroblasts were present in similar levels for non-crosslinked and Permacol™, with slightly fewer present for implants from highly-crosslinked group.

Permacol™ had a higher number of macrophages (activated and total) than non-crosslinked and highly-crosslinked implants. One implant from the Permacol™ implantation set had a cell count 3.5 times higher than the average. If this implant was removed from the quantitative analysis all three implant sets had similar αASD counts (figure 5.8). Figure 5.10 shows monocytes, macrophages and histiocytes in host tissue concentrating at the implant / host interface.

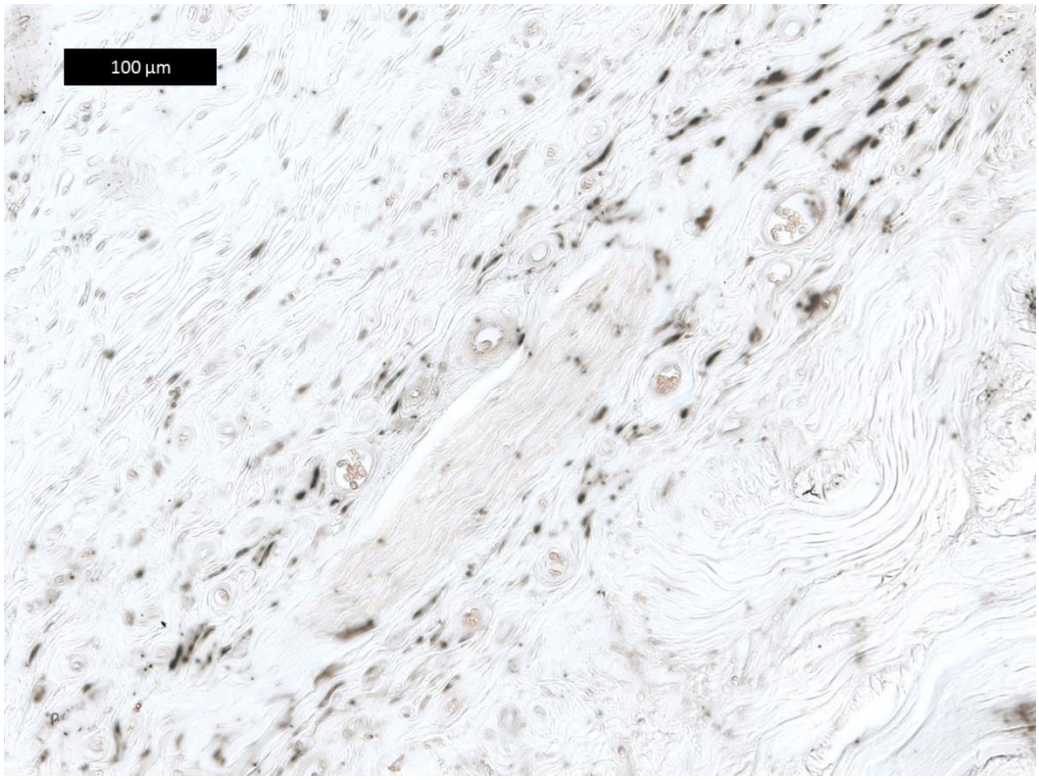

Figure 5.10 αASD staining of monocytes, macrophages and histiocytes (20x magnification)

Microscopic observations Deposition of ECM and immature collagen was similar around all implants. Non-crosslinked implants were integrating most with the surrounding host tissue. Implants with the highest crosslinking level were showing least integration with surrounding host tissue. Non-crosslinked implants had less organised matrix in the interface between host tissue and implant than crosslinked implants. Staining for collagen type I at the host / implant interface showed positive staining of the implant but minimal staining of host tissue (figure 5.11). Staining for collagen type III showed the inverse relationship with staining present in the host tissue but absent in the implants (figure 5.12) Non-crosslinked implants and Permacol™ implants had similar collagen I/III ratios, highly-crosslinked implants had a lower I/III ratio (figure 5.13), indicating a greater deposition of collagen III around the implants.

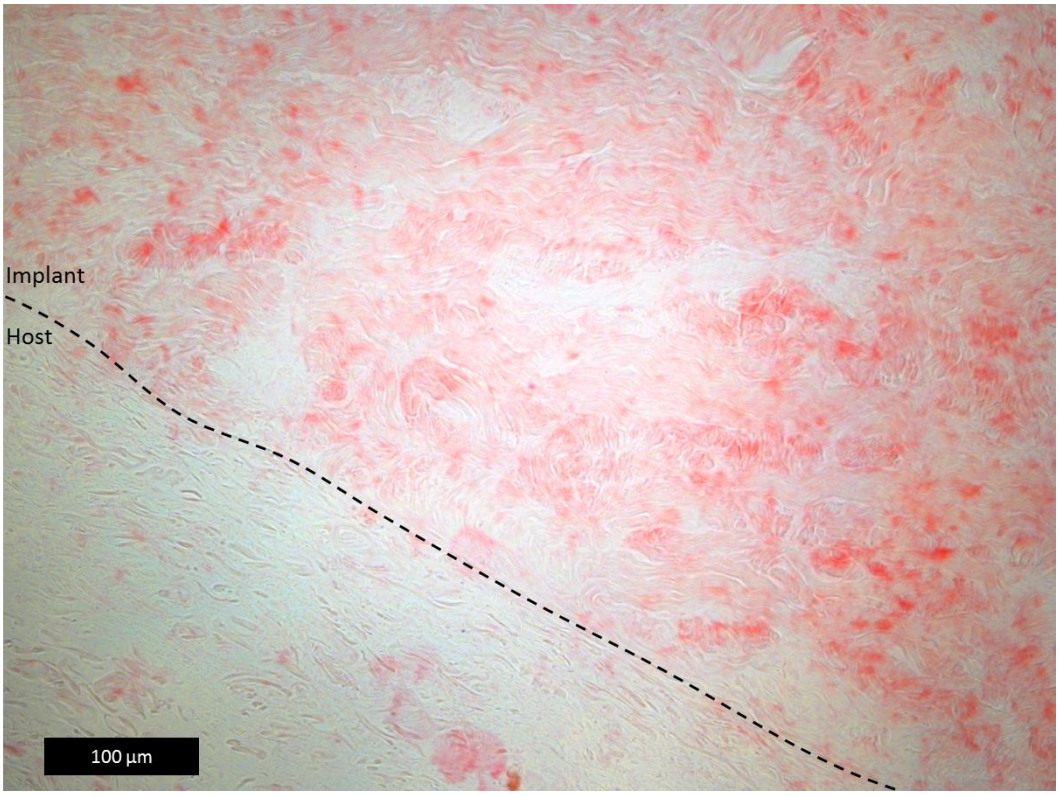

Figure 5.11 Collagen I staining of Permacol™ implant / host interface (dashed line) after 2 days implantation, 20x H&E.

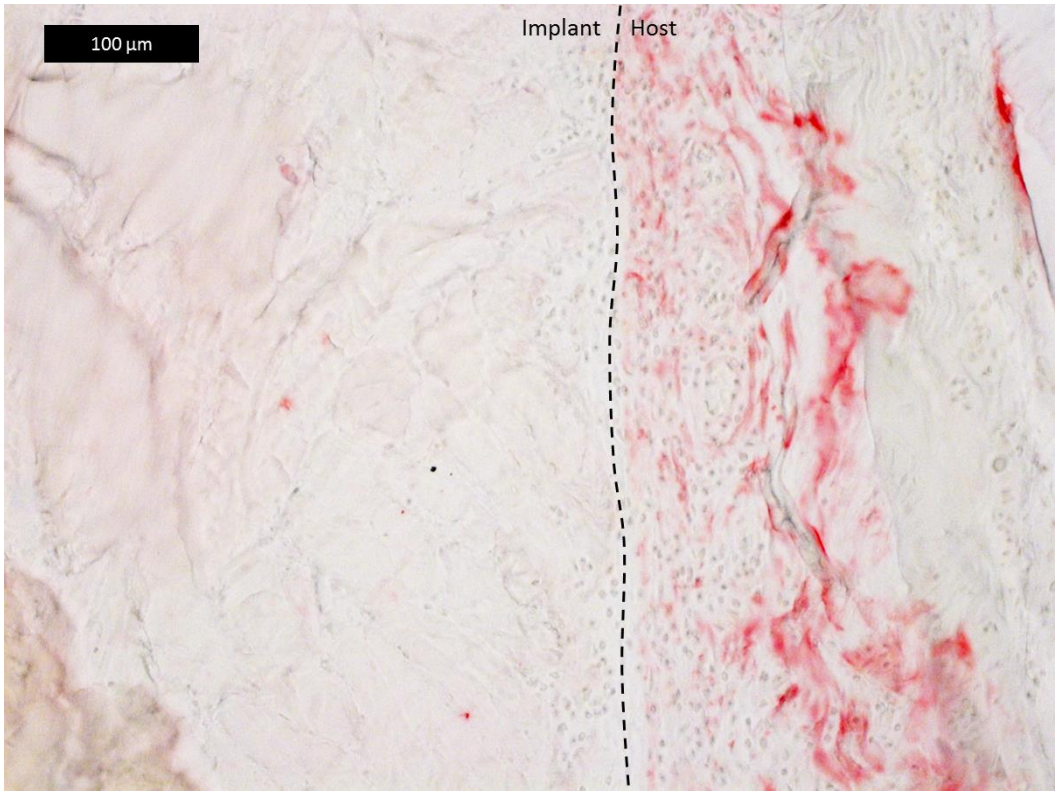

Figure 5.12 Collagen III staining of Permacol™ implant / host interface (dashed line) after 2 days implantation, 20x H&E.

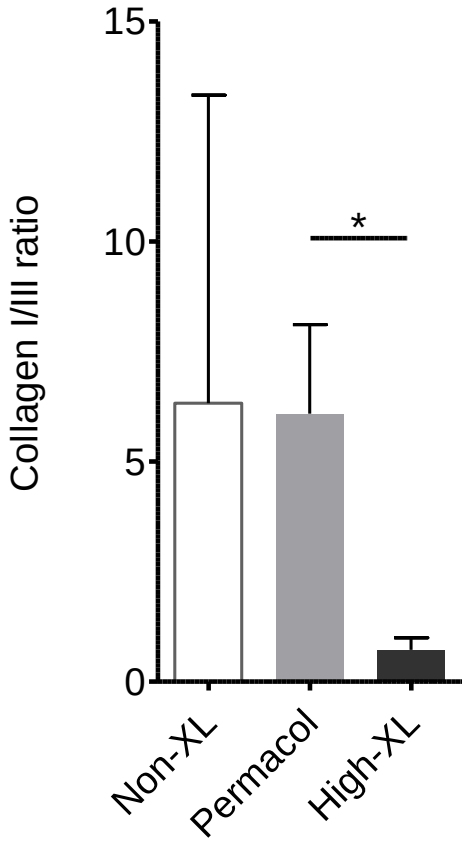

Figure 5.13 Quantitative collagen ratio for day 2 non-crosslinked, Permacol™ and highly-crosslinked implants, error bars + 1 standard deviation from the mean, n= 6 for non-crosslinked and Permacol™ and n=4 for highly-crosslinked.

5.3.2 **Day 7 implant observations**

After 7 days, overall seroma / hematoma levels had subsided with only one present associated with highly-crosslinked implant (figure 5.14). By day 7 vessels were clearly visible on the surface of some implants (figure 5.15). All implants were attached to the underlying musculature. No degradation of the implants was visible. No macroscopic inflammatory differences were observed between the different crosslinking levels.

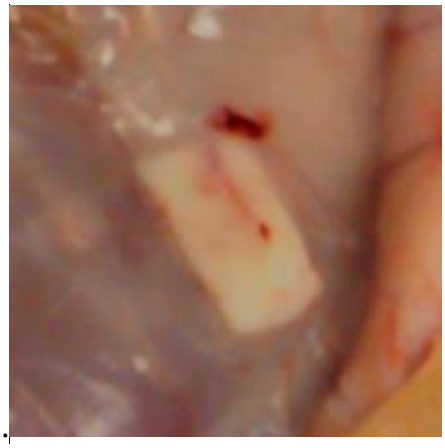

Figure 5.14 Implant image, highly-crosslinked implant 7 days post implantation, with vessel visible over implant.

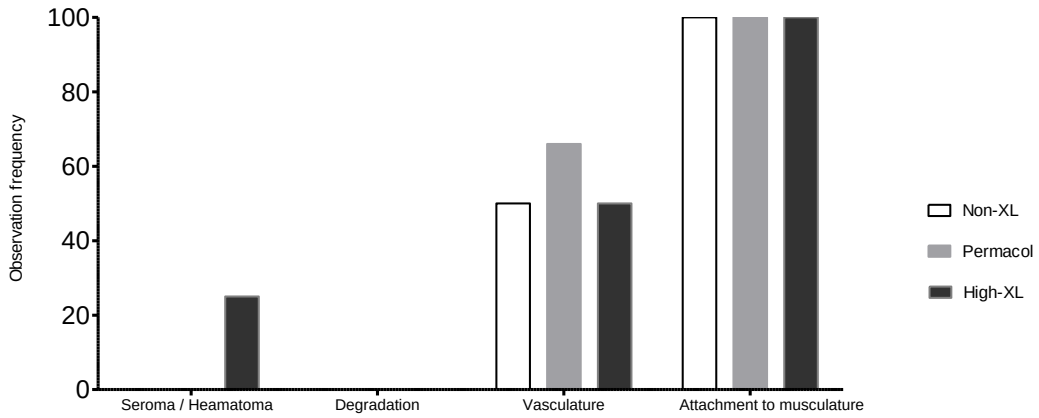

Figure 5.15 Macroscopic observations for day 7 implants

The structure of all implants remained intact with the basket weave pattern present. Limited degradation of implants was observed across all implants.

None of the implants had giant cells, oedema or necrosis.

Figures 5.16 and 5.17 are example H&E images of the implants taken at 40x and 20x magnification. A clearly defined host / implant interface was visible in all groups. Host tissue surrounding the implants had good vascularisation as seen in figure 5.16a.

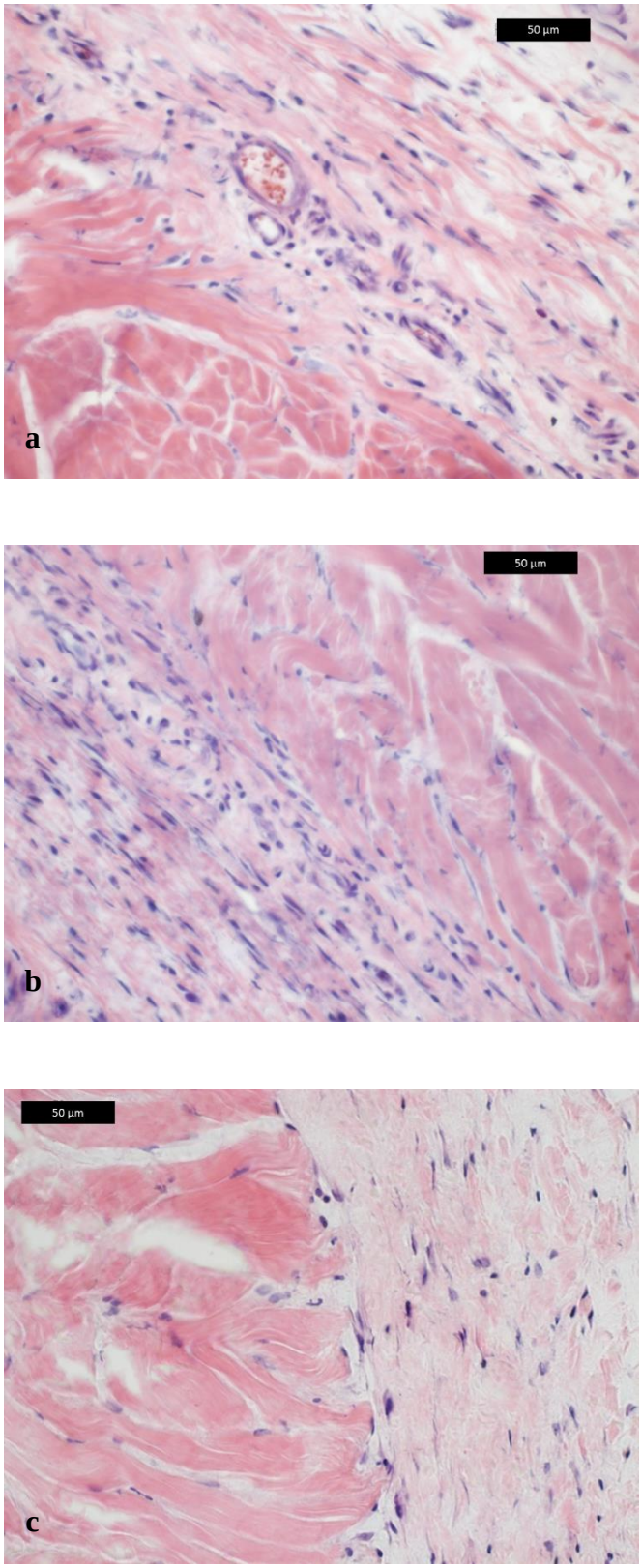

Figure 5.16 Day 7 implants, a) non-crosslinked b)Permacol™ c) highly-crosslinked H&E 40X magnification

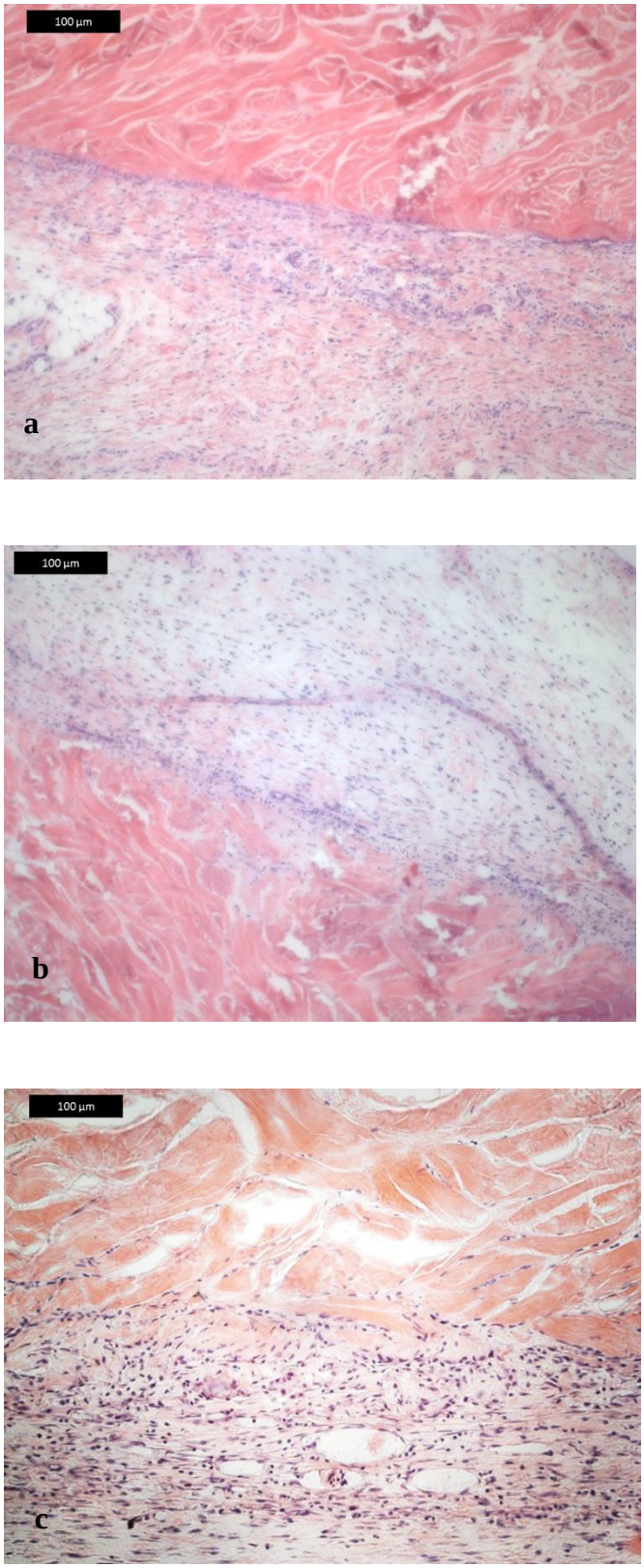

Figure 5.17 Day 7 implants, a) non-crosslinked b)Permacol™ c) highly-crosslinked H&E 20X magnification

Granulocytes were present in similar levels to day 2 implants for the non-crosslinked implants. Granulocyte levels present in Permacol™ and highly-crosslinked groups had fallen from levels present at day 2, bringing them in line with the non-crosslinked implants (figures 5.6 and 5.20).

Fibroblast levels increased from day 2 to day 7. The trend remained consistent with the number of fibroblasts observed in relation to the crosslinked variants decreased as the crosslinking level increased (not significant).

Permacol™ implants had similar macrophage levels observed at day 7 as at day 2. Non-crosslinked and highly-crosslinked implants had more macrophages at day 7 than day 2. As with the fibroblasts, macrophage levels decreased as crosslinking levels increased, this was not a significant trend.

Fibroplasia score increased from day 2 implants to day 7. No trend was present relevant to the crosslinking groups.

Colonisation histological scores were significantly different between the crosslinking groups at day 7. Cells had penetrated significantly further into highly-crosslinked implants than Permacol™. No significant difference was present for the non-crosslinked samples with these scores falling between Permacol™ and highly-crosslinked groups. As with day 2, the cells had mainly penetrated along the collagen fibres (figures 5.16 and 5.17).

Lymphocyte presence and neovascularisation was consistent for all implant groups, with histological scores being similar to day 2 implants (figures 5.6 and 5.8). Vessles can be seen at the host / implant interface in figure 5.18.

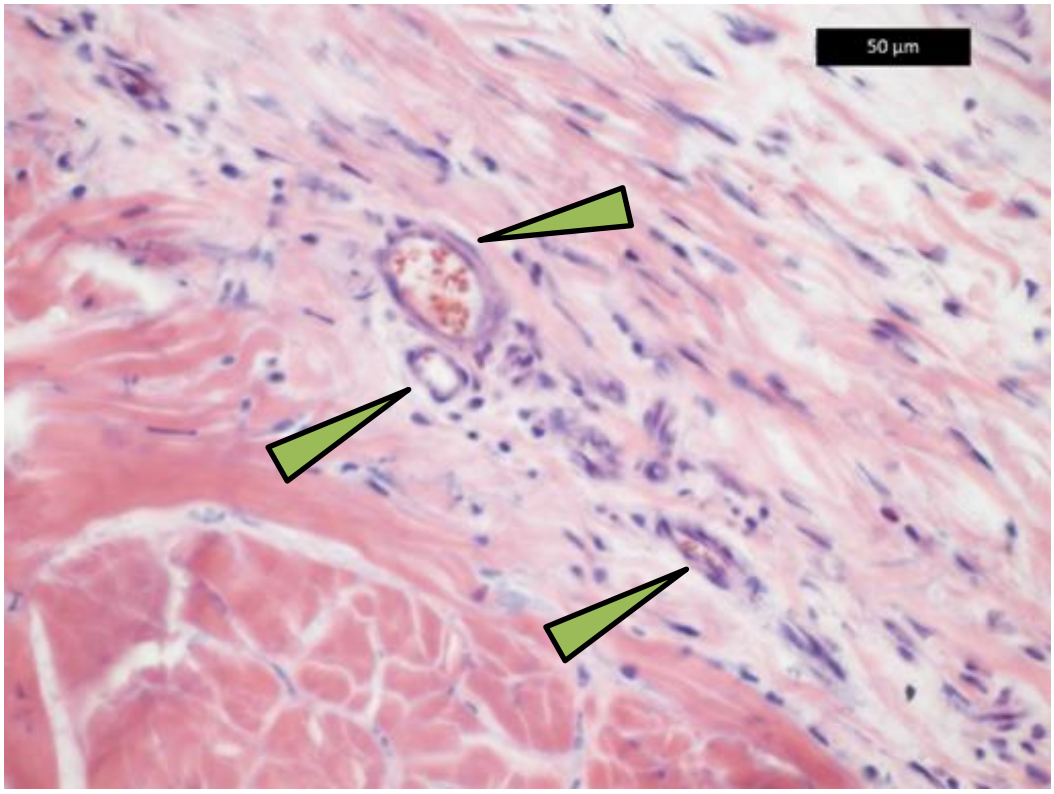

Figure 5.18 Permacol™ implant 7 days after implantation, integration of the implant with the host tissue with vessels (green arrows) along the interface (dashed line), H & E 40X magnification.

All implant groups doubled the percentage of implant integration with host tissue between day 2 and day 7 (figure 5.19). The trend of increased crosslinking levels associated with lower host integration continued from day 2 to day 7 observations. An inverse trend was observed for cellular colonisation of the implants with a higher crosslinking level associated with greater colonisation and no crosslinking with lower colonisation.

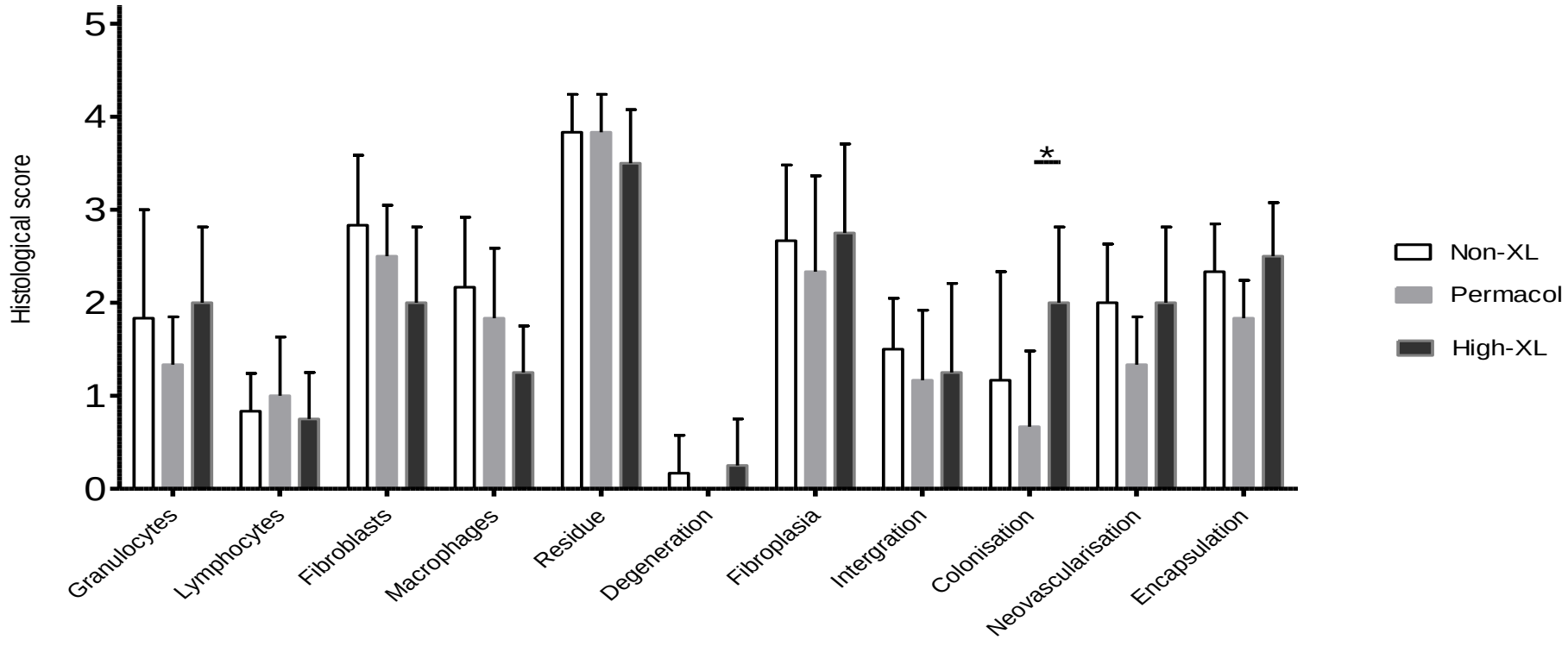

Figure 5.19 Semi-quantitative histological scores for day 7 implants with 0.0, 1.7 and highly-crosslinked, error bars + 1 standard deviation from the mean, n= 6 for non-crosslinked and Permacol™ and n=4 for highly-crosslinked.

Collagen degradation was minimal for all of the implants with the basket weave pattern present in all implants (figure 5.20).

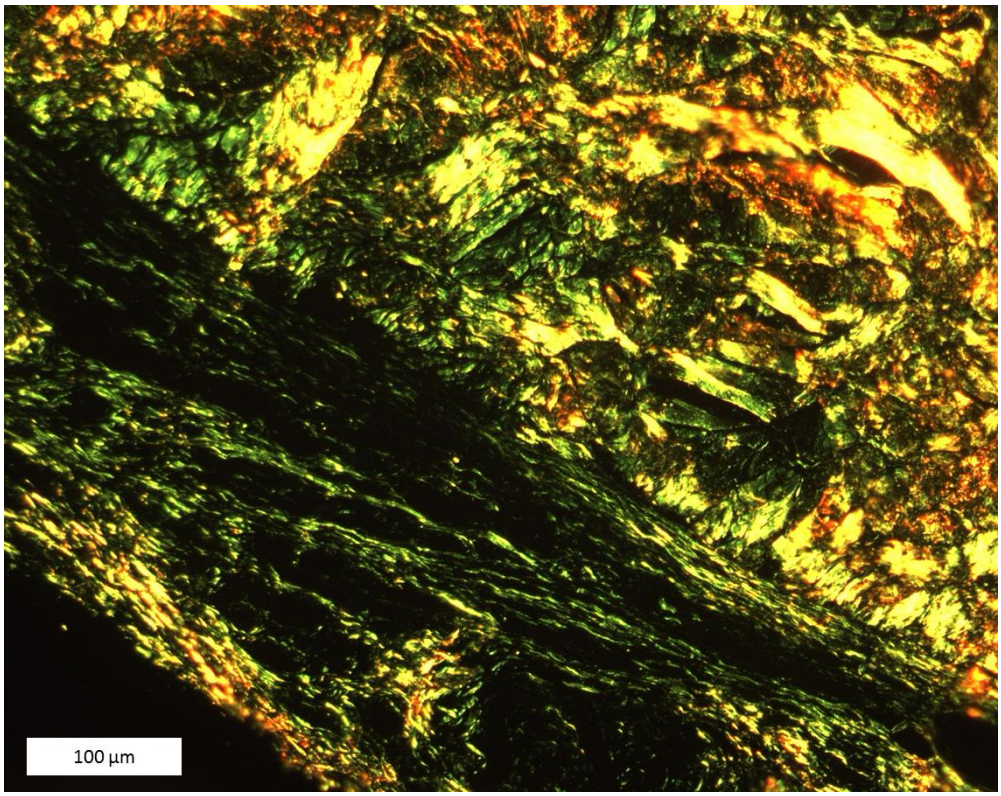

Figure 5.20 Non-crosslinked implant, 7 days after implantation showing host implant interface, Picro sirius red (polarised light) 20X magnification.

Non-crosslinked and Permacol™ implants had similar total cell counts, highly-crosslinked implants had significantly higher total cell counts, almost double

(figure5.21). Each implant group had lower total cell counts at day 7 compared to day 2.

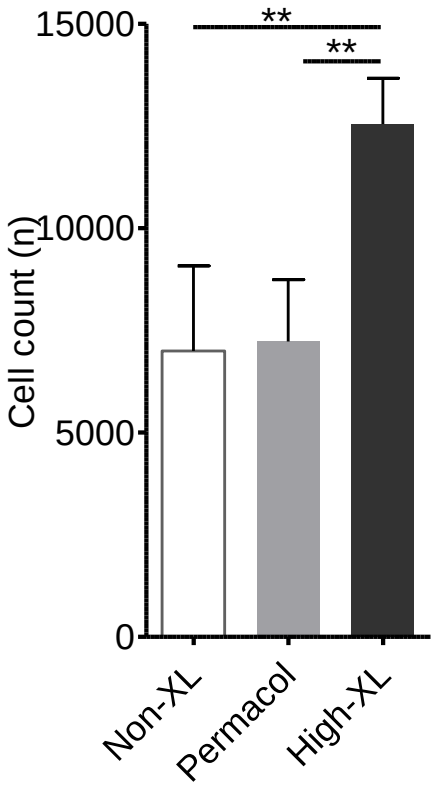

Figure 5.21 Quantitative cell count for day 7 non-crosslinked, Permacol™ and highly-crosslinked implants, error bars + 1 standard deviation from the mean, n= 6 for non-crosslinked and Permacol™ and n=4 for highly-crosslinked.

Less than 1% of the total cells were granulocytes for Permacol™ and non-crosslinked, a higher percentage of the cells around the highly-crosslinked were granulocytes (figure 5.23a). For all implants the proportion of mast cells present around the implants was higher than the day 2 implants. Figure 5.22 shows granulocytes concentrating at the implant host interface. The mast cell subpopulation was only observed in the host tissue.

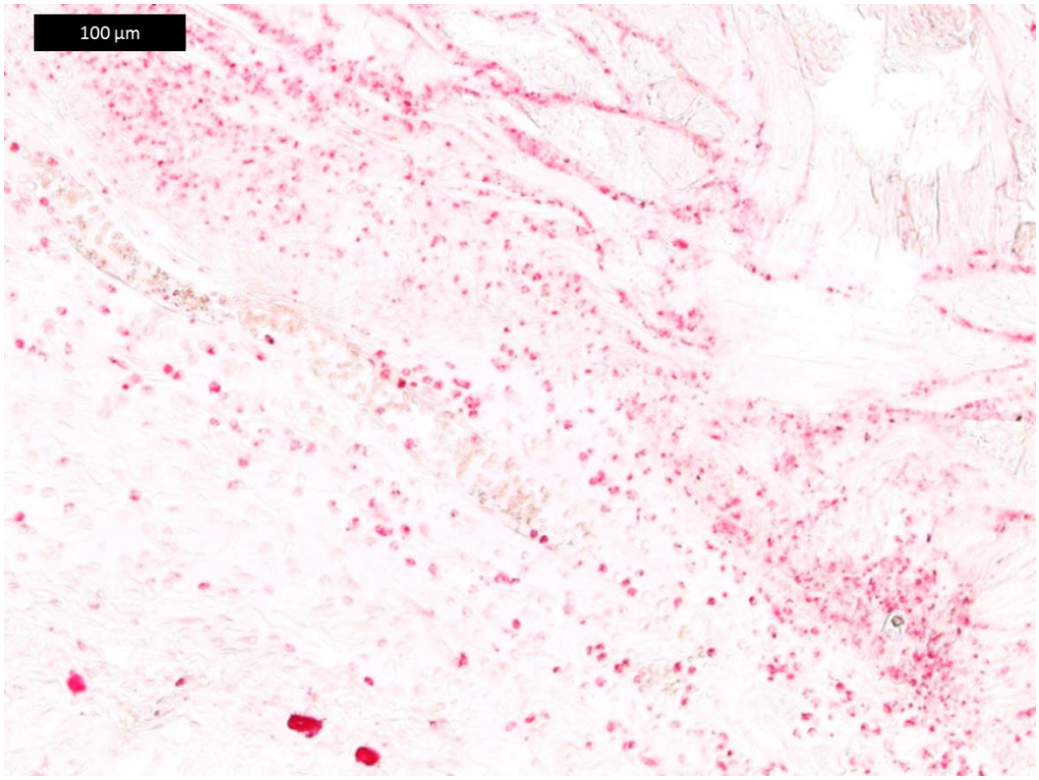

Figure 5.22 ASD stating of granulocytes, day 7 implant, 20x magnification.

The quantitative image analysis showed a trend in αASD staining with non-crosslinked samples having the highest proportion of monocytes, macrophages and histiocytes and highly-crosslinked having the lowest (figure 5.23). This trend was repeated for the activated macrophages (CD68 positive) (figure 5.23), with the highest proportion observed in non-crosslinked implants. Activated macrophages were observed 'lining up' along the implant edge (figure 5.24).

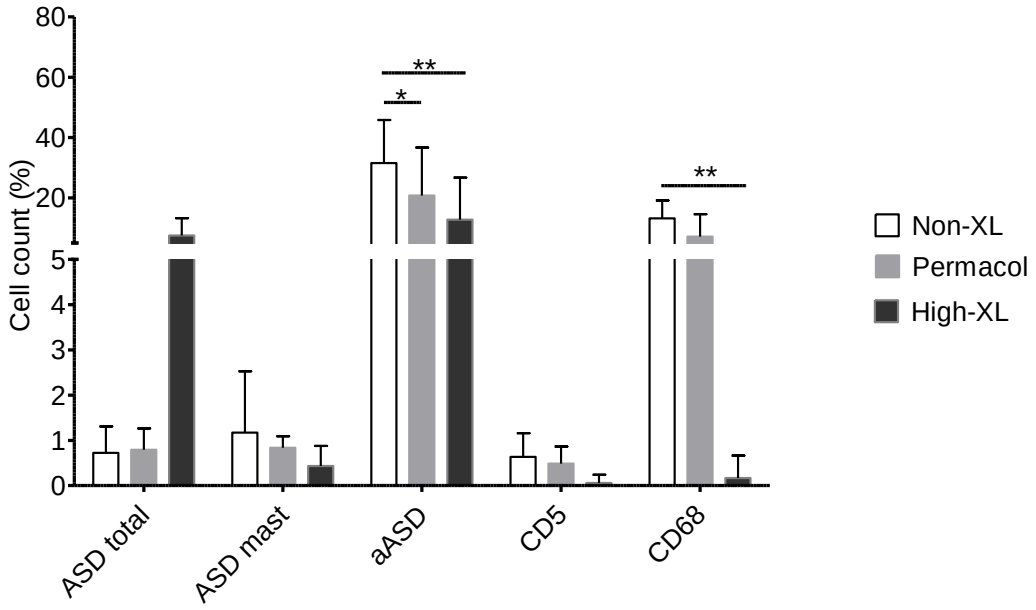

Figure 5.23 Quantitative cell percentages for day 7 non-crosslinked, Permacol™ and highly-crosslinked implants, error bars + 1 standard deviation from the mean, n= 6 for non-crosslinked and Permacol™ and n=4 for highly-crosslinked.

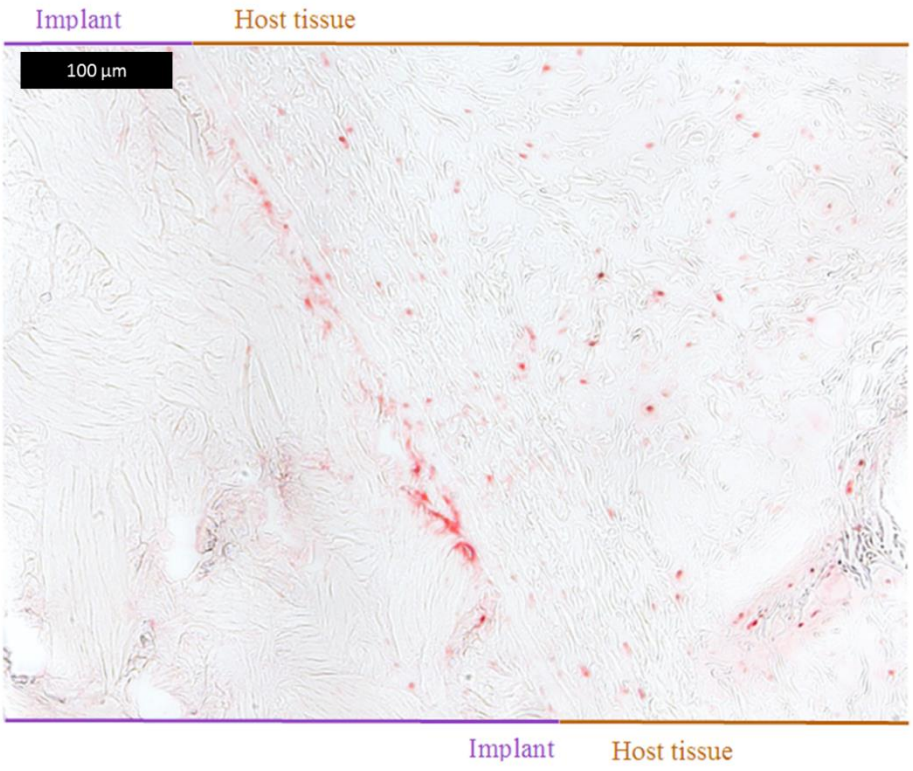

Figure 5.24 Immunohistochemistry stain CD68 for activated macrophages, host tissue right and implant left (20X magnification).

Average collagen I/III ratio was highest for Permacol™, implants with highly-crosslinked having the lowest ratio (figure 5.25).

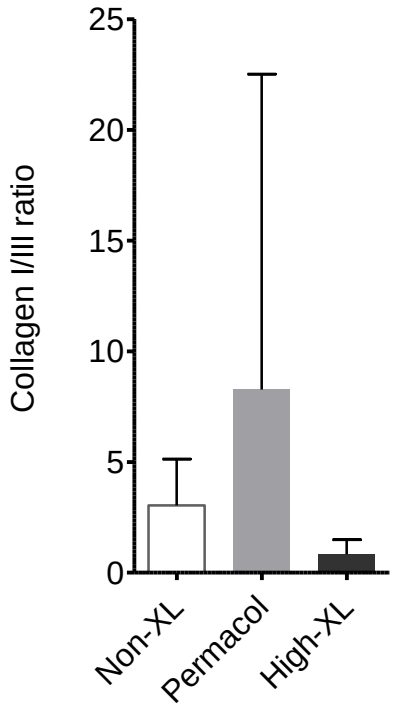

Figure 5.25 Quantitative collagen ratio for day 7 implants with 0.0, 1.7 and highly-crosslinked, error bars + 1 standard deviation from the mean, n= 6 for non-crosslinked and Permacol™ and n=4 for highly-crosslinked.

5.3.3 **Day 14 implant observations**

Seroma / hematoma levels were similar to day 7, with only one present in association with a non-crosslinked implant (figure 5.26). Vessels were clearly visible on the surface of most implants. No macroscopic inflammatory differences were observed between the different crosslinking levels.

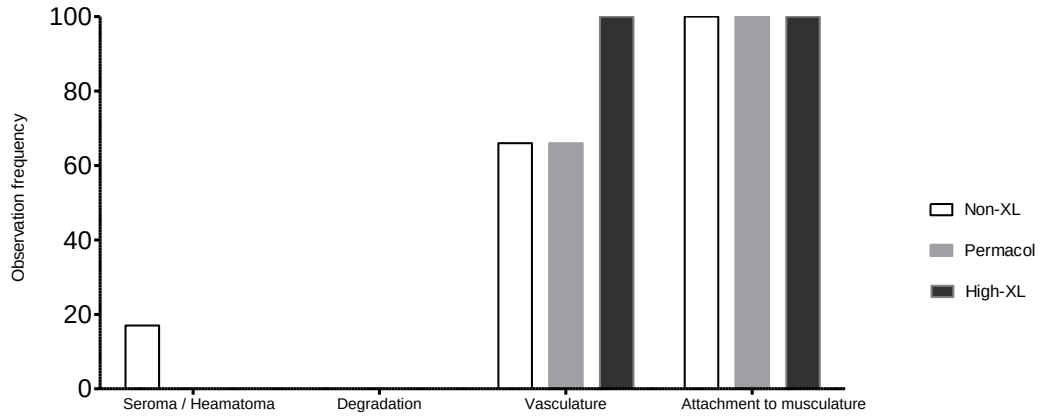

Figure 5.26 Macroscopic observations for day 14 implants

Giant cells were observed in one of the Permacol™ implants. No oedema or necrosis was observed in relation to any of the implants.

Figures 5.27 and 5.28 are example H&E images of the implants taken at 40x and 20 x magnification. The host / implant interface was clearly defined in all groups.

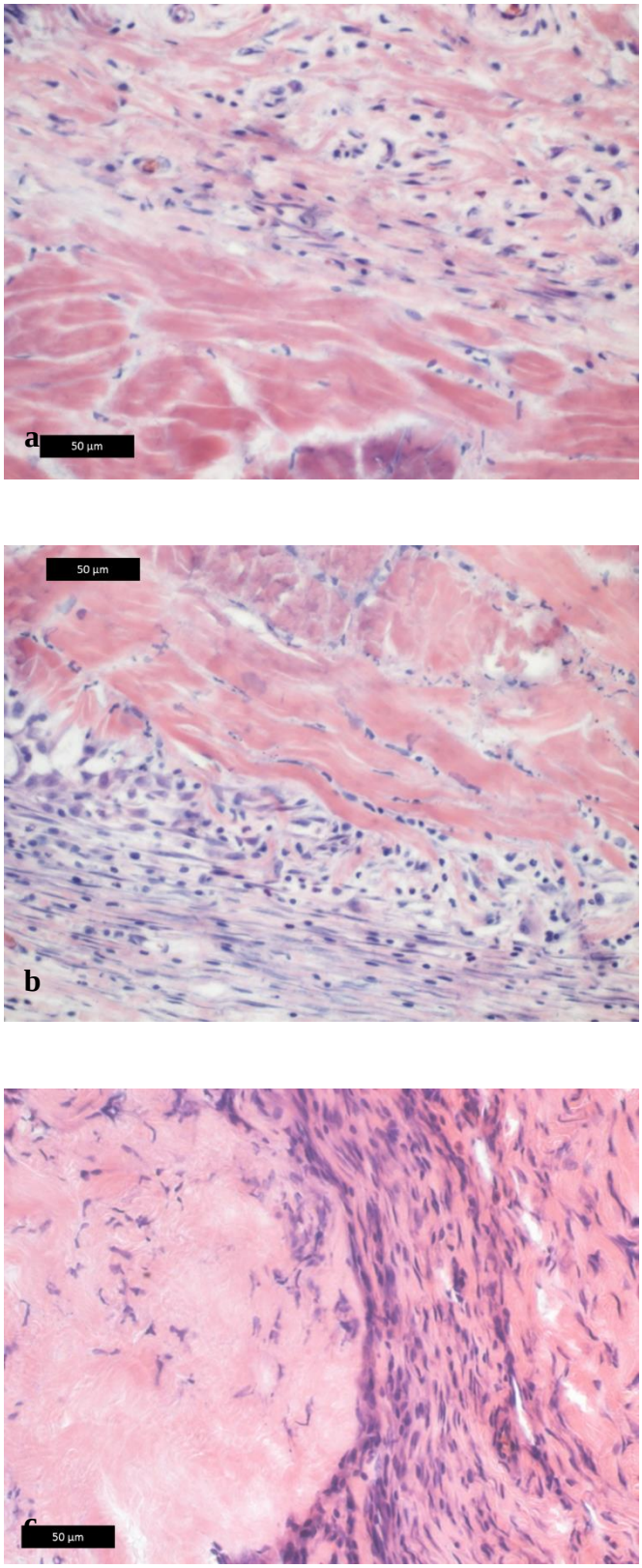

Figure 5.27 Day 14 implants, a) non-crosslinked b)Permacol™ c) highly-crosslinked H&E 40X magnification

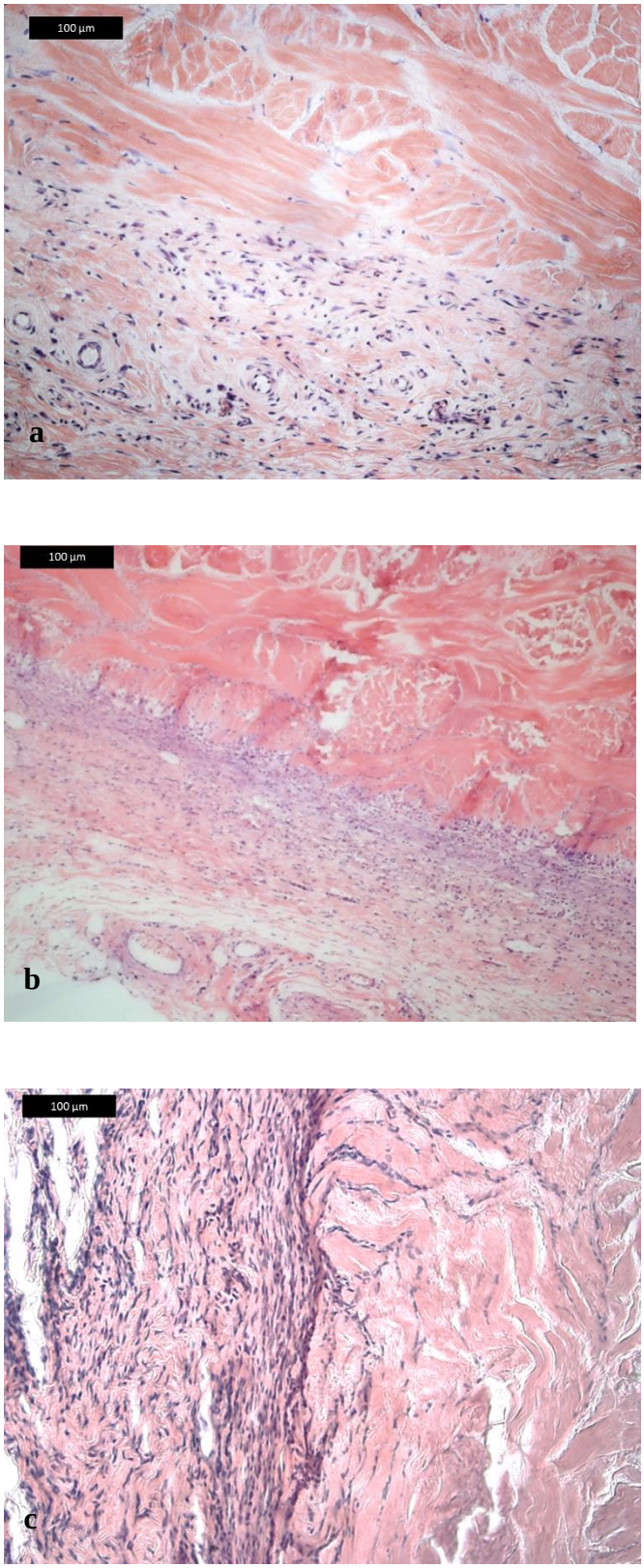

Figure 5.28 Day 14 implants, a) non-crosslinked b)Permacol™ c) highly-crosslinked H&E 20X magnification

From the semi quantitative histological scoring; granulocyte, lymphocyte, fibroblast, implant integration, encapsulation and neovascularisation levels were at similar levels to day 7 implants (figures 5.19 and 5.30), with no significant differences observed between the groups implanted at day 14.

In figure 5.29 good integration of the non-crosslinked implant with the host tissue was observed, with vessels formed within the implant and close to the interface within the host tissue. Pockets of non-vascularised cellular infiltration are also present within the implant.

Macrophages were observed at a similar frequency for the non-crosslinked implants and Permacol™. Significantly ($p<0.01$) fewer macrophages were observed in relation to the highly-crosslinked implants when compared to Permacol™ (figure 5.30).

A slight drop in fibroplasia was observed between day 7 and 14 implants.

Implant colonisation by cells increased across all groups between days 7 and 14. As crosslinking level of the implant increased the degree of cell penetration also increased. Cells penetrated significantly further into the highest crosslinking group when compared to the non-crosslinked implants.

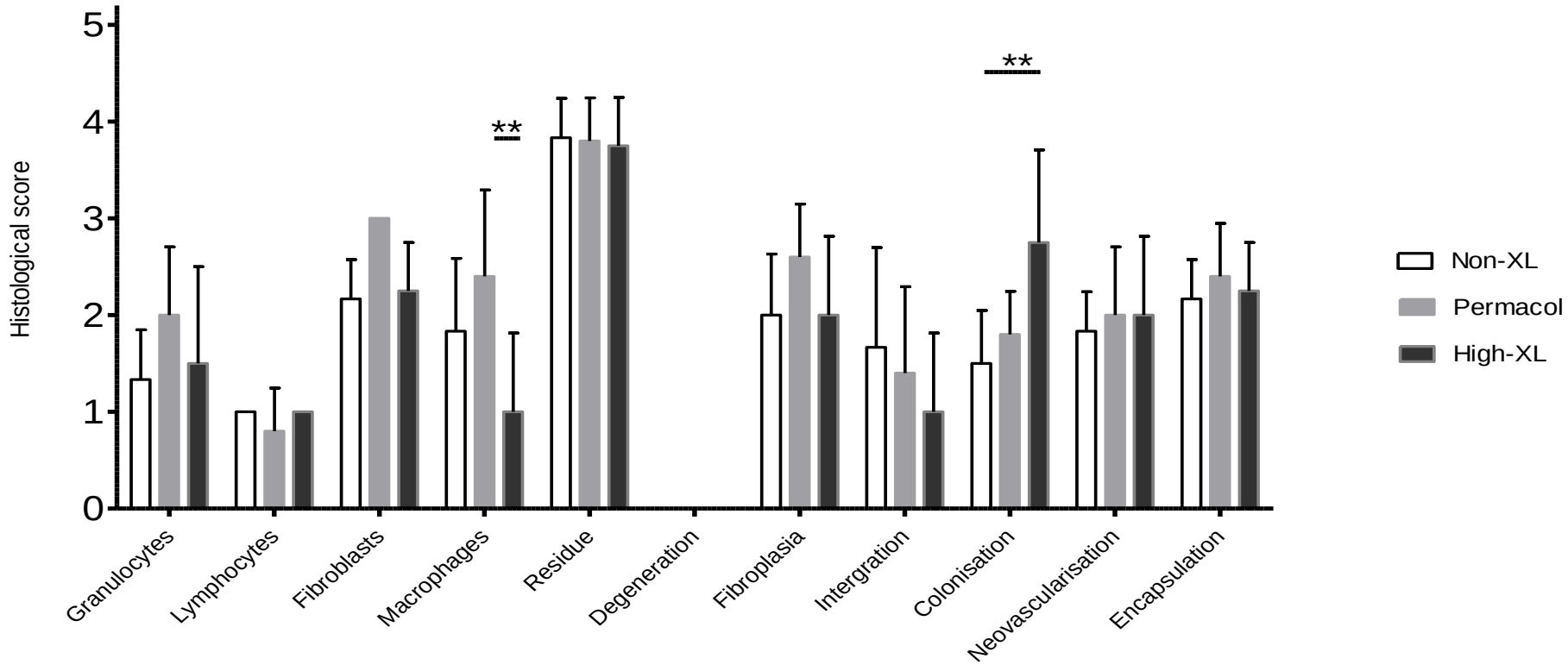

Figure 5.29 Semi-quantitative histological scores for day 14 implants with 0.0, 1.7 and highly-crosslinked, error bars + 1 standard deviation from the mean, n= 6 for non-crosslinked and Permacol™ and n=4 for highly-crosslinked.

Total cell counts were similar for non-crosslinked and Permacol™ implants which was consistent with the day 7 implants. Highly-crosslinked implants had a higher total cell count than the other implants (figure 5.31). Three of the implants had similar total cell counts to the day 7 implants, one of the day 14 implants had almost twice the cell density of the other implants, raising the implant group average.

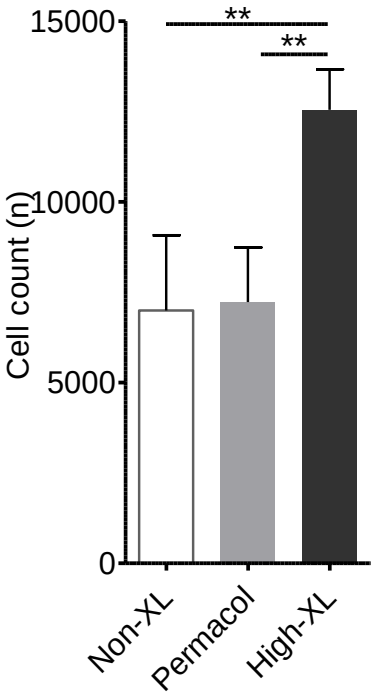

Figure 5.30 Quantitative cell count for day 14 non-crosslinked, Permacol™ and highly-crosslinked implants, error bars + 1 standard deviation from the mean, n= 6 for non-crosslinked and Permacol™ and n=4 for highly-crosslinked.

A higher percentage of the cells identified in the non-crosslinked and Permacol™ implants were granulocytes compared to highly-crosslinked implants (figure 5.32). For all implants the proportion of mast cells present around the implants remained similar too day 7 implants.

Number of lymphocytes remained constant from day 7 to day 14 implants, quantitative image analysis showed a trend in αASD staining with non-crosslinked

samples having the highest proportion of monocytes, macrophages and histiocytes and the highly-crosslinked group having the lowest (figure 5.32). This trend was repeated for the activated macrophages (figure 5.32).

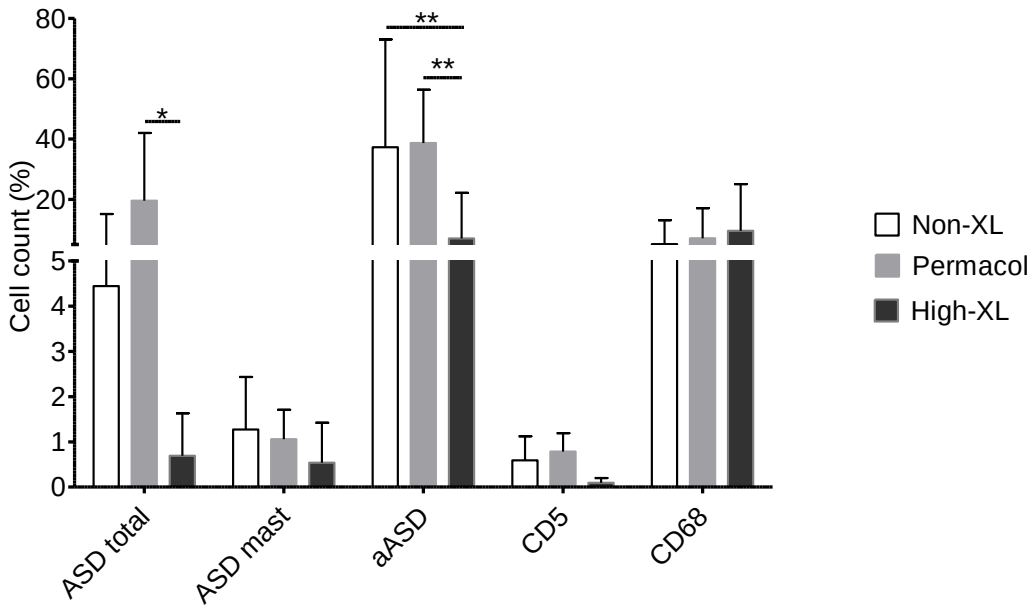

Figure 5.31 Quantitative cell percentages for day 14 non-crosslinked, Permacol™ and highly-crosslinked implants, error bars + 1 standard deviation from the mean, n= 6 for non-crosslinked and Permacol™ and n=4 for highly-crosslinked.

Average collagen I/III ratio was highest for the non-crosslinked group, highly-crosslinked implants had the lowest ratio (figure 5.33).

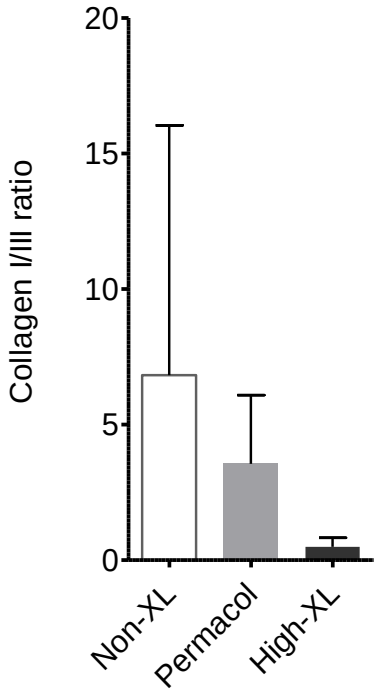

Figure 5.32 Quantitative collagen ratio for day 14 non-crosslinked, Permacol™ and highly-crosslinked implants, error bars + 1 standard deviation from the mean, n= 6 for non-crosslinked and Permacol™ and n=4 for highly-crosslinked.

5.3.4 **Day 28 implant observations**

28 days post implantation no seromas / hematomas were present. Vasculature was visible on the surface of implants from all groups. No macroscopic inflammatory differences were observed between the different crosslinking levels.

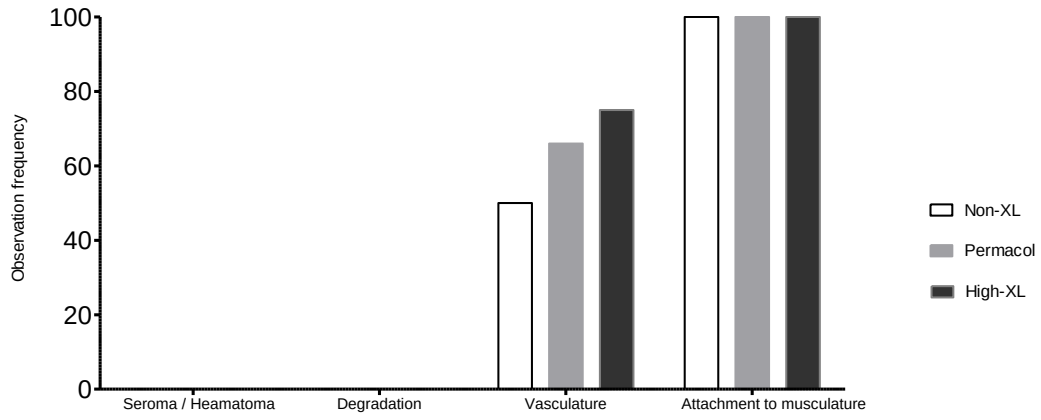

Figure 5.33 Macroscopic observations for day 28 implants.

No oedema, giant cells or necrosis was observed in any of the implants.

Figure 5.30 shows representative H&E images of the implants taken at 20 or 40 x magnification. The host / implant interface is clearly defined in all groups.

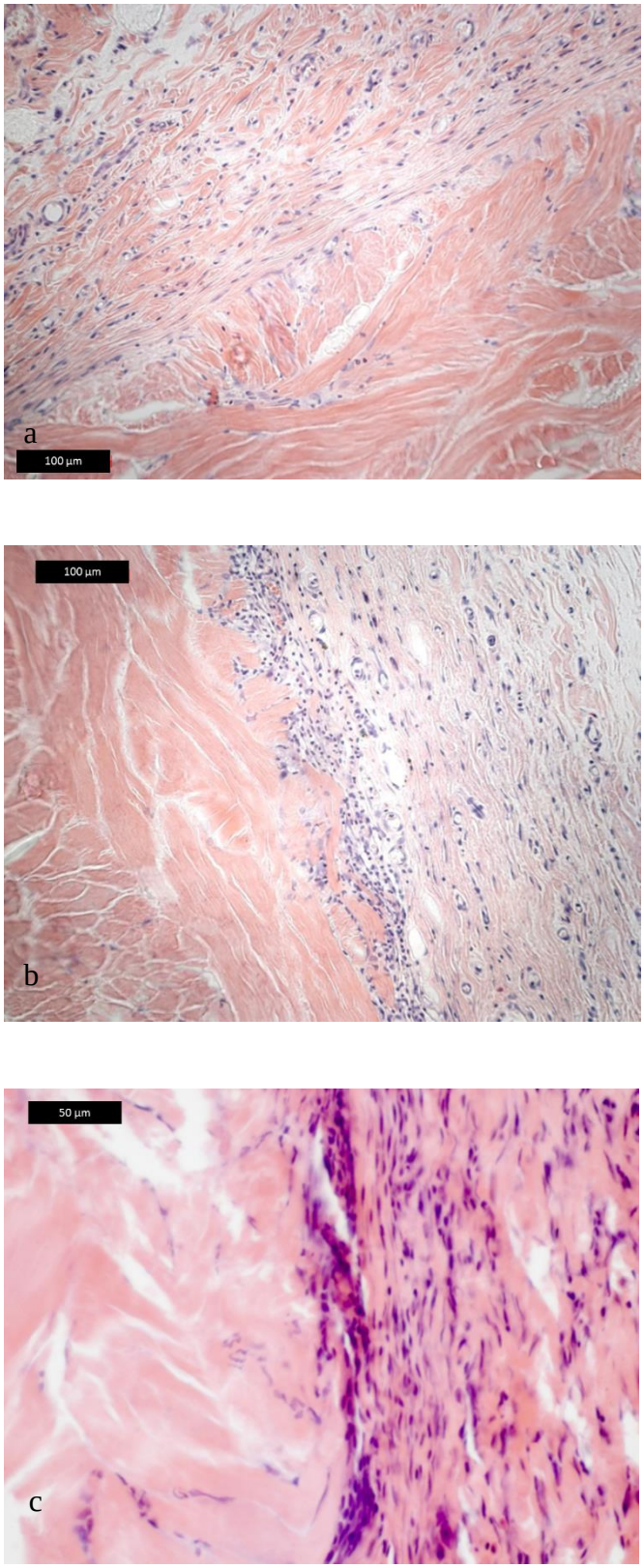

Figure 5.34 Day 28 implants, a a) non-crosslinked b)Permacol™ c) highly-crosslinked H&E 20X (a, b) 40X (c) magnification

From the semi quantitative histological scoring; granulocyte, lymphocyte, fibroblast, residue integration, encapsulation, colonisation and neovascularisation levels were at similar levels to day 14 implants (figure 5.30 and 5.36), with no significant differences observed between the crosslinking groups.

Continuing the trend between day 7 and 14 implants, a slight drop in fibroplasia was observed between day 14 and 28 implants.

Macrophages were observed at a similar frequency for the non-crosslinked implants and Permacol™. Significantly ($p<0.01$) fewer macrophages were observed in relation to highly-crosslinked implants when compared to Permacol™ and the non-crosslinked group.

All three implant groups had similar numbers of fibroblasts present. Non-crosslinked and highly-crosslinked groups remained consistent with levels observed at day 14. Fibroblast levels had dropped for the Permacol™ group from the day 14 implants bringing them in line with the other 2 groups.

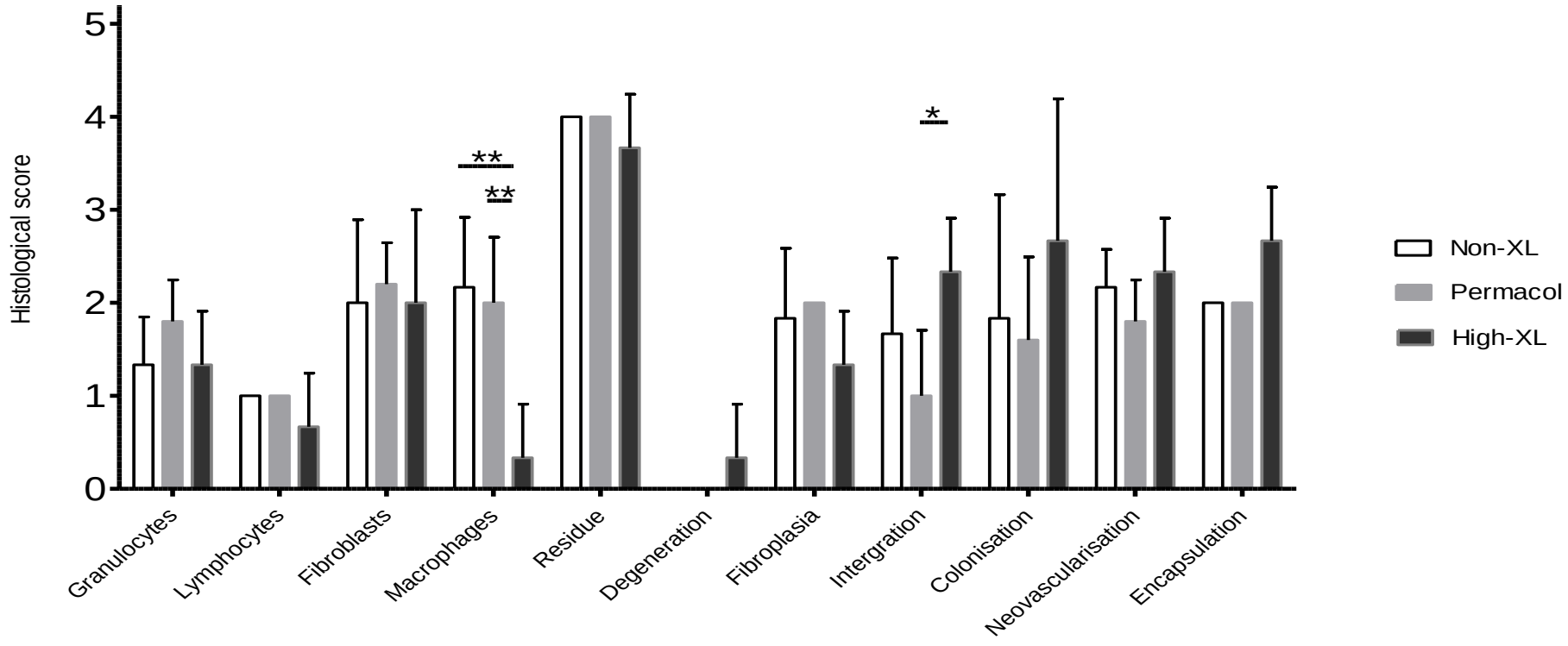

Figure 5.35 Semi-quantitative histological scores for day 28 implants with 0.0, 1.7 and highly-crosslinked, error bars + 1 standard deviation from the mean, n= 6 for non-crosslinked and Permacol™ and n=4 for highly-crosslinked.

Little degradation of the implants was observed at 28 days, with the basket weave pattern present and no damaged collagen observed (figure 5.37).

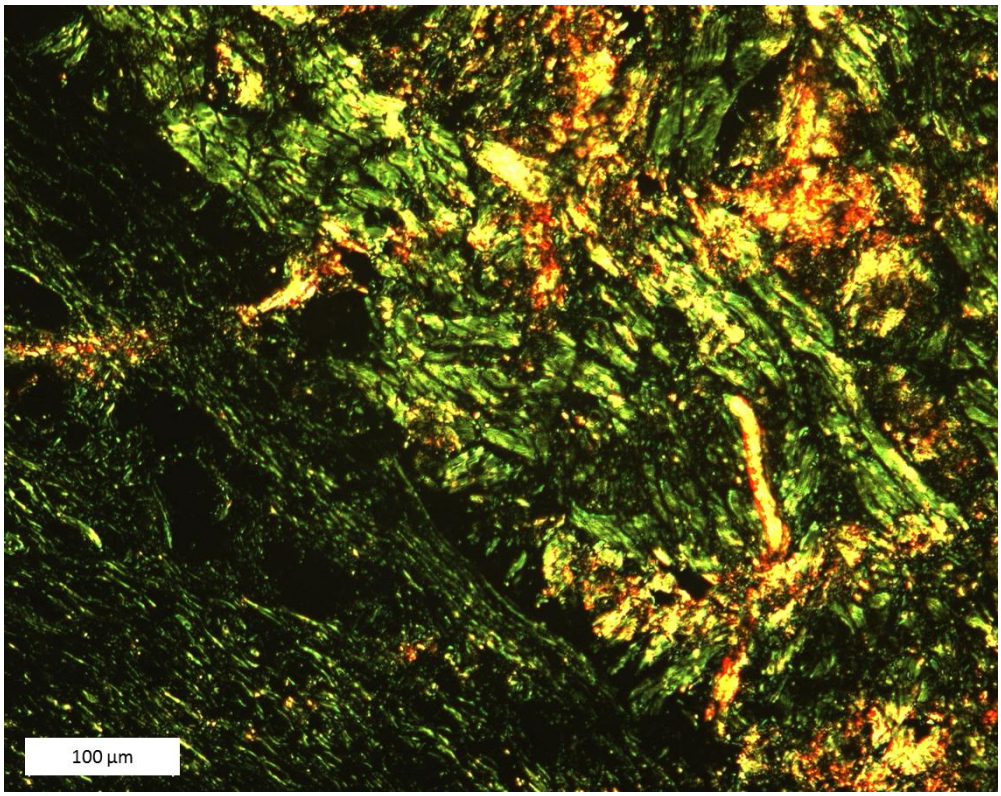

Figure 5.36 Permacol™ implant after 28 day implantation, implant showing basket weave pattern, Picro siris red (polarised light) 20X magnification.

Total cell counts at day 28 remained consistant with day 14 implants for non-crosslinked implants and highly-crosslinked implants. The highest crosslinked implants showed approximately triple the total cell count of non-crosslinked implants, the Permacol™ implants had an increase in total cell number over day 14 implants, falling between the other two implant groups (figure 5.38).

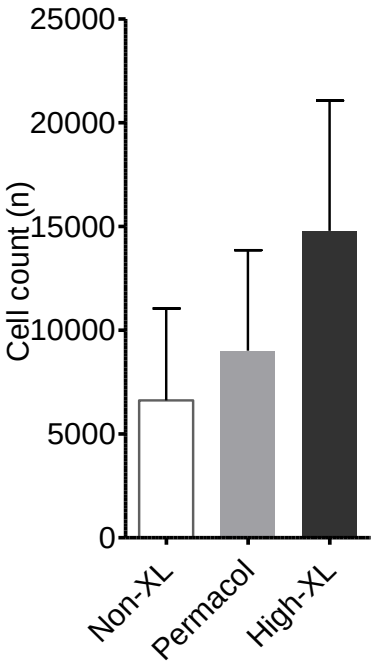

Figure 5.37 Quantitative cell count for day 28 non-crosslinked, Permacol™ and highly-crosslinked implants, error bars + 1 standard deviation from the mean, n= 6 for non-crosslinked and Permacol™ and n=4 for highly-crosslinked.

The proportion of cells identified in all implants as granulocytes was low, all below 5% of the total cell number. Nearly all of the granulocytes present (>90%) were identified as mast cells (figures 5.39 and 5.40). For all the implant groups the mast cell populations around the implants had remained consistent with day 7 and 14.

Lymphocyte numbers remained similar to day 14 implants for Permacol™ implants. A slight drop in lymphocyte numbers was measured between days 14 and 28 for the non-crosslinked and highly-crosslinked implant groups.

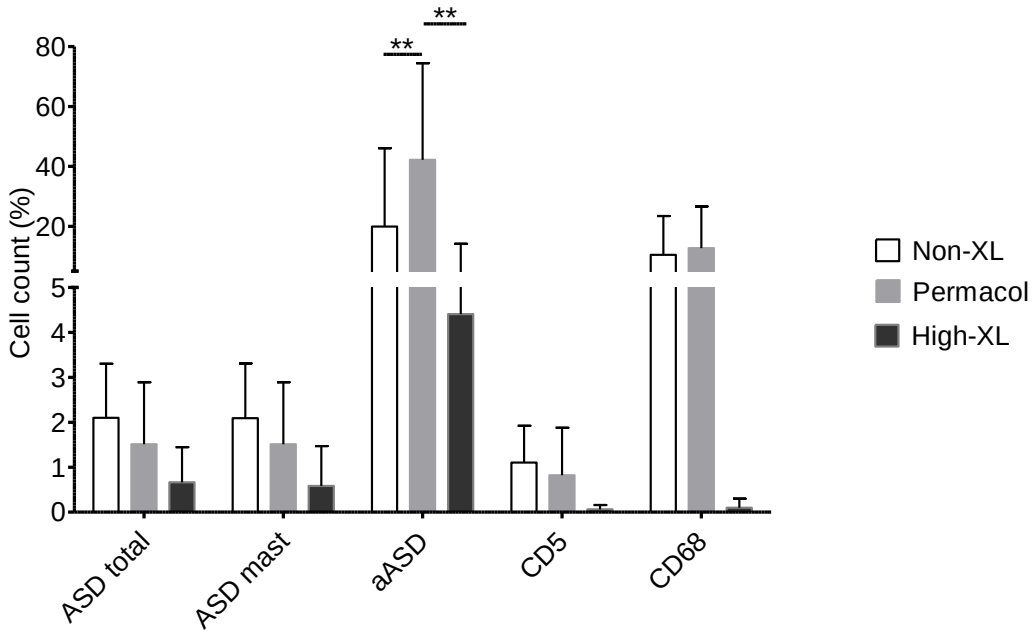

Figure 5.38 Quantitative cell percentages for day 28 non-crosslinked, Permacol™ and highly-crosslinked implants, error bars + 1 standard deviation from the mean, n= 6 for non-crosslinked and Permacol™ and n=4 for highly-crosslinked.

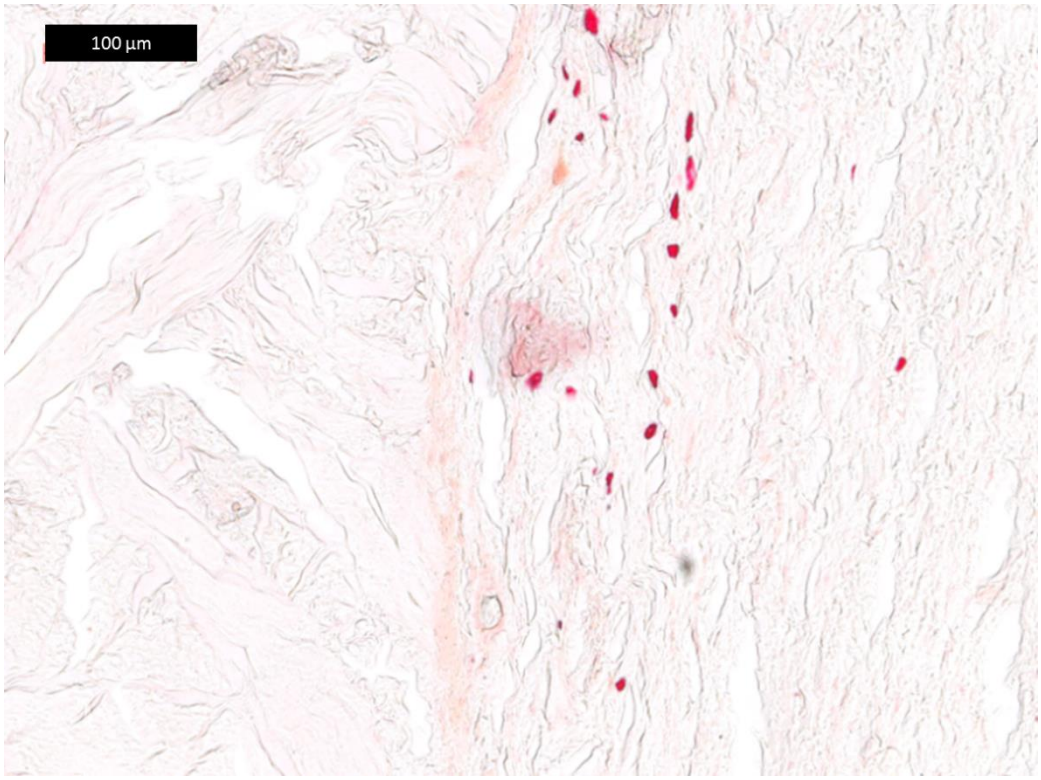

Figure 5.39 Non-crosslinked ASD staining of granulocytes, day 28 implant 20X magnification

5.3.5 **Overall implant observations**

General linear model (GLM) was used to test statistical significance of semi-quantitative and quantitative histopathology scores.

Table 5.1 and figures 5.41 and 5.42 show the results for implant type, duration of implantation and interaction between the two variables for the semi quantitative histological scoring.

Table 5.1 Statistical results for semi-quantitative histological scoring, P values determined by general linear model.

	Implant	Time	Implant x time
Granulocytes	Not significant	$p < 0.05$	Not significant
Lymphocytes	Not significant	Not significant	Not significant
Fibroblasts	Not significant	$p < 0.05$	Not significant
Macrophages	$p < 0.05$	Not significant	Not significant
Residue	Not significant	Not significant	Not significant
Degradation	Not significant	Not significant	Not significant
Fibroplasia	Not significant	$p < 0.05$	Not significant
Integration	Not significant	$p < 0.05$	Not significant
Colonisation	$p < 0.05$	$p < 0.05$	Not significant
Neovascularisation	Not significant	Not significant	Not significant
Encapsulation	Not significant	Not significant	Not significant

Grouping together all time points and assessing the effects of crosslinking levels of the implants, macrophage numbers and colonisation show significance in GLM. Performing an ANOVA with Tukeys post hoc test on these data sets showed highly-crosslinked implants were different from the other implant groups (figure 5.41).

Fewer macrophages and greater colonisation was observed in the highly-crosslinked group. Although not significant, a relationship is apparent for granulocytes and encapsulation with scores for both increasing with crosslinking level (figure 5.3).

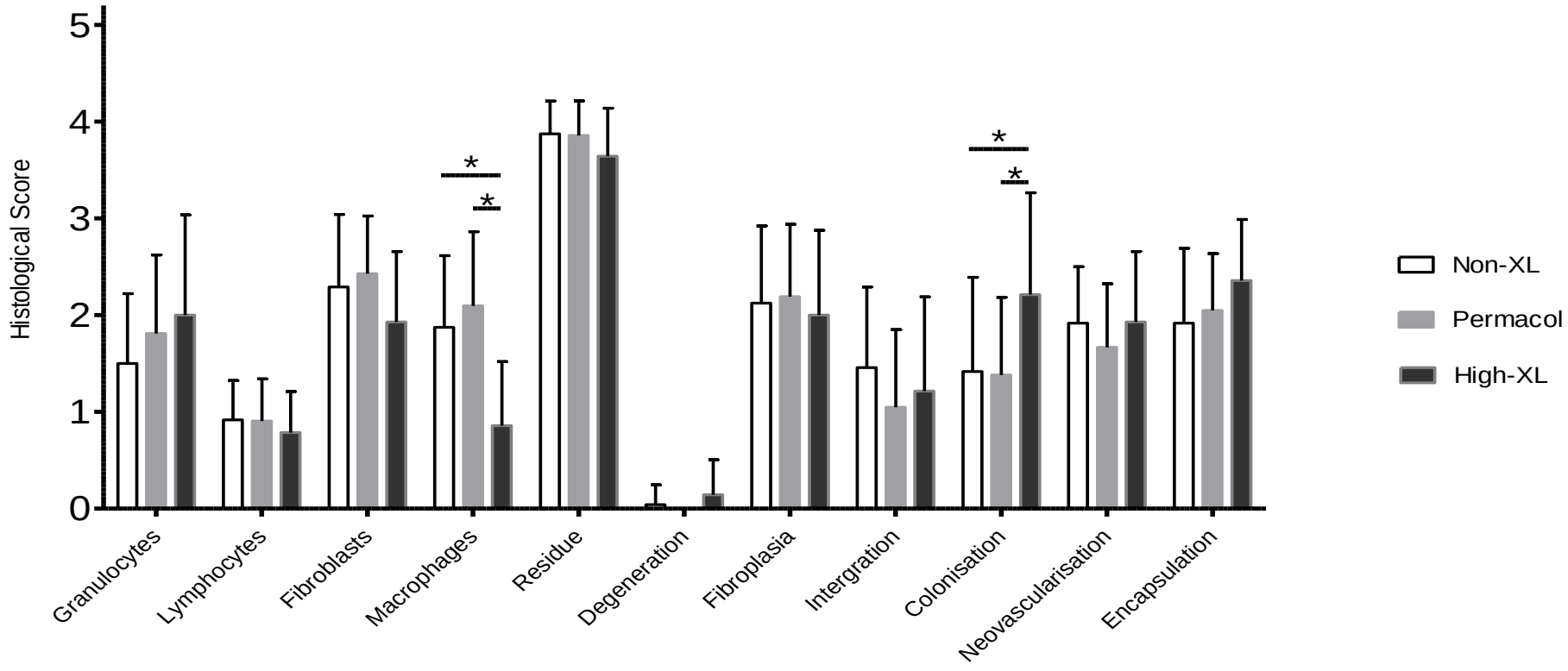

Figure 5.40 Semi-quantitative histological scores for all implant timepoints for non-crosslinked, Permacol™ and highly-crosslinked implants, error bars + 1 standard deviation from the mean, n= 24 for non-crosslinked and Permacol™ and n=16 for highly-crosslinked.

Grouping together implant groups and assessing effect of implant duration; granulocyte, fibroblast, fibroplasia, integration, colonisation and encapsulation scores show significance in the GLM. From figure 5.42 trends within these criteria can be seen;

Granulocyte – Decrease in histological score from days 2- 28, with the largest decrease observed between days 2 and 7.

Fibroblast and fibroplasia – Increase in histological score between days 2 and 7 then a decrease from days 7 to 28.

Integration - Increase in histological score from days 2- 28, with the largest increase observed between days 2 and 7.

Colonisation – Slight decrease in histological score between days 2 and 7, then an increase between days 7 and 14, remaining constant at day 28.

Encapsulation – Increase in histological score between days 2 and 7 remaining constant until day 28.

Analysing each histological criteria individually with ANOVA and Tukeys post hoc, fibroplasia between days 7 and 28 and integration between days 2 and 28 were significantly different (table 5.5).

For the semi quantitative scores the duration of implantation had a greater effect on differences observed.

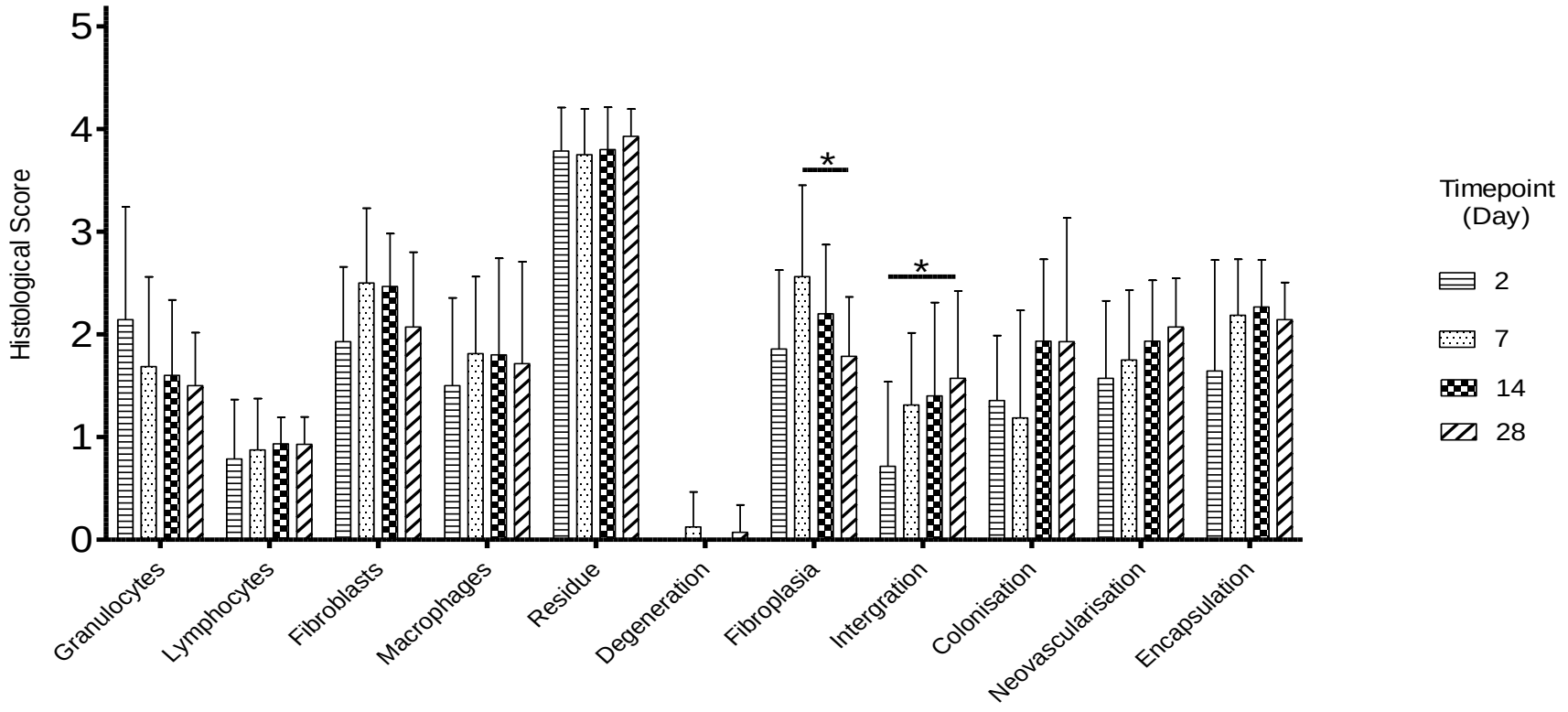

Figure 5.41 Semi-quantitative histological scores for all implants from days 2, 7, 14 and 28, error bars + 1 standard deviation from the mean, n= 21.

Table 5.5 Statistical results for quantitative histological scoring, P values determined by general linear model.

	Implant	Time	Implant x time
Total cell count	p <0.01	Not significant	Not significant
ASD (%)	Not significant	p <0.01	Not significant
Mast cells (%)	p <0.05	Not significant	Not significant
αASD (%)	p <0.01	Not significant	Not significant
CD5 cells (%)	p <0.01	Not significant	Not significant
CD68 cells (%)	p <0.05	Not significant	p <0.05
Collagen I/III ratio	Not significant	Not significant	Not significant

Grouping together all time points and assessing effect of crosslinking level of the implant, total cell count, mast cells, αASD, CD5 and CD68 positive cells show significance in GLM. Analysing each parameter separately with ANOVA and Tukeys post hoc these significant differences can be attributed to variances between highly crosslinked implants and either / or non-crosslinked and Permacol™ implants(figure 5.43). Trends observed across each parameter;

Total cell count – Increase in cell count from low to high crosslinking level. Highly-crosslinked implants have a significantly higher cell count than the other 2 groups.

ASD cells – No trend.

Mast cells – Decrease in mast cells present from low to high crosslinking level. Significant between the non-crosslinked and highly-crosslinked groups.

αASD – Slight increase between non-crosslinked and Permacol™ groups. Significantly fewer αASD positive cells in the highly-crosslinked implant group.

CD5 - Decrease in CD5 positive cells present from low to high crosslinking level. Significant between highly-crosslinked and other two groups.

CD68 - Slight increase between non-crosslinked and Permacol™ groups. Significantly fewer CD68 positive cells in the highly-crosslinked implant group than Permacol™.

Collagen ratio – Non-crosslinked and Permacol™ had similar ratios, highly-crosslinked implants had a lower overall ratio. Due to the large variation between the individual implants no significance was observed.

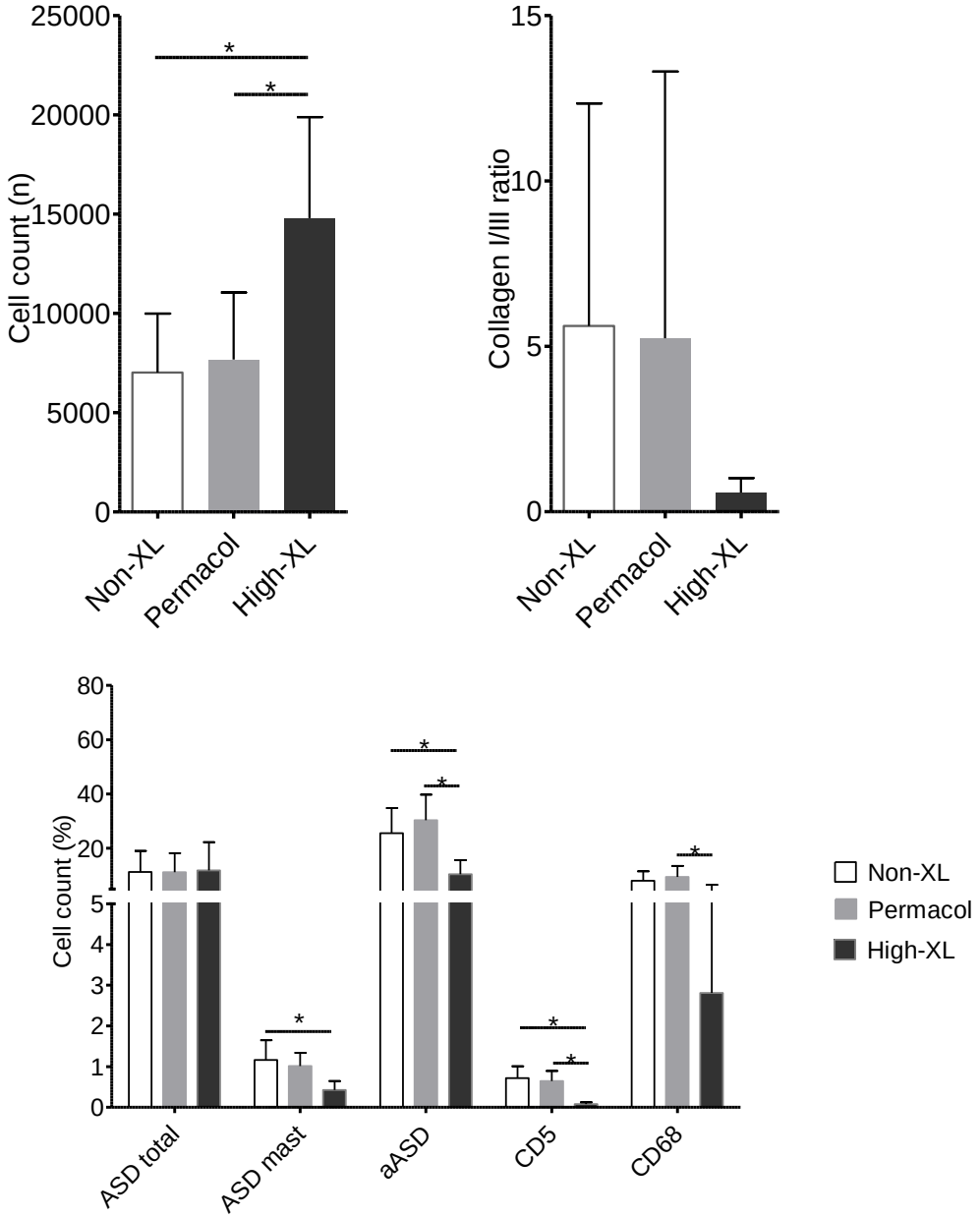

Figure 5.42 Quantitative histological analysis for non-crosslinked, Permacol™ and highly-crosslinked implants, error bars + 1 standard deviation from the mean, n= 24 for non-crosslinked and Permacol™ and n=16 for highly-crosslinked.

Grouping together all crosslinking levels and assessing implant duration, ASD positive cells show significance in GLM. Analysing each parameter separately with ANOVA and Tukeys post hoc these significant differences can be attributed to differences between day 2 time point and later time points (figure 5.44). Trends observed across each parameter;

Total cell count – No trend

ASD cells – First time point had significantly higher ASD positive cells than all later time points.

Mast cells – Increase in mast cells present from early to late time points. Significant between first (day2) and last (day 28) implants.

αASD – Slight increase between days 2 and 14 starting to drop by day 28.

CD5 – Similar for day 2 and 7 implant with a slight increase across day 14 and 28 implants.

CD68 - Slight increase between day 2 and 7 implants, remaining similar between days 7 and 28.

Collagen ratio – Decrease in collagen ratio as implant duration increased. Due to the large variation between the individual implants no significance was observed.

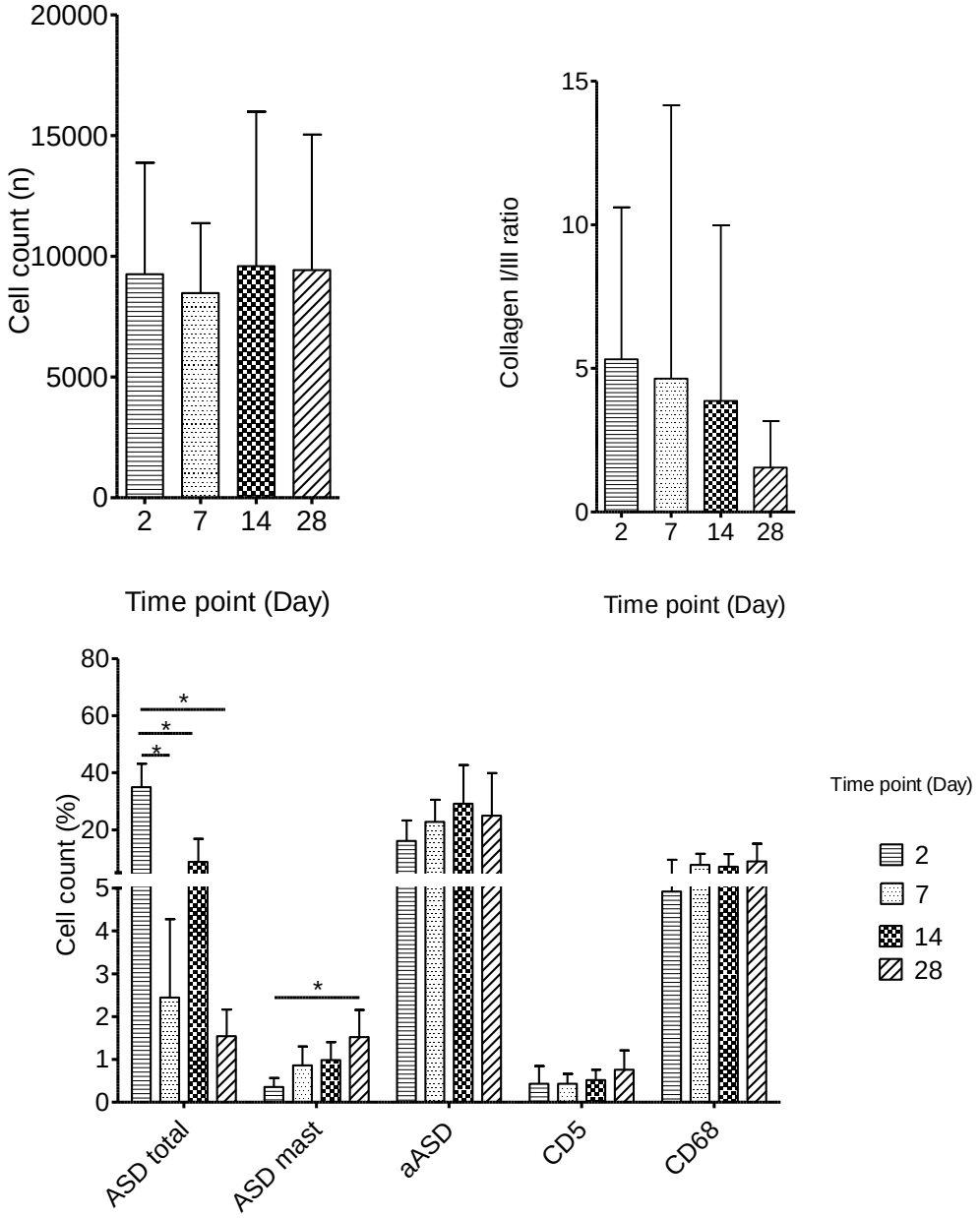

Figure 5.43 Quantitative histological score for 2, 7, 14 and 28 day implants, error bars + 1 standard deviation from the mean, n= 15.

5.4 Discussion

The effect crosslinking levels of biomaterials on immune response was assessed by subcutaneously implanting non-crosslinked, Permacol™ and highly crosslinked biomaterials. The first stage of this assessment was the observation of macroscopic characteristics upon explanation.

After only 48 hours, all of the implanted materials had attached to the underlying fascia. Seroma / hematomas were present across all crosslinking groups, no correlation could be drawn linking a specific group to incidence. These seromas and hematomas were likely due to surgical trauma rather than being implant driven. By day 7 all seromas had resolved, the small number of hematomas recorded at 48-hour implantation were not specific to a crosslinking group. From 7 days, angiogenesis and vasculature were observed across the three-crosslinking groups, with no bias towards any group. No visible degradation of any of the implants was observed through the time course.

Across the 28 day time course similar characteristics and host / tissue interactions were observed for all implant groups. The level of crosslinking of the implant did not have an effect on the macroscopic implant observations.

Following on from the macroscopic observations tissue and cell morphology was quantified on a microscopic level. These investigations were focused on the host implant interface, determining effects directly attributable to the implants.

In a normal immune response cells of the innate immune response are drawn to the injury / foreign body. In these studies the implant and implantation site represented these areas. After 48 hours an immune response at the host implant interface was

observed in all hosts. A clear indication of this was the large populations of granulocytes present [38], [61], accounting for 20 – 50 % of the total cell populations (figure 5.8). Granulocytes accounted for nearly all the cellular penetration into the implants, following the basket weave pattern of the implant's collagen fibres (figure 5.9). Similar levels of cell penetration were observed across all implant groups.

Crosslinking level of the implants did not influence implant degeneration with no significant degeneration observed over the time course. Pascual *et al.* carried out subcutaneous and intraperitoneal implantation models of commercially available crosslinked and non-crosslinked biological hernia implants [103]. They reported initial implant thickness had a greater impact on *in vivo* degradation than crosslinking, with Permacol™ (crosslinked) and Strattice® (non-crosslinked) having similar degradation and collagen profiles. Permacol™ implanted from three patients (at 16, 36 and 60 months) was examined for type I collagen of porcine (implant) and human (host) origin [119]. Original implant location could be clearly identified at 16 months, by 36 months collagen structure similar to host tissue was observed, both implants stained positive for host collagen rather than native implant collagen. One small area of collagen was identified at 60 months staining positive for original implant collagen, with the rest of the implant demonstrating host collagen only. This study showed that over time crosslinked implants are successfully remodelled by the host replacing the implant collagen with host collagen.

Integration of the implants with the host tissue was greater for the non-crosslinked implant group compared to the crosslinked implants groups, except for the highly-

crosslinked implants at day 28. For the Permacol™ group of implants the integration profile was more similar to the non-crosslinked group than the highly-crosslinked group. Reduced integration of crosslinked implants has previously been suggested by other authors [95], [102], [120]. This trend has been observed during this study; however the amount of overlap between the groups indicated that it is not significant at a clinical level, especially between the non-crosslinked and Permacol™ groups.

Cellular penetration into the implants was similar for the non-crosslinked and Permacol™ implant groups, with the highly-crosslinked group having slightly more cellular penetration. This trend has been observed in human implants of non-crosslinked implants (Strattice) and Permacol™ [121].

Cellular density of the implants was greater for the highly-crosslinked group compared to the non-crosslinked and Permacol™ groups, which had similar cell densities across the study. At day 7 and 14 explanations, this difference was significant. This indicated that highly-crosslinking the implant material elicits a stronger host response than 'lightly' crosslinking as in the Permacol™ group when compared to the non-crosslinked implants.

It was noted in the histopathology that the highly-crosslinked implants had significantly more granulocytes present than the non-crosslinked implants after 2 days implantation (figure 5.6). This trend is confirmed by the specific staining, although the percentage of granulocytes in the highly-crosslinked group was only slightly greater than the non-crosslinked group (figure 5.8) the total numbers of cells present was higher. Therefore the total number of granulocytes present in the highly-crosslinked implants was greater than the non-crosslinked implants. No

significant differences in granulocyte levels were observed between Permacol™ and the non-crosslinked implants.

Monocytes and T-cells were present in all implants, as expected at 48 hours post implantation, their frequency was lower than the granulocytes. Interestingly mature macrophages were not observed in the highly-crosslinked group.

Following the expected cell profile of the innate immune response, by day 7 the proportion of granulocytes had dropped significantly from day 2. Most of the granulocytes had disappeared from the implant / host interface for the non-crosslinked and Permacol™ groups with less than 1% remaining. In relation to this drop, the proportion of monocytes, macrophages and fibroblasts had increased from day 2 to 7 in the non-crosslinked and Permacol™ groups. The highly-crosslinked group showed a marked decrease of granulocytes from day 2 to 7 implants however, the levels of granulocytes surrounding these implants remained higher than the non-crosslinked and Permacol™ groups. It has been reported in the literature that macrophages play a critical role in the non-phlogistic removal of neutrophils [122]. Mature macrophages were not observed around highly-crosslinked implants at 48 hours, this could be part of the reason a greater level of granulocytes were present around the highly-crosslinked implants compared to the non-crosslinked and Permacol™ implants. The level of observed monocytes and macrophages remained constant between the day 2 and day 7 implants, though at day 7 a few mature macrophages were observed and fibroblast levels had increased over day 2. These shifts in cell types from granulocytes to monocytes mark the transition in the host's immune response towards resolution of the immune response. This indicated that the host response was similar for non-crosslinked and Permacol™ groups, the

highly-crosslinked group appeared to elicit a stronger immune response, which took longer to resolve.

Non-crosslinked and Permacol™ implant groups maintained similar cell profiles and matrix characteristics between implantation periods 7, 14 and 28 days. By day 14 and continuing at day 28, the highly-crosslinked groups granulocyte populations had dropped and were consistent with the non-crosslinked and Permacol™ groups. Interestingly the overall monocyte and macrophage levels of the highly crosslinked group did not rise, remaining proportionally lower than the non-crosslinked and Permacol™ groups. The only time any cells from these lineages were concordant was at the 14-day time point, when all three groups had similar proportions of mature macrophages present.

Many studies have been carried out comparing non-crosslinked and crosslinked biomaterials. The studies reported in this thesis were designed to eliminate the ambiguities brought into these studies by comparing differently processed and sources of donor material.

This study demonstrated that at lower levels of crosslinking, such as those present in Permacol™, the host's immune response was not significantly different to the same material omitting the crosslinks. However, implants with greater levels of crosslinking, in this study nearly 7 times, had a higher induction effect on the host immune response, eliciting a stronger innate immune response from the host and delaying resolution.

6 General Discussion and Conclusions

6.1 General Discussion

Three research objectives were investigated;

i. Characterisation of the biophysical properties of biomaterials prepared using various crosslinking reactions with HMDI.

ii. Evaluation of how biomaterial crosslinking affects leukocyte activation, using an *in vitro* reactive oxygen species assay.

iii. Assessment of how biomaterial crosslinking affects the immune response, using an *in vivo* rat model.

Biomaterials for soft tissue repair are a growing area, with more materials and increased indications being identified for use every year. One topic that has been highly discussed is the effect of the addition of chemical crosslinks to these materials. Many chemicals have been used for crosslinking biomaterials over the years including; glutaraldehyde, genipin, HMDI and EDC/NHS. The aim of adding these crosslinks is mainly to improve implant stability and physical properties, in the case of sponges and gels generating a cohesive 3D structure from the composite materials or, for sheet materials, manipulating handling characteristics and degradation resistance. Any foreign body that is implanted will initiate the host immune response, one area that is poorly understood is the direct effect crosslinking alone has on the host immune response. All materials produced for this study were decellularised using the proprietary Permacol™ process, only the crosslinking step was altered. Using the data generated in this project the effect crosslinking has on the biomaterial and subsequently the *in vivo* response elicited by the biomaterial

was established. This has developed the understanding of the effect crosslinking decellularised biomaterials with HMDI has on the host immune response.

Changes within the biomaterials biophysical characteristics induced by crosslinking were considered in chapter 3. HMDI was used as the crosslinking agent within these studies, HMDI has two reactive isocyanate groups which can bond with amine groups present on lysine and hydroxylysine molecules within collagen fibres.

Subtle changes in the crosslinking levels present within the collagen-derived biomaterials had a dramatic effect on resistance to collagenase enzyme degradation. It was established that the crosslinking parameters used in the manufacture of Permacol™ imparts 1.7 crosslinks per 1000 AA, this level of crosslinking increased the biomaterials resistance, over 20 hours, to degradation by collagenase from 30% to 85%. Doubling this level of crosslinking to 3 crosslinks per 1000 AA increased the resistance to 95% and increasing again to 7 crosslinks per 1000 AA no degradation was observed. Resistance against collagenase digestion can be used as an indication of the implants stability and longevity *in vivo*, especially in chronic and infected wounds. Surgeons can use the collagenase degradation information to help inform their selection of an implant for the procedure. If the implant is to be used in a contaminated field, the additional collagenase resistance offered by crosslinking may be of benefit, providing extended support when compared to a non-crosslinked varient. However, collagenase is not the only enzymes by which collagen based biomaterials can be degraded, *in vivo* many enzyme are present during the host immune response. It would be useful to conduct an *in vivo* study of non-crosslinked and crosslinked implants in clean and dirty contaminated fields.

The information provided by carrying out such a study would be very useful for scientist and surgeons.

The degree of crosslinking present in the implants affected the temperature at which the collagen fibres denatured, the point when tertiary structure is lost. As the crosslinking level increased the denaturation temperature increased proportionally. Several studies have been carried out where the denaturation temperature of crosslinked materials has been investigated, both of these studies found glutaraldehyde had a greater effect than isocyanate or genipin crosslinking [33], [70]. Miles *et al* determined that the rise in denaturation temperature from crosslinking rat-tail tendons reduced fibre hydration [70]. For biomaterials processed by the proprietary Permacol™ process the denaturation temperature recorded can be used as an indication of the level of crosslinking present within specific samples.

Once the relationship between crosslinking level and denaturation temperature has been established for an implants produced via a specified processing protocol. The implants denaturation temperature could be a useful quality control tool for manufacturing companies, allowing the level of crosslinking attained during the manufacturing process to be quickly and cheaply quantified. Initially determining the crosslinking level by HPLC amino acid analysis involves a technically complicated and potentially dangerous extraction procedure, taking several days to quantify crosslinking level. Establishing implant denaturation temperature only requires a small portion of the implant to be sealed inside a crucible, taking less than 15 minutes to quantify the crosslinking level.

When comparing the different crosslinking levels for tensile properties no trends could be linked to the number of crosslinks present within the biomaterials. Ultimate tensile strength, Young's modulus and maximum extension were established for all crosslinking groups, lack of differences between groups for these measurements indicates that at implantation, elasticity and tensile strength of materials processed by the Permacol™ proprietary process will be similar irrespective of crosslinking level. Once implanted it is likely that tensile properties of non-crosslinked material will reduce before those containing crosslinks, Deeken *et al* observed this trend over a 12 month time course of commercially available biological hernia implants, one of which was Permacol™ [123]. Over the 12 month course of this study they found that tensile strength and maximum load of Permacol™ remained higher than native abdominal wall.

In vitro testing of the crosslinked implants was completed by assessing their ability to activate leukocytes over a 2-hour time course. When comparing crosslinking levels to leukocyte activation, clear trends were observed across the whole data set. When comparing data from individuals, large inter-person variations were observed, since not all donor blood was tested against every crosslinking variant, the inter-person variations made statistical analysis of the data difficult. When the study compared 10 donor's leukocyte activation on the same day to a subset of crosslinking levels (non-crosslinked, Permacol™ and highly-crosslinked) the statistical analysis became more robust. In this study, 8 out of the 10 donors demonstrated higher leukocyte activation by the highly-crosslinked biomaterial than non-crosslinked or Permacol™ biomaterials. When averaging over the 10 donors the difference between highly-crosslinked versus non-crosslinked and Permacol™ was significant, we have reported that non-crosslinked and Permacol™

materials activated leukocytes to a similar degree [85]. When considering implant selection for surgery, testing the patients' leukocyte activation in relation to implant materials may be advantageous, allowing a personalised approach to medicine. Chapter 4 concentrated on crosslinked variants prepared using the Permacol process, 3 other commercial implants (Strattice, Alloderm and Sugisis) were also tested. Permacol, Strattice and Alloderm all recorded similar leukocyte activation levels. However Surgisis achieved much higher activation levels, this higher response could be indicative of an implant that could generate a greater host response. Bryan *et. al*, implanted these materials in a full thickness abdominal wall defect model, Permacol, Strattice and Alloderm all performed at a similar level, Surgisis showed significant degeneration and a higher level of polymorphonuclear cells associated with the implantation site [98]. This supports the theory that *in vitro* testing of leukocyte activation could be used as an indication host response. It would be interesting to carry out an *in vivo* study where blood was taken pre and post implantation for leuckocyte activation testing and comparing the results to the surgery's outcome.

In vivo a clear trend in immune response was observed towards the three implant groups, non-crosslinked, Permacol™ and highly-crosslinked. As with the *in vitro* leukocyte activation study of 10 donors, non-crosslinked and Permacol™ had very similar host immune responses, the host immune response observed towards highly-crosslinked implants was greater. Differences in observed characteristics and cell profiles that were observed between Permacol™ and non-crosslinked implants did not affect the overall progress of the host immune response. The main indicator of an increased immune response towards highly-crosslinked implants was the level of cell recruitment, which remained consistently higher throughout these studies.

Initially the proportion of different cells recruited was similar to non-crosslinked and Permacol™ implants with granulocytes most prominent. For non-crosslinked and Permacol™ implants, these granulocytes were rapidly cleared being replaced by monocytes and fibroblasts, for highly-crosslinked implants the initial host interrogation of the implants by granulocytes continued into the second time point (7 days). This delay may be partly due to the lack of macrophages present, which play a pivotal role in the removal of neutrophils [124]. Even with the delay in the resolution of the immune response towards highly-crosslinked implants, all implants examined within these studies were accepted by the hosts showing good integration with the surrounding tissue.

This thesis has focused on the effect crosslinking has on implant characteristics and host response. One of the advantages of this study is only the crosslinking manufacturing step was modified between implants. Many previous studies have compared implants prepared using different manufacturing parameters, grouping implants together as either non-crosslinked or crosslinked regardless of crosslinking level and manufacturing processes. The data generated demonstrated that the low level of crosslinks present in Permacol imparted beneficial properties like resistance to collagenase degradation, however the host response was unaffected by the addition of the crosslinks when compared to non-crosslinked material. Previous studies have shown that crosslinking implants can have a detrimental effect on the host response; these studies have backed up this statement to a degree, with the highly-crosslinked implant producing an increased host response both *in vitro* and *in vivo*. However, scientists can use the data and methodologies contained within this thesis to aid the design of new biomaterials utilising the benefits of additional crosslinks whilst minimising detrimental *in vivo* effects.

6.2 Conclusions

Chapter 3 – Biomaterial characterisation

- Lysine and hydroxylysine concentrations fell as exposure to HMDI increased either by duration or concentration, indicating the molecules had been chemically modified and crosslinked.
- Crosslinking did not favour lysine or hydroxylysine with a ratio of 3:1 being maintained throughout the reactions.
- The concentration of HMDI had a greater effect on the crosslinking level than increasing exposure time.
- Introducing crosslinks to the collagen matrix imparted resistance to degradation by collagenase enzyme.
- As the level of crosslinking increased the denaturation temperature of the material increased.
- The addition of crosslinks in to the collagen matrix did not affect the tensile properties of the material.

Chapter 4 – Effect of crosslinking on leukocyte activation

- The addition of crosslinks to the collagen matrix did not have an effect on the leukocyte activation profile.
- Differences were observed between donors.

Chapter 5 – Effect of crosslinking on immune response

- Low levels of crosslinking, as in Permacol™ did not affect the host immune response.
- High levels of crosslinking increased and delayed resolution of the hosts immune response.

6.3 Suggestions for future work

Host immune responses to crosslinked biomaterials are still not fully understood, these studies have indicated that crosslinking at low levels, as used in Permacol™, does not significantly impact the host immune response. From the *in vitro* leukocyte activation studies, donor variability was more important to leukocyte activation. If further studies were carried out it would be interesting prior to implantation and possibly during the study to measure the host *in vitro* leukocyte activation towards the biomaterial which is planned to be implanted.

One of the major strengths of crosslinking biomaterials is the increase in resistance to enzyme degradation. These studies investigated this trend *in vitro,* it would be interesting to see how the addition of crosslinks affected biomaterial integrity in a compromised model.

Studies such as those mentioned above could help improve patient outcomes when they need a soft tissue repair that would benefit from the use of a biomaterial. The first point could help tailor the implant to the patient, ensuring the host does not have an increased immune response due to material selection. Selection of the correct material could improve recovery and reduce the chance of reoccurrence in the case of hernia surgery. Crosslinked biomaterials are not currently indicated for use in contaminated fields, anecdotally these materials have a better outcome in

complicated wounds. Since use is currently classed as ‘off catalogue’ many surgeons are unwilling / unable to use these implants in cases which they may benefit. Controlled trials to confirm or refute this anecdotal evidence would assist surgeon implant selection.

7 References

[1] D. J. S. Hulmes, “Collagen Diversity , Synthesis and Assembly,” in *Collagen*, P. Fratzl, Ed. Springer, 2008, pp. 15–48.

[2] J. Bella, “Collagen structure: new tricks from a very old dog,” *Biochem. J.*, vol. 473, no. 8, pp. 1001–25, 2016.

[3] M. Mienaltowski and D. Birk, “Progress in Heritable Soft Connective Tissue Diseases,” in *Advances in Experimental Medicine and Biology*, J. Halper, Ed. 2014, pp. 77–94.

[4] D. S. Greenspan, “Biosynthetic processing of collagen molecules,” *Top. Curr. Chem.*, vol. 247, pp. 149–183, 2005.

[5] N. C. Avery and A. J. Bailey, “The effects of the Maillard reaction on the physical properties and cell interactions of collagen.,” *Pathol. Biol. (Paris).*, vol. 54, no. 7, pp. 387–95, Sep. 2006.

[6] L. Cen, W. Liu, L. Cui, W. Zhang, and Y. Cao, “Collagen tissue engineering: Development of novel biomaterials and applications,” *Pediatr. Res.*, vol. 63, no. 5, pp. 492–496, 2008.

[7] P. Balasubramanian, M. P. Prabhakaran, and M. Sireesha, “Collagen in Human Tissues: Structure, Function, and Biomedical Implications from a Tissue Engineering Perspective,” in *Polymer Composites – Polyolefin Fractionation – Polymeric Peptidomimetics – Collagens*, vol. 251, no. August 2012, A. Abe, H.-H. Kausch, M. Möller, and H. Pasch, Eds. Berlin, Heidelberg: Springer Berlin Heidelberg, 2013, pp. 173–206.

[8] A. L. Kwansa, R. De Vita, and J. W. Freeman, “Mechanical recruitment of N- and C-crosslinks in collagen type I.,” *Matrix Biol.*, vol. 34, pp. 161–9, Feb. 2014.

[9] P. Brown, “Abdominal wall reconstruction using biological tissue grafts,” *Aorn*, vol. 90, no. 4, pp. 513–524, Oct. 2009.

[10] D. R. Hopkins, S. Keles, and D. S. Greenspan, “The bone morphogenetic protein 1/Tolloid-like metalloproteinases.,” *Matrix Biol.*, vol. 26, no. 7, pp. 508–23, Sep. 2007.

[11] D. E. Birk and P. Bruckner, “Collagen suprastructures,” *Top. Curr. Chem.*, vol. 247, pp. 185–205, 2005.

[12] K. Bisbort, Gretchen and Oberholser, “Collagen tutorial,” 2013. [Online]. Available: http://www.messiah.edu/departments/chemistry/molscilab/Jmol/collagen/chapter1.htm.

[13] S. Porter, I. M. Clark, L. Kevorkian, and D. R. Edwards, “The ADAMTS metalloproteinases.,” *Biochem. J.*, vol. 386, no. Pt 1, pp. 15–27, Feb. 2005.

[14] T. J. Wess, “Collagen Fibrillar Structure and Hierarchies,” in *Collagen structure and mechanics*, Peter Fratzl, Ed. 2008, pp. 49–80.

[15] J. P. Orgel, T. J. Wess, and a Miller, “The in situ conformation and axial location of the intermolecular cross-linked non-helical telopeptides of type I collagen.,” *Structure*, vol. 8, no. 2, pp. 137–42, Feb. 2000.

[16] N. C. Avery and A. J. Bailey, “Restraining Cross-Links Responsible for the Mechanical Properties of Collagen Fibers: Natural and Artificial,” in *Collagen*, P. Fratzl, Ed. Boston, MA: Springer US, 2008, pp. 81–110.

[17] B. Depalle, Z. Qin, S. J. Shefelbine, and M. J. Buehler, “Influence of cross-link structure, density and mechanical properties in the mesoscale deformation mechanisms of collagen fibrils,” *J. Mech. Behav. Biomed. Mater.*, vol. 52, pp. 1–13, 2015.

[18] S. P. Robins, “Biochemistry and functional significance of collagen cross-linking.,” *Biochem. Soc. Trans.*, vol. 35, no. Pt 5, pp. 849–52, Nov. 2007.

[19] J. P. R. O. Orgel, T. C. Irving, A. Miller, and T. J. Wess, “Microfibrillar structure of type I collagen in situ.,” *Proc. Natl. Acad. Sci. U. S. A.*, vol. 103, no. 24, pp. 9001–5, Jun. 2006.

[20] M. Yamauchi, R. E. London, C. Guenat, F. Hashimoto, and G. L. Mechanic, "Structure and formation of a stable histidine-based trifunctional cross-link in skin collagen.," *J. Biol. Chem.*, vol. 262, no. 24, pp. 11428–34, Aug. 1987.

[21] D. F. Williams, "On the nature of biomaterials.," *Biomaterials*, vol. 30, no. 30, pp. 5897–909, Oct. 2009.

[22] B. D. Ratner, "A history of biomaterials," in *Biomaterials Science*, Third., B. Ratner, A. Hoffman, F. Schoen, and J. Lemons, Eds. 2013, pp. 41–53.

[23] A. K. Lynn, I. V Yannas, and W. Bonfield, "Antigenicity and immunogenicity of collagen.," *J. Biomed. Mater. Res. B. Appl. Biomater.*, vol. 71, no. 2, pp. 343–54, Nov. 2004.

[24] Y. Yang, Y. Kang, M. Sen, and S. Park, "Biomaterials for Tissue Engineering Applications," in *Bioceramics in Tissue Engineerng*, J. A. Burdick and R. L. Mauck, Eds. Vienna: Springer Vienna, 2011, pp. 179–207.

[25] J. Glowacki and S. Mizuno, "Collagen scaffolds for tissue engineering.," *Biopolymers*, vol. 89, no. 5, pp. 338–44, May 2008.

[26] D. W. Courtman, B. F. Errett, and G. J. Wilson, "The role of crosslinking in modification of the immune response elicited against xenogenic vascular acellular matrices.," *J. Biomed. Mater. Res.*, vol. 55, no. 4, pp. 576–86, Jun. 2001.

[27] G. Krishnamoorthy, R. Selvakumar, T. P. Sastry, A. B. Mandal, and M. Doble, "Effect of d-amino acids on collagen fibrillar assembly and stability: Experimental and modelling studies," *Biochem. Eng. J.*, vol. 75, pp. 92–100, 2013.

[28] C. Englert, T. Blunk, R. Müller, S. S. von Glasser, J. Baumer, J. Fierlbeck, I. M. Heid, M. Nerlich, and J. Hammer, "Bonding of articular cartilage using a combination of biochemical degradation and surface cross-linking.," *Arthritis Res. Ther.*, vol. 9, no. 3, p. R47, Jan. 2007.

[29] P. J. Dijkstra, J. Feijen, C. Biology, L. H. H. Olde Damink, P. J. Dijkstra, M. J. A. Luyn, P. B. Wachem, P. Nieuwenhuis, and J. Feijen, "Crosslinking of dermal sheep collagen using hexamethylene diisocyanate," *J. Mater. Sci. Mater. Med.*, vol. 6, no. 7, pp. 429–434, 1995.

[30] D. T. Cheung, N. Perelman, E. C. Ko, and M. e. Nimni, "Mechanism of crosslinking of proteins by glutaraldehyde III. Reaction with collagen in tissues," *Connect. Tissue Res.*, vol. 13, no. 2, pp. 109–115, Jan. 1985.

[31] I. Migneault, C. Dartiguenave, M. J. Bertrand, and K. C. Waldron, "Glutaraldehyde: behavior in aqueous solution, reaction with proteins, and application to enzyme crosslinking.," *Biotechniques*, vol. 37, no. 5, pp. 790–6, 798–802, Nov. 2004.

[32] L. H. H. Olde Damink, P. J. Dijkstra, M. J. A. Luyn, P. B. Wachem, P. Nieuwenhuis, and J. Feijen, "Glutaraldehyde as a crosslinking agent for collagen-based biomaterials," *J. Mater. Sci. Mater. Med.*, vol. 6, no. 8, pp. 460–472, Aug. 1995.

[33] H. W. Sung, I. L. Liang, C. N. Chen, R. N. Huang, and H. F. Liang, "Stability of a biological tissue fixed with a naturally occurring crosslinking agent (genipin).," *J. Biomed. Mater. Res.*, vol. 55, no. 4, pp. 538–46, Jun. 2001.

[34] L. Huang-Chien, C. Yen, H. Cheng-Kuo, L. Meng-Horng, and S. Hsing-Wen, "Effects of crosslinking degree of an acellular biological tissue on its tissue regeneration pattern," *Biomaterials*, vol. 25, no. 17, pp. 3541–3552, Aug. 2004.

[35] D. M. Klinman, "Immunotherapeutic uses of CpG oligodeoxynucleotides.," *Nat. Rev. Immunol.*, vol. 4, no. 4, pp. 249–58, Apr. 2004.

[36] G. Dranoff, "Cytokines in cancer pathogenesis and cancer therapy," *Nat. Rev. Cancer*, vol. 4, no. 1, pp. 11–22, Jan. 2004.

[37] B. H. Harris and J. A. Gelfand, "The immune response to trauma.," *Semin. Pediatr. Surg.*, vol. 4, no. 2, pp. 77–82, May 1995.

[38] S. Franz, S. Rammelt, D. Scharnweber, and J. C. Simon, “Immune responses to implants - a review of the implications for the design of immunomodulatory biomaterials.,” *Biomaterials*, vol. 32, no. 28, pp. 6692–709, Oct. 2011.

[39] N. Bryan, H. Ashwin, N. J. J. Smart, Y. Bayon, and J. a a Hunt, “In vitro activation of human leukocytes in response to contact with synthetic hernia meshes.,” *Clin. Biochem.*, vol. 45, no. 9, pp. 672–6, Jun. 2012.

[40] E. A. Nicu and B. G. Loos, “Polymorphonuclear neutrophils in periodontitis and their possible modulation as a therapeutic approach.,” *Periodontol. 2000*, vol. 71, no. 1, pp. 140–63, 2016.

[41] R. Warrington, W. Watson, H. L. Kim, and F. R. Antonetti, “An introduction to immunology and immunopathology.,” *Allergy Asthma. Clin. Immunol.*, vol. 7, no. Suppl 1, p. S1, Jan. 2011.

[42] N. Woolf, *Cell, tissue and disease. The basis of pathology*, 3rd ed. Harcourt, 2000.

[43] D. Hashimoto, J. Miller, and M. Merad, “Dendritic cell and macrophage heterogeneity in vivo.,” *Immunity*, vol. 35, no. 3, pp. 323–35, Sep. 2011.

[44] D. Ferenbach and J. Hughes, “Macrophages and dendritic cells: what is the difference?,” *Kidney Int.*, vol. 74, no. 1, pp. 5–7, Jul. 2008.

[45] S. Gordon and P. R. Taylor, “Monocyte and macrophage heterogeneity.,” *Nat. Rev. Immunol.*, vol. 5, no. 12, pp. 953–64, Dec. 2005.

[46] E. Vivier, E. Tomasello, M. Baratin, T. Walzer, and S. Ugolini, “Functions of natural killer cells.,” *Nat. Immunol.*, vol. 9, no. 5, pp. 503–10, May 2008.

[47] C. R. Almeida, D. P. Vasconcelos, R. M. Gonçalves, and M. a Barbosa, “Enhanced mesenchymal stromal cell recruitment via natural killer cells by incorporation of inflammatory signals in biomaterials.,” *J. R. Soc. Interface*, vol. 9, no. 67, pp. 261–71, Feb. 2012.

[48] J. Zimmer, *Natural killer cells: at the forefront of modern immunology*. Berlin, Heidelberg: Springer Berlin Heidelberg, 2010.

[49] K. A. Fitzgerald, L. A. J. O'Neill, and A. J. H. Gearing, *Cytokine factsbook and webfacts*, 2nd ed. Academic Press, 2001.

[50] J. A. Stenken and A. J. Poschenrieder, "Analytica Chimica Acta Bioanalytical chemistry of cytokines – A review," *Anal. Chim. Acta*, vol. 853, pp. 95–115, 2015.

[51] A. Kelso, "Educating T cells : early events in the differentiation and commitment of cytokine-producing CD4 + and CD8 + T cells," *Springer Semin. Immunopathol.*, vol. 21, no. 3, pp. 231–248, 1999.

[52] J. V. Sarma and P. a. Ward, "The complement system," *Cell Tissue Res.*, vol. 343, pp. 227–235, 2011.

[53] H. Oxlund, H. Christensen, M. Seyer-Hansen, and T. T. Andreassen, "Collagen deposition and mechanical strength of colon anastomoses and skin incisional wounds of rats.," *J. Surg. Res.*, vol. 66, no. 1, pp. 25–30, Nov. 1996.

[54] L. T. Sørensen, "Effect of lifestyle, gender and age on collagen formation and degradation.," *Hernia*, vol. 10, no. 6, pp. 456–61, Dec. 2006.

[55] D. T. Luttikhuizen, M. J. van Amerongen, P. C. de Feijter, A. H. Petersen, M. C. Harmsen, and M. J. a van Luyn, "The correlation between difference in foreign body reaction between implant locations and cytokine and MMP expression.," *Biomaterials*, vol. 27, no. 34, pp. 5763–70, Dec. 2006.

[56] J. M. Anderson, A. Rodriguez, and D. T. Chang, "Foreign body reaction to biomaterials," *Seminars in Immunology*, vol. 20, no. 2. pp. 86–100, 2008.

[57] J. Wetterö, P. Tengvall, and T. Bengtsson, "Platelets stimulated by IgG-coated surfaces bind and activate neutrophils through a selectin-dependent pathway," *Biomaterials*, vol. 24, pp. 1559–1573, 2003.

[58] A. C. Vasconcelos, P. P. Campos, N. B. Pereira, T. O. Socarra, J. P. C. Souza, and S. P. Andrade, “Foreign Body Response to Subcutaneous Implants in Diabetic Rats,” vol. 9, no. 11, 2014.

[59] K. S. Ltd., “ABLE Oxidative Stree Kits with Pholasin,” *kit insert*, 2013. .

[60] C. H. I. Chiung, G. Chen, B. Ridgeway, and M. F. R. Paraiso, “Biologic Grafts and Synthetic Meshes in Pelvic Reconstructive Surgery,” *Clin. Obstet. Gynecol.*, vol. 50, no. 2, pp. 383–411, 2007.

[61] S. F. Badylak, “Decellularized allogeneic and xenogeneic tissue as a bioscaffold for regenerative medicine: Factors that influence the host response,” *Ann. Biomed. Eng.*, vol. 42, no. 7, pp. 1517–1527, 2014.

[62] W. B. Gaertner, M. E. Bonsack, and J. P. Delaney, “Experimental evaluation of four biologic prostheses for ventral hernia repair.,” *J. Gastrointest. Surg.*, vol. 11, no. 10, pp. 1275–85, Oct. 2007.

[63] Y. W. Novitsky, S. B. Orenstein, and D. L. Kreutzer, “Comparative analysis of histopathologic responses to implanted porcine biologic meshes,” *Hernia*, vol. 18, no. 5, pp. 713–721, Oct. 2014.

[64] A. M. S. Ibrahim, O. a Ayeni, K. B. Hughes, B. T. Lee, S. A. Slavin, and S. J. Lin, “Acellular dermal matrices in breast surgery: a comprehensive review.,” *Ann. Plast. Surg.*, vol. 70, no. 6, pp. 732–8, Jun. 2013.

[65] H. Zhao, M. Qu, Y. Wang, Z. Wang, and W. Shi, “Xenogeneic acellular conjunctiva matrix as a scaffold of tissue-engineered corneal epithelium,” *PLoS One*, vol. 9, no. 11, pp. 1–9, 2014.

[66] R. F. Oliver, R. a Grant, C. M. Kent, and M. Kent, “The fate of cutaneously and subcutaneously implanted trypsin purified dermal collagen in the pig.,” *Br. J. Exp. Pathol.*, vol. 53, no. 5, pp. 540–9, Oct. 1972.

[67] E. Woodroof, “Use of glutaraldehyde and formaldehyde to process tissue heart valves.,” *J. Bioeng.*, vol. 2, no. 1–2, p. 1, 1978.

[68] R. Oliver, H. Barker, A. Cooke, and R. Grant, “Dermal collagen implants,” *Biomaterials*, vol. 3, no. 1, pp. 38–40, 1982.

[69] M. L. Jarman-smith, T. Bodamyali, C. Stevens, J. a Howell, M. Horrocks, and J. B. Chaudhuri, “Porcine collagen crosslinking, degradation and its capability for fibroblast adhesion and proliferation.,” *J. Mater. Sci. Mater. Med.*, vol. 15, no. 8, pp. 925–32, Aug. 2004.

[70] C. A. Miles, N. C. Avery, V. V Rodin, and A. J. Bailey, “The increase in denaturation temperature following cross-linking of collagen is caused by dehydration of the fibres,” *J. Mol. Biol.*, vol. 346, no. 2, pp. 551–556, Feb. 2005.

[71] L. E. De Castro Brás, “Characterisation of collagen-derived biomaerials,” Brunel University, 2009.

[72] A. Antunes, G. Attenburrow, A. Covington, and J. Ding, “Utilisation of oleuropein as a crosslinking agent in collagenic films,” *J. leather Sci.*, vol. 2, no. 2, pp. 17–23, 2008.

[73] E. Harris and M. Farrell, “Reistance to collagenase: a characterisitc of collagen fibrils cross-linked by formaldehyde,” *Biochim. Biophys. Acta*, vol. 278, pp. 133–141, 1972.

[74] G. Pascual, M. Rodr, J. Manuel, R. García-Pumarino, G. Pascual, M. Rodríguez, B. Pérez-Köhler, J. M. Bellón, M. Rodr, J. Manuel, R. García-Pumarino, G. Pascual, M. Rodríguez, B. Pérez-Köhler, and J. M. Bellón, “Do collagen meshes offer any benefits over preclude® ePTFE implants in contaminated surgical fields? A comparative in vitro and in vivo study.,” *J. Biomed. Mater. Res. B. Appl. Biomater.*, vol. 2008, pp. 1–10, Sep. 2013.

[75] L. Lee, J. Mata, T. Landry, K. A. Khwaja, M. C. Vassiliou, G. M. Fried, and L. S. Feldman, “A systematic review of synthetic and biologic materials for abdominal wall reinforcement in contaminated fields,” *Surg. Endosc. Other Interv. Tech.*, vol. 28, no. 9, pp. 2531–2546, 2014.

[76] M. Hiles, R. D. Record Ritchie, and A. M. Altizer, “Are biologic grafts effective for hernia repair?: a systematic review of the literature.,” *Surg. Innov.*, vol. 16, no. 1, pp. 26–37, Mar. 2009.

[77] T. M. Saettele, S. L. Bachman, C. R. Costello, S. a Grant, D. S. Cleveland, T. S. Loy, D. G. Kolder, and B. J. Ramshaw, “Use of porcine dermal collagen as a prosthetic mesh in a contaminated field for ventral hernia repair: a case report.,” *Hernia*, vol. 11, no. 3, pp. 279–85, Jun. 2007.

[78] I. Melnik, D. Goldstein, and B. Yoffe, “Use of a porcine dermal collagen implant for contaminated abdominal wall reconstruction in a 105-year-old woman: a case report and review of the literature,” *J. Med. Case Rep.*, vol. 9, no. 1, p. 95, 2015.

[79] H. M. J. Oliver. R.F., Grant. R.A., Cox. R.W., “Hisological studies of subculaneous and intraperitoneal implants of trypsin-prepared dermal collagen allograft in rat,” *Clincal Orthop. Relat. Res.*, no. March-April, pp. 291–302, 1976.

[80] L. E. De Castro Brás, S. Shurey, and P. D. Sibbons, “Evaluation of crosslinked and non-crosslinked biologic prostheses for abdominal hernia repair,” *Hernia*, vol. 16, pp. 77–89, 2012.

[81] W. A. Naimark, C. A. Pereira, K. Tsang, and J. M. Lee, “HMDC crosslinking of bovine pericardial tissue: A potential role of the solvent environment in the design of bioprosthetic materials,” *J. Mater. Sci. Mater. Med.*, vol. 6, no. 4, pp. 235–241, 1995.

[82] N. Bryan, H. Ahswin, N. Smart, Y. Bayon, S. Wohlert, and J. a Hunt, “Reactive oxygen species (ROS)--a family of fate deciding molecules pivotal in constructive inflammation and wound healing.,” *Eur. Cell. Mater.*, vol. 24, pp. 249–65, Jan. 2012.

[83] M. U. Ehrengruber, T. Geiser, and D. A. Deranleau, “Activation of human neutrophils by C3a and C5A Comparison of the effects on shape changes, chemotaxis, secretion, and respiratory burst,” *FEBS Lett.*, vol. 346, no. 2–3, pp. 181–184, Jun. 1994.

[84] W. M. Nauseef and N. Borregaard, “Neutrophils at work.,” *Nat. Immunol.*, vol. 15, no. 7, pp. 602–11, 2014.

[85] N. Bryan, H. Ashwin, N. Smart, Y. Bayon, N. Scarborough, and J. a Hunt, “The innate oxygen dependant immune pathway as a sensitive parameter to predict the performance of biological graft materials.,” *Biomaterials*, vol. 33, no. 27, pp. 6380–92, Sep. 2012.

[86] V. Witko-Sarsat, P. Rieu, B. Descamps-Latscha, P. Lesavre, and L. Halbwachs-Mecarelli, “Neutrophils: molecules, functions and pathophysiological aspects.,” *Lab. Invest.*, vol. 80, no. 5, pp. 617–653, 2000.

[87] L. Schwab, L. Goroncy, S. Palaniyandi, S. Gautam, A. Triantafyllopoulou, A. Mocsai, W. Reichardt, F. J. Karlsson, S. V Radhakrishnan, K. Hanke, A. Schmitt-Graeff, M. Freudenberg, F. D. von Loewenich, P. Wolf, F. Leonhardt, N. Baxan, D. Pfeifer, O. Schmah, A. Schönle, S. F. Martin, R. Mertelsmann, J. Duyster, J. Finke, M. Prinz, P. Henneke, H. Häcker, G. C. Hildebrandt, G. Hacker, and R. Zeiser, “Neutrophil granulocytes recruited upon translocation of intestinal bacteria enhance graft-versus-host disease via tissue damage.,” *Nat. Med.*, vol. 20, no. 6, pp. 648–654, 2014.

[88] R. Noubade, K. Wong, N. Ota, S. Rutz, C. Eidenschenk, P. a Valdez, J. Ding, I. Peng, A. Sebrell, P. Caplazi, J. DeVoss, R. H. Soriano, T. Sai, R. Lu, Z. Modrusan, J. Hackney, and W. Ouyang, “NRROS negatively regulates reactive oxygen species during host defence and autoimmunity.,” *Nature*, vol. 509, no. 7499, pp. 235–9, 2014.

[89] T. Assari, “Chronic Granulomatous Disease; fundamental stages in our understanding of CGD.,” *Med. Immunol.*, vol. 5, p. 4, Jan. 2006.

[90] N. K. Burns, M. V. Jaffari, C. N. Rios, A. B. Mathur, and C. E. Butler, “Non-cross-linked porcine acellular dermal matrices for abdominal wall reconstruction,” *Plast. Reconstr. Surg.*, vol. 125, no. 1, pp. 167–176, Jan. 2010.

[91] S. Misra, P. K. Raj, S. M. Tarr, and R. C. Treat, “Results of AlloDerm use in abdominal hernia repair.,” *Hernia*, vol. 12, no. 3, pp. 247–50, Jun. 2008.

[92] N. J. J. Slater, M. van der Kolk, T. Hendriks, H. van Goor, and R. P. P. Bleichrodt, “Biologic grafts for ventral hernia repair: a systematic review.,” *Am. J. Surg.*, vol. 205, no. 2, pp. 220–30, Feb. 2013.

[93] J. Hodde and M. Hiles, “Transforming surgery through biomaterial template technology,” *Br. J. Hosp. Med.*, vol. 77, no. 3, pp. 162–166, 2016.

[94] W. F. Liu, M. Ma, K. M. Bratlie, T. T. Dang, R. Langer, and D. G. Anderson, “Real-time in vivo detection of biomaterial-induced reactive oxygen species,” *Biomaterials*, vol. 32, no. 7, pp. 1796–1801, 2011.

[95] J. a. Cavallo, S. C. Greco, J. Liu, M. M. Frisella, C. R. Deeken, and B. D. Matthews, “Remodeling characteristics and biomechanical properties of a crosslinked versus a non-crosslinked porcine dermis scaffolds in a porcine model of ventral hernia repair,” *Hernia*, vol. 19, pp. 207–218, 2015.

[96] O. Mestak, E. Matouskova, Z. Spurkova, K. Benkova, P. Vesely, J. Mestak, M. Molitor, A. Pombinho, and A. Sukop, “Mesenchymal Stem Cells Seeded on Cross-Linked and Noncross-Linked Acellular Porcine Dermal Scaffolds for Long-Term Full-Thickness Hernia Repair in a Small Animal Model,” *Artif. Organs*, vol. 38, pp. 572–579, 2014.

[97] M. Sandor, H. Xu, J. Connor, J. Lombardi, J. R. Harper, R. P. Silverman, and D. J. McQuillan, “Host response to implanted porcine-derived biologic materials in a primate model of abdominal wall repair.,” *Tissue Eng. Part A*, vol. 14, no. 12, pp. 2021–31, Dec. 2008.

[98] N. Bryan, H. Ashwin, N. Smart, Y. Bayon, S. Wohlert, and J. A. Hunt, “The in vivo evaluation of tissue-based biomaterials in a rat full-thickness abdominal wall defect model.,” *J. Biomed. Mater. Res. B. Appl. Biomater.*, vol. 102, no. 4, pp. 709–20, May 2014.

[99] K. W. Lee, L. M. Pierce, D. Sc, T. L. Carlson, K. W. Lee, and L. M. Pierce, “Effect of cross-linked and non-cross-linked acellular dermal matrices on the expression of mediators involved in wound healing and matrix remodeling.,” *Plast. Reconstr. Surg.*, vol. 131, no. 4, pp. 697–705, Apr. 2013.

[100] S. B. Orenstein, Y. Qiao, U. Klueh, D. L. Kreutzer, and Y. W. Novitsky, “Activation of human mononuclear cells by porcine biologic meshes in vitro.,” *Hernia*, vol. 14, no. 4, pp. 401–407, Aug. 2010.

[101] C. R. Deeken, L. Melman, E. D. Jenkins, S. C. Greco, M. M. Frisella, and B. D. Matthews, “Histologic and biomechanical evaluation of crosslinked and non-crosslinked biologic meshes in a porcine model of ventral incisional hernia repair,” *J. Am. Coll. Surg.*, vol. 212, no. 5, pp. 880–888, 2011.

[102] L. Melman, E. D. Jenkins, N. a. Hamilton, L. C. Bender, M. D. Brodt, C. R. Deeken, S. C. Greco, M. M. Frisella, and B. D. Matthews, “Early biocompatibility of crosslinked and non-crosslinked biologic meshes in a porcine model of ventral hernia repair,” *Hernia*, vol. 15, pp. 157–164, 2011.

[103] G. Pascual, S. Sotomayor, M. Rodr, V. Arteaga, and J. M. Bell, “Extraperitoneal and intraperitoneal behavior of several biological meshes currently used to repair abdominal wall defects,” *J. Biomed. Mater. Res. Part B Appl. Biomater.*, vol. 103, no. 2, pp. 365–372, 2015.

[104] S. Lucke, A. Hoene, U. Walschus, A. Kob, J.-W. Pissarek, and M. Schlosser, “Acute and Chronic Local Inflammatory Reaction after Implantation of Different Extracellular Porcine Dermis Collagen Matrices in Rats,” *Biomed Res. Int.*, vol. 2015, pp. 1–10, 2015.

[105] L. M. Delgado, Y. Bayon, A. Pandit, and D. I. Zeugolis, “To Cross-Link or Not to Cross-Link? Cross-Linking Associated Foreign Body Response of Collagen-Based Devices,” *Tissue Eng. Part B Rev.*, vol. 21, no. 3, pp. 298–313, 2015.

[106] B. C. Shah, M. M. Tiwari, M. R. Goede, M. J. Eichler, R. R. Hollins, C. L. McBride, J. S. Thompson, and D. Oleynikov, “Not all biologics are equal!,” *Hernia*, vol. 15, no. 2, pp. 165–171, 2011.

[107] F. E. Primus and H. W. Harris, “A critical review of biologic mesh use in ventral hernia repairs under contaminated conditions.,” *Hernia*, vol. 17, no. 1, pp. 21–30, Feb. 2013.

[108] J. G. Neyt, J. A. Buckwalter, and N. C. Carroll, “Use of animal models in musculoskeletal research.,” *Iowa Orthop. J.*, vol. 18, pp. 118–23, 1998.

[109] A. Stavropoulos, A. Sculean, D. D. Bosshardt, D. Buser, and B. Klinge, “Pre-clinical in vivo models for the screening of bone biomaterials for oral/craniofacial indications: focus on small-animal models,” *Periodontol. 2000*, vol. 68, no. 1, pp. 55–65, 2015.

[110] L. E. De Castro Brás, J. L. Proffitt, S. Bloor, and P. D. Sibbons, “Effect of crosslinking on the performance of a collagen-derived biomaterial as an implant for soft tissue repair: A rodent model,” *J. Biomed. Mater. Res. - Part B Appl. Biomater.*, vol. 95 B, pp. 239–249, 2010.

[111] D. Eberli, S. Rodriguez, A. Atala, and J. J. Yoo, “In vivo evaluation of acellular human dermis for abdominal wall repair.,” *J. Biomed. Mater. Res. A*, vol. 93, no. 4, pp. 1527–38, 2010.

[112] V. Kishore, J. A. Uquillas, A. Dubikovsky, M. a. Alshehabat, P. W. Snyder, G. J. Breur, and O. Akkus, “In vivo response to electrochemically aligned collagen bioscaffolds,” *J. Biomed. Mater. Res. - Part B Appl. Biomater.*, vol. 100 B, no. 2, pp. 400–408, 2012.

[113] S. Mayer, H. Decaluwe, M. Ruol, S. Manodoro, M. Kramer, H. Till, and J. Deprest, “Diaphragm Repair with a Novel Cross-Linked Collagen Biomaterial in a Growing Rabbit Model,” *PLoS One*, vol. 10, no. 7, p. e0132021, 2015.

[114] H. Sugiura, S. Yunoki, E. Kondo, T. Ikoma, J. Tanaka, and K. Yasuda, “In vivo biological responses and bioresorption of tilapia scale collagen as a potential biomaterial.,” *J. Biomater. Sci. Polym. Ed.*, vol. 20, no. 10, pp. 1353–1368, 2009.

[115] C. J. Pendegrass, M. J. Oddy, S. Sundar, S. R. Cannon, a E. Goodship, and G. W. Blunn, “The novel use of resorbable Vicryl mesh for in vivo tendon reconstruction to a metal prosthesis.,” *J. Bone Joint Surg. Br.*, vol. 88, no. 9, pp. 1245–1251, 2006.

[116] D. Enea, J. Gwynne, S. Kew, M. Arumugam, J. Shepherd, R. Brooks, S. Ghose, S. Best, R. Cameron, and N. Rushton, “Collagen fibre implant for tendon and ligament biological augmentation. In vivo study in an ovine model,” *Knee Surgery, Sport. Traumatol. Arthrosc.*, vol. 21, no. 8, pp. 1783–1793, 2013.

[117] J. H. Lee, H. G. Kim, and W. J. Lee, “Characterization and tissue incorporation of cross-linked human acellular dermal matrix,” *Biomaterials*, vol. 44, pp. 195–205, 2015.

[118] J. Goodman, a. Chandna, and K. Roe, “Trends in animal use at US research facilities,” *J. Med. Ethics*, pp. 1–3, 2015.

[119] P. D. Sibbons, R. D. Pullan, and L. E. de Castro Brás, “Biopsies of Permacol™ implant in humans after use in abdominal wall repair: histological and immunohistochemical analysis,” *Comp. Clin. Path.*, vol. 24, no. 4, pp. 831–840, 2014.

[120] T. M. Macleod, G. Williams, R. Sanders, and C. J. Green, “Histological evaluation of Permacol as a subcutaneous implant over a 20-week period in the rat model.,” *Br. J. Plast. Surg.*, vol. 58, no. 4, pp. 518–32, Jun. 2005.

[121] G. S. De Silva, D. M. Krpata, Y. Gao, C. N. Criss, J. M. Anderson, H. T. Soltanian, M. J. Rosen, and Y. W. Novitsky, “Lack of identifiable biologic behavior in a series of porcine mesh explants,” *Surg. (United States)*, vol. 156, no. 1, pp. 183–189, 2014.

[122] T. J. Koh and L. A. DiPietro, “Inflammation and wound healing: the role of the macrophage,” *Expert Rev. Mol. Med.*, vol. 13, no. 2008, p. e23, Oct. 2011.

[123] E. D. Jenkins, L. Melman, C. R. Deeken, S. C. Greco, M. M. Frisella, and B. D. Matthews, “Biomechanical and histologic evaluation of fenestrated and nonfenestrated biologic mesh in a porcine model of ventral hernia repair.,” *J. Am. Coll. Surg.*, vol. 212, no. 3, pp. 327–39, Mar. 2011.

[124] T. J. Koh and L. A. DiPietro, “Inflammation and wound healing: the role of the macrophage,” *Expert Rev. Mol. Med.*, vol. 13, no. 2008, p. e23, Oct. 2011.